OPTIMIZATION OF SURFACE ROUGHNESS, MATERIAL REMOVAL RATE AND CUTTING TOOL FLANK WEAR IN TURNING USING EXTENDED TAGUCHI APPROACH

A thesis submitted in partial fulfillment
of the requirements for the degree of

Master of Technology

In

Production Engineering

By

UMESH KHANDEY
Roll No. 207ME208

NATIONAL INSTITUTE OF TECHNOLOGY
ROURKELA 769008, INDIA

OPTIMIZATION OF SURFACE ROUGHNESS, MATERIAL REMOVAL RATE AND CUTTING TOOL FLANK WEAR IN TURNING USING EXTENDED TAGUCHI APPROACH

A thesis submitted in partial fulfillment
of the requirements for the degree of

Master of Technology

In

Mechanical Engineering

By

UMESH KHANDEY

Under the guidance of

DR. SAURAV DATTA

NATIONAL INSTITUTE OF TECHNOLOGY
ROURKELA 769008, INDIA

NATIONAL INSTITUTE OF TECHNOLOGY
ROURKELA 769008, INDIA

Certificate

This is to certify that the project report entitled "OPTIMIZATION OF SURFACE ROUGHNESS, MATERIAL REMOVAL RATE AND CUTTING TOOL FLANK WEAR IN TURNING USING EXTENDED TAGUCHI APPROACH" submitted by *Sri Umesh Khandey* has been carried out under my supervision in partial fulfillment of the requirements for the degree of *Master of Technology* in *Production Engineering* at National Institute of Technology, Rourkela and this work has not been submitted elsewhere before for any academic degree/diploma.

Dr. Saurav Datta

Lecturer

Department of Mechanical Engineering

NIT Rourkela

Rourkela-769008

Date:

ACKNOWLEDGEMENT

I would like to express my sincere gratitude to **Dr. Saurav Datta**, Lecturer of Department of Mechanical Engineering, NIT Rourkela, for his guidance and help extended at every stage of this project work. I am deeply indebted to him for giving me a definite direction and moral support to complete the project successfully.

I am also thankful to **Prof. Ranjit Kumar Sahoo**, Professor and Head, **Prof. Siba Sankar Mahapatra**, Professor, Department of Mechanical Engineering, NIT Rourkela, for extending support to complete the project effectively. I wish to express sincere thanks to **Dr. Asish Bandyopadhyay**, Reader, Department of Mechanical Engineering, Jadavpur University, Kolkata, for his support to complete the project.

Last, but not the least I extend my sincere thanks to other faculty members of the Department of Mechanical Engineering, NIT Rourkela, for their valuable advice in every stage for successful completion of this project report.

UMESH KHANDEY
Roll No. 207ME208
NIT, Rourkela

CONTENTS

ABSTRACT

Quality and productivity play significant role in today's manufacturing market. From customers' viewpoint quality is very important because the extent of quality of the procured item (or product) influences the degree of satisfaction of the consumers during usage of the procured goods. Therefore, every manufacturing or production unit should concern about the quality of the product. Apart from quality, there exists another criterion, called productivity which is directly related to the profit level and also goodwill of the organization. Every manufacturing industry aims at producing a large number of products within relatively lesser time. But it is felt that reduction in manufacturing time may cause severe quality loss. In order to embrace these two conflicting criteria it is necessary to check quality level of the item either on-line or off-line. The purpose is to check whether quality lies within desired tolerance level which can be accepted by the customers. Quality of a product can be described by various quality attributes. The attributes may be quantitative or qualitative. In on-line quality control controller and related equipments are provided with the job under operation and continuously the quality is being monitored. If quality falls down the expected level the controller supplies a feedback in order to reset the process environment. In off-line quality control the method is either to check the quality of few products from a batch or lot (acceptance sampling) or to evaluate the best process environment capable of producing desired quality product. This invites optimization problem which seeks identification of the best process condition or parametric combination for the said manufacturing process. If the problem is related to a single quality attribute then it is called single objective (or response) optimization. If more than one attribute comes into consideration it is very difficult to select the optimal setting which can achieve all quality requirements simultaneously. Otherwise optimizing one quality feature may lead severe quality loss to other quality characteristics which may not be accepted by the customers. In order to tackle such a multi-objective optimization problem, the present study applied extended Taguchi method through a case study in straight turning of mild

steel bar using HSS tool. The study aimed at evaluating the best process environment which could simultaneously satisfy requirements of both quality and as well as productivity with special emphasis on reduction of cutting tool flank wear. Because reduction in flank wear ensures increase in tool life. The predicted optimal setting ensured minimization of surface roughness, height of flank wear of the cutting tool and maximization of MRR (Material Removal Rate). In view of the fact, that traditional Taguchi method cannot solve a multi-objective optimization problem; to overcome this limitation grey relational theory has been coupled with Taguchi method. Furthermore to follow the basic assumption of Taguchi method i.e. quality attributes should be uncorrelated or independent. But is practical case it may not be so. To overcome this shortcoming the study applied Principal Component analysis (PCA) to eliminate response correlation that exists between the responses and to evaluate independent or uncorrelated quality indices called Principal Components. Finally the study combined PCA, grey analysis, utility concept and Taguchi method for predicting the optimal setting. Optimal result was verified through confirmatory test. This indicates application feasibility of the aforesaid techniques for correlated multi-response optimization and off-line quality control in turning operation.

Key words: *quality, productivity, straight turning, surface roughness, MRR (Material Removal Rate), flank wear, grey-Taguchi method, Principal Component analysis (PCA)*

TABLES AND FIGURES

CHAPTER 1

CHAPTER 1: INTRODUCTION

1.1 TURNING OPERATION

Turning is the removal of metal from the outer diameter of a rotating cylindrical work piece. Turning is used to reduce the diameter of the work piece, usually to a specified dimension, and to produce a smooth finish on the metal. Often the work piece will be turned so that adjacent sections have different diameters.

Turning is the machining operation that produces cylindrical parts. In its basic form, it can be defined as the machining of an external surface:

- With the work piece rotating.
- With a single-point cutting tool, and
- With the cutting tool feeding parallel to the axis of the work piece and at a distance that will remove the outer surface of the work.

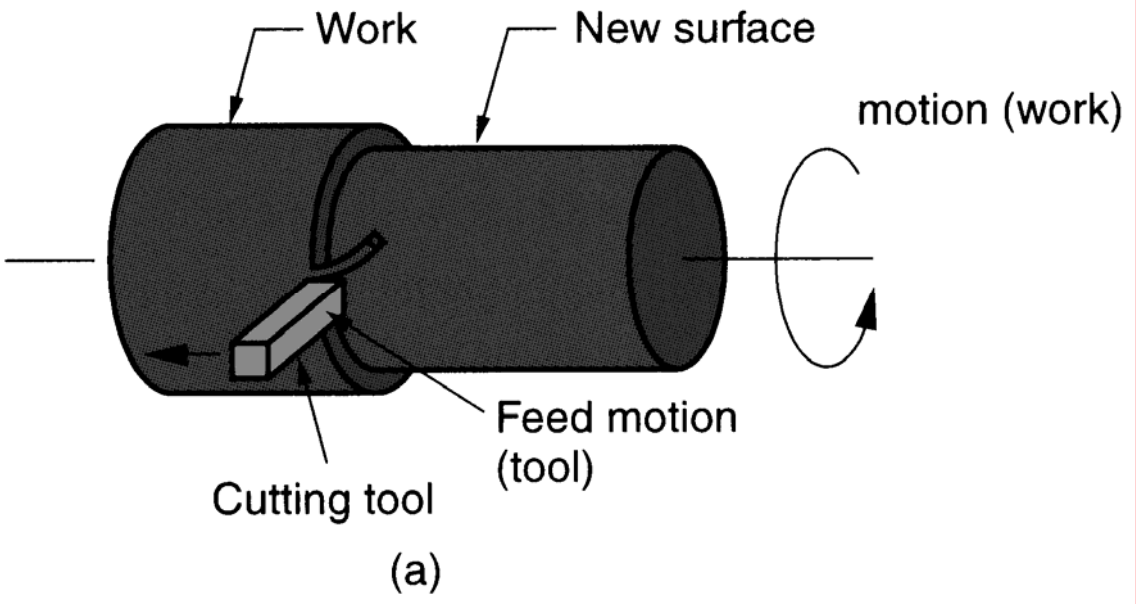

Figure 1.1: Adjustable parameters in turning operation

Taper turning is practically the same, except that the cutter path is at an angle to the work axis. Similarly, in contour turning, the distance of the cutter from the work axis is varied to produce the desired shape. Even though a single-point tool is specified, this does not

exclude multiple-tool setups, which are often employed in turning. In such setups, each tool operates independently as a single-point cutter.

1.1.1 ADJUSTABLE CUTTING FACTORS IN TURNING

The three primary factors in any basic turning operation are speed, feed, and depth of cut. Other factors such as kind of material and type of tool have a large influence, of course, but these three are the ones the operator can change by adjusting the controls, right at the machine.

Speed:

Speed always refers to the spindle and the work piece. When it is stated in revolutions per minute (rpm) it tells their rotating speed. But the important feature for a particular turning operation is the surface speed, or the speed at which the work piece material is moving past the cutting tool. It is simply the product of the rotating speed times the circumference of the work piece before the cut is started. It is expressed in meter per minute (m/min), and it refers only to the work piece. Every different diameter on a work piece will have a different cutting speed, even though the rotating speed remains the same.

$$v = \frac{\pi DN}{1000} m \min^{-1}$$

Here, v is the cutting speed in turning, D is the initial diameter of the work piece in mm, and N is the spindle speed in RPM.

Feed:

Feed always refers to the cutting tool, and it is the rate at which the tool advances along its cutting path. On most power-fed lathes, the feed rate is directly related to the spindle speed and is expressed in mm (of tool advance) per revolution (of the spindle), or mm/rev.

$$F_m = f.N \; mm.\min^{-1}$$

Here, F_m is the feed in mm per minute, f is the feed in mm/rev and N is the spindle speed in RPM.

Depth of Cut:

Depth of cut is practically self explanatory. It is the thickness of the layer being removed (in a single pass) from the work piece or the distance from the uncut surface of the work to the cut surface, expressed in mm. It is important to note, though, that the diameter of the work piece is reduced by two times the depth of cut because this layer is being removed from both sides of the work.

$$d_{cut} = \frac{D-d}{2} mm$$

Here, D *and* d represent initial and final diameter (in mm) of the job respectively.

1.1.2 CUTTING TOOLS FOR LATHES: TOOL GEOMETRY

Tool Geometry:

For cutting tools, geometry depends mainly on the properties of the tool material and the work material. The standard terminology is shown in the following figure. For single point tools, the most important angles are the rake angles and the end and side relief angles.

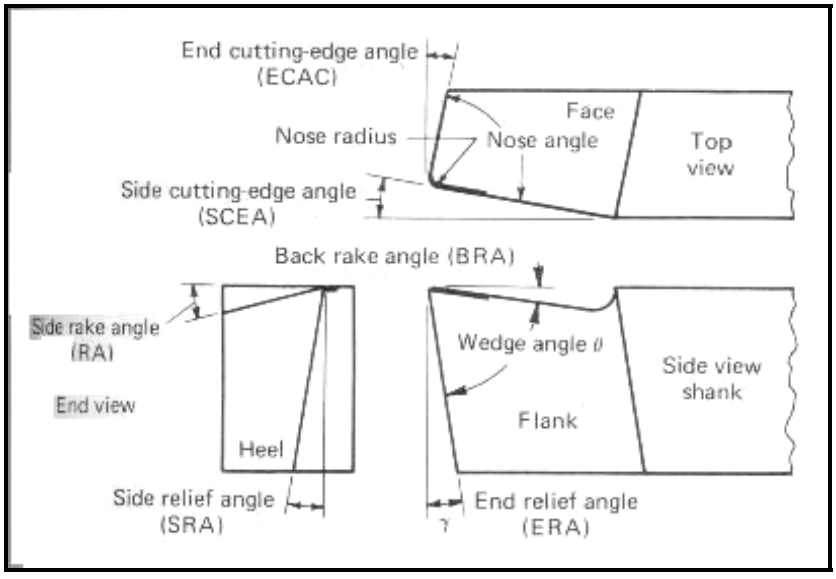

Figure 1.2: Geometry of a single point turning tool

Flank:

A flat surface of a single-point tool that is adjacent to the face of the tool. During turning, the side flank faces the direction that the tool is fed into the work piece, and the end flank passes over the newly machined surface.

Face:

The flat surface of a single point tool through which, the work piece rotates during turning operation. On a typical turning setup, the face of the tool is positioned upwards.

Back rake angle:

If viewed from the side facing the end of the work piece, it is the angle formed by the face of the tool and a line parallel to the floor. A positive back rake angle tilts the tool face back, and a negative angle tilts it forward and up.

Side rake angle:

If viewed behind the tool down the length of the tool holder, it is the angle formed by the face of the tool and the centerline of the work piece. A positive side rake angle tilts the tool face down toward the floor, and a negative angle tilts the face up and toward the work piece.

Side cutting edge angle:

If viewed from above looking down on the cutting tool, it is the angle formed by the side flank of the tool and a line perpendicular to the work piece centerline. A positive side cutting edge angle moves the side flank into the cut, and a negative angle moves the side flank out of the cut.

End cutting edge angle:

If viewed from above looking down on the cutting tool, it is the angle formed by the end flank of the tool and a line parallel to the work piece centerline. Increasing the end cutting edge angle tilts the far end of the cutting edge away from the work piece.

Side relief angle:

If viewed behind the tool down the length of the tool holder, it is the angle formed by the side flank of the tool and a vertical line down to the floor. Increasing the side relief angle tilts the side flank away from the work piece.

End relief angle:

If viewed from the side facing the end of the work piece, it is the angle formed by the end flank of the tool and a vertical line down to the floor. Increasing the end relief angle tilts the end flank away from the work piece.

Nose radius:

It is the rounded tip on the cutting edge of a single point tool. A zero degree nose radius creates a sharp point of the cutting tool.

Lead angle:

It is the common name for the side cutting edge angle. If a tool holder is built with dimensions that shift the angle of an insert, the lead angle takes this change into consideration.

The back rake angle affects the ability of the tool to shear the work material and form the chip. It can be positive or negative. Positive rake angles reduce the cutting forces resulting in smaller deflections of the work piece, tool holder, and machine. If the back rake angle is too large, the strength of the tool is reduced as well as its capacity to conduct heat. In machining hard work materials, the back rake angle must be small, even negative for carbide and diamond tools. The higher the hardness, the smaller will be the back rake angle. For high-speed steels, back rake angle is normally chosen in the positive range.

1.1.3 CUTTING TOOL MATERIALS

The classes of cutting tool materials currently in use for machining operation are high-speed tool steel, cobalt-base alloys, cemented carbides, ceramic, polycrystalline cubic boron nitride and polycrystalline diamond. Different machining applications require

different cutting tool materials. The Ideal cutting tool material should have all of the following characteristics:

- Harder than the work it is cutting
- High temperature stability
- Resists wear and thermal shock
- Impact resistant
- Chemically inert to the work material and cutting fluid

To effectively select tools for machining, a machinist or engineer must have specific information about:

- The starting and finished part shape
- The work piece hardness
- The material's tensile strength
- The material's abrasiveness
- The type of chip generated
- The work holding setup
- The power and speed capacity of the machine tool

Some common cutting tool materials are described below:

Carbon steels:

Carbon steels have been used since the 1880s for cutting tools. However carbon steels start to soften at a temperature of about 180^{o}C. This limitation means that such tools are rarely used for metal cutting operations. Plain carbon steel tools, containing about 0.9% carbon and about 1% manganese, hardened to about 62 Rc, are widely used for woodworking and they can be used in a router to machine aluminium sheet up to about 3mm thick.

High speed steels (HSS):

HSS tools are so named because they were developed to cut at higher speeds. Developed around 1900 HSS are the most highly alloyed tool steels. The tungsten (T series) was developed first and typically contains 12 - 18% tungsten, plus about 4% chromium and 1

- 5% vanadium. Most grades contain about 0.5% molybdenum and most grades contain 4 - 12% cobalt.

It was soon discovered that molybdenum (smaller proportions) could be substituted for most of the tungsten resulting in a more economical formulation which had better abrasion resistance than the T series and undergoes less distortion during heat treatment. Consequently about 95% of all HSS tools are made from M series grades. These contain 5 - 10% molybdenum, 1.5 - 10% tungsten, 1 - 4% vanadium, 4% Chromium and many grades contain 5 - 10% cobalt.

HSS tools are tough and suitable for interrupted cutting and are used to manufacture tools of complex shape such as drills, reamers, taps, dies and gear cutters. Tools may also be coated to improve wear resistance. HSS accounts for the largest tonnage of tool materials currently used. Typical cutting speeds: 10 - 60 m/min.

Cast Cobalt alloys:

Introduced in early 1900s these alloys have compositions of about 40 - 55% cobalt, 30% chromium and 10 - 20% tungsten and are not heat treatable. Maximum hardness values of 55 - 64 Rc. They have good wear resistance but are not as tough as HSS but can be used at somewhat higher speeds than HSS. Now only in limited use.

Carbides:

Also known as cemented carbides or sintered carbides were introduced in the 1930s and have high hardness over a wide range of temperatures, high thermal conductivity, high Young's modulus making them effective tool and die materials for a range of applications. The two groups used for machining are tungsten carbide and titanium carbide; both types may be coated or uncoated. Tungsten carbide particles (1 to 5 micrometer) are bonded together in a cobalt matrix using powder metallurgy. The powder is pressed and sintered to the required insert shape. Titanium and niobium carbides may also be included to impart special properties. A wide range of grades are available for different applications. Sintered carbide tips are the dominant type of material used in metal cutting. The proportion of cobalt (the usual matrix material) present has a significant effect on the properties of carbide tools. 3 - 6% matrix of cobalt gives greater

hardness while 6 - 15% matrix of cobalt gives a greater toughness while decreasing the hardness, wear resistance and strength. Tungsten carbide tools are commonly used for machining steels, cast irons and abrasive non-ferrous materials. Titanium carbide has a higher wear resistance than tungsten but is not as tough. With a nickel-molybdenum alloy as the matrix, TiC is suitable for machining at higher speeds than those which can be used for tungsten carbide. Typical cutting speeds are: 30 - 150 m/min or 100 - 250 when coated.

Coatings:

Coatings are frequently applied to carbide tool tips to improve tool life or to enable higher cutting speeds. Coated tips typically have lives 10 times greater than uncoated tips. Common coating materials include titanium nitride, titanium carbide and aluminium oxide, usually 2 - 15 micro-m thick. Often several different layers may be applied, one on top of another, depending upon the intended application of the tip. The techniques used for applying coatings include chemical vapour deposition (CVD) plasma assisted CVD and physical vapour deposition (PVD). Diamond coatings are also in use and being further developed.

Cermets:

Developed in the 1960s, these typically contain 70% aluminium oxide and 30% titanium carbide. Some formulation contains molybdenum carbide, niobium carbide and tantalum carbide. Their performance is between those of carbides and ceramics and coatings seem to offer few benefits. Typical cutting speeds: 150 - 350 m/min.

Ceramics:

Alumina

Introduced in the early 1950s, two classes are used for cutting tools: fine grained high purity aluminium oxide (Al_2O_3) and silicon nitride (Si_3N_4) are pressed into insert tip shapes and sintered at high temperatures. Additions of titanium carbide and zirconium oxide (ZrO_2) may be made to improve properties. But while ZrO_2 improves the fracture toughness, it reduces the hardness and thermal conductivity. Silicon carbide (SiC)

whiskers may be added to give better toughness and improved thermal shock resistance. The tips have high abrasion resistance and hot hardness and their superior chemical stability compared to HSS and carbides means they are less likely to adhere to the metals during cutting and consequently have a lower tendency to form a built up edge. Their main weakness is low toughness and negative rake angles are often used to avoid chipping due to their low tensile strengths. Stiff machine tools and work set ups should be used when machining with ceramic tips as otherwise vibration is likely to lead to premature failure of the tip. Typical cutting speeds: 150-650 m/min.

Silicon Nitride:

In the 1970s a tool material based on silicon nitride was developed, these may also contain aluminium oxide, yttrium oxide and titanium carbide. SiN has an affinity for iron and is not suitable for machining steels. A specific type is 'Sialon', containing the elements: silicon, aluminium, oxygen and nitrogen. This has higher thermal shock resistance than silicon nitride and is recommended for machining cast irons and nickel based super alloys at intermediate cutting speeds.

Cubic Boron Nitride (CBN):

Introduced in the early 1960s, this is the second hardest material available after diamond. cBN tools may be used either in the form of small solid tips or or as a 0.5 to 1 mm thick layer of of polycrystalline boron nitride sintered onto a carbide substrate under pressure. In the latter case the carbide provides shock resistance and the cBN layer provides very high wear resistance and cutting edge strength. Cubic boron nitride is the standard choice for machining alloy and tool steels with a hardness of 50 Rc or higher. Typical cutting speeds: 30 - 310 m/min.

Diamond:

The hardest known substance is diamond. Although single crystal diamond has been used as a tool, they are brittle and need to be mounted at the correct crystal orientation to obtain optimal tool life. Single crystal diamond tools have been mainly replaced by

polycrystalline diamond (PCD). This consists of very small synthetic crystals fused by a high temperature high pressure process to a thickness of between 0.5 and 1mm and bonded to a carbide substrate. The result is similar to cBN tools. The random orientation of the diamond crystals prevents the propagation of cracks, improving toughness. Because of its reactivity, PCD is not suitable for machining plain carbon steels or nickel, titanium and cobalt based alloys. PCD is most suited to light uninterrupted finishing cuts at almost any speed and is mainly used for very high speed machining of aluminium - silicon alloys, composites and other non - metallic materials. Typical cutting speeds: 200 - 2000 m/min.

To improve the toughness of tools, developments are being carried out with whisker reinforcement, such as silicon nitride reinforced with silicon carbide whiskers.

As rates of metal removal have increased, so has the need for heat resistant cutting tools. The result has been a progression from high-speed steels to carbide, and on to ceramics and other super hard materials.

High-speed steels cut four times faster than the carbon steels they replaced. There are over 30 grades of high-speed steel, in three main categories: tungsten, molybdenum, and molybdenum-cobalt based grades.

In industry today, carbide tools have replaced high-speed steels in most applications. These carbide and coated carbide tools cut about 3 to 5 times faster than high-speed steels. Cemented carbide is a powder metal product consisting of fine carbide particles cemented together with a binder of cobalt. The major categories of hard carbide include tungsten carbide, titanium carbide, tantalum carbide, and niobium carbide.
Ceramic cutting tools are harder and more heat-resistant than carbides, but more brittle. They are well suited for machining cast iron, hard steels, and the super alloys. Two types of ceramic cutting tools are available: the alumina-based and the silicon nitride-based ceramics. The alumina-based ceramics are used for high speed semi- and final-finishing of ferrous and some non-ferrous materials. The silicon nitride-based ceramics are generally used for rougher and heavier machining of cast iron and the super alloys.

1.1.4 TURNING MACHINES

The turning machines are, of course, every kind of lathes. Lathes used in manufacturing can be classified as engine, turret, automatics, and numerical control etc.

They are heavy duty machine tools and have power drive for all tool movements. They commonly range in size from 12 to 24 inches swing and from 24 to 48 inches center distance, but swings up to 50 inches and center distances up to 12 feet are not uncommon. Many engine lathes are equipped with chip pans and built-in coolant circulating system.

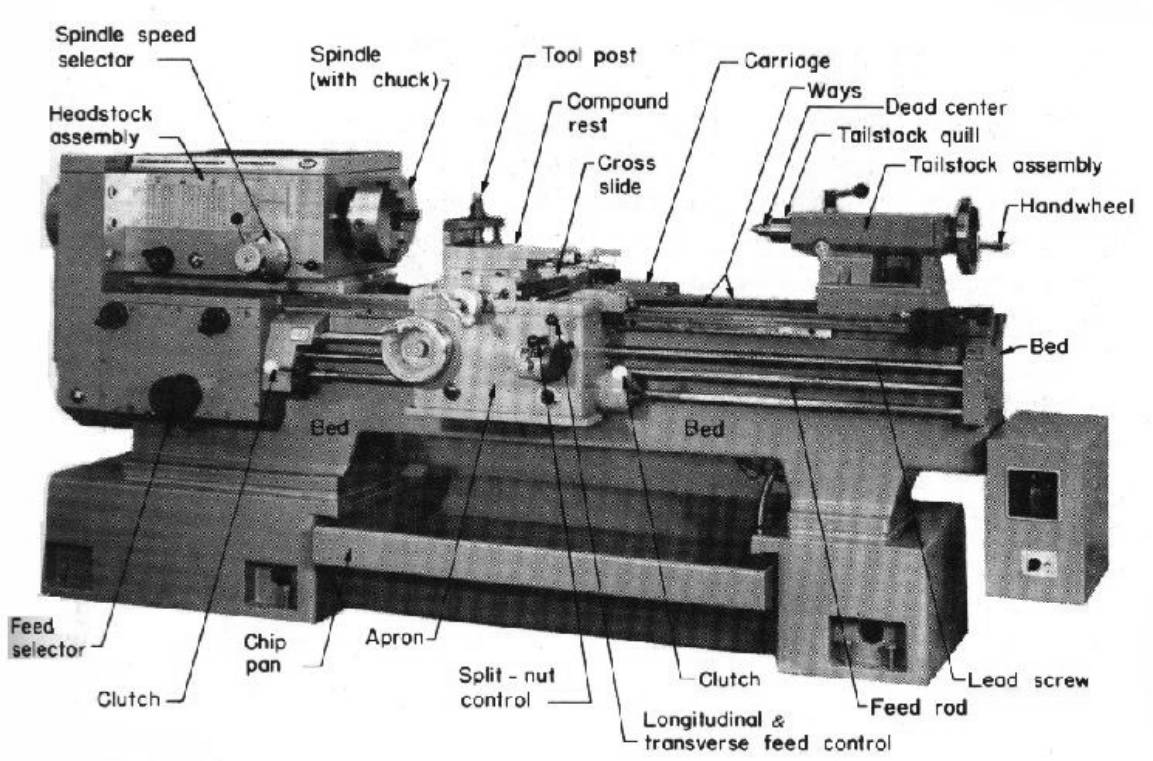

Figure 1.3: Centre lathe used for turning

Turret Lathes:

In a turret lathe, a longitudinally feedable, hexagon turret replaces the tailstock. The turret, on which six tools can be mounted, can be rotated about a vertical axis to bring each tool into operating position, and the entire unit can be moved longitudinally, either annually or by power, to provide feed for the tools. When the turret assembly is backed away from the spindle by means of a capstan wheel; the turret indexes automatically at the end of its movement, thus, bring each of the six tools into operating position. The square turret on the cross slide can be rotated manually about a vertical axis to bring each

of the four tools into operating position. On most machines, the turret can be moved transversely, either manually or by power, by means of the cross slide, and longitudinally through power or manual operation of the carriage. In most cased, a fixed tool holder also is added to the back end of the cross slide; this often carries a parting tool.

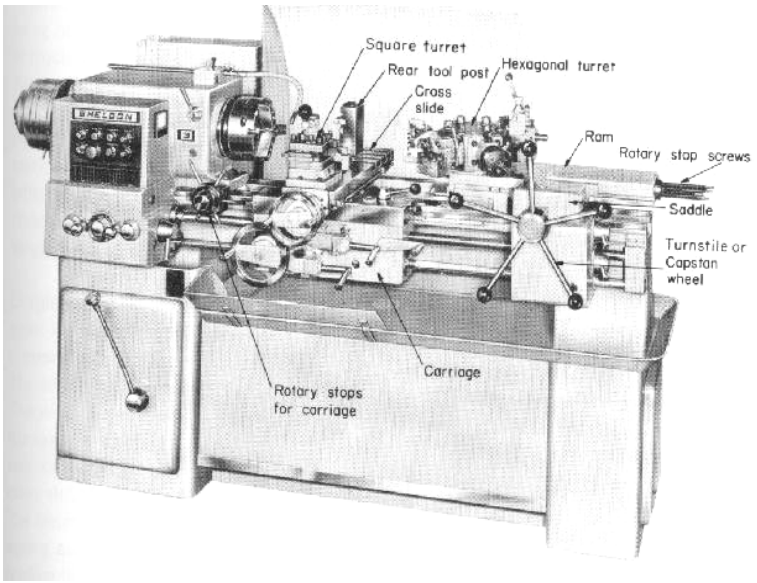

Figure 1.4: Turret lathe

Through these basic features of a turret lathe, a number of tools can be set on the machine and then quickly be brought successively into working position so that a complete part can be machined without the necessity for further adjusting, changing tools, or making measurements.

Single-Spindle Automatic Screw Machines:

There are two common types of single-spindle screw machines, One, an American development and commonly called the turret type (Brown & Sharp), is shown in the following figure. The other is of Swiss origin and is referred to as the Swiss type. The Brown & Sharp screw machine is essentially a small automatic turret lathe, designed for bar stock, with the main turret mounted on the cross slide. All motions of the turret, cross slide, spindle, chuck, and stock-feed mechanism are controlled by cams. The turret cam is essentially a program that defines the movement of the turret during a cycle. These

machines usually are equipped with an automatic rod feeding magazine that feeds a new length of bar stock into the collect as soon as one rod is completely used.

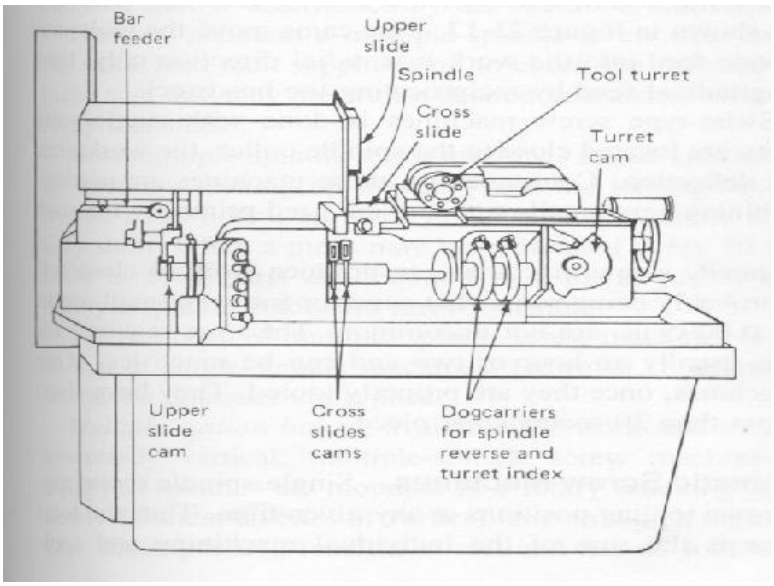

Figure 1.5: Single-Spindle Automatic Screw Machine

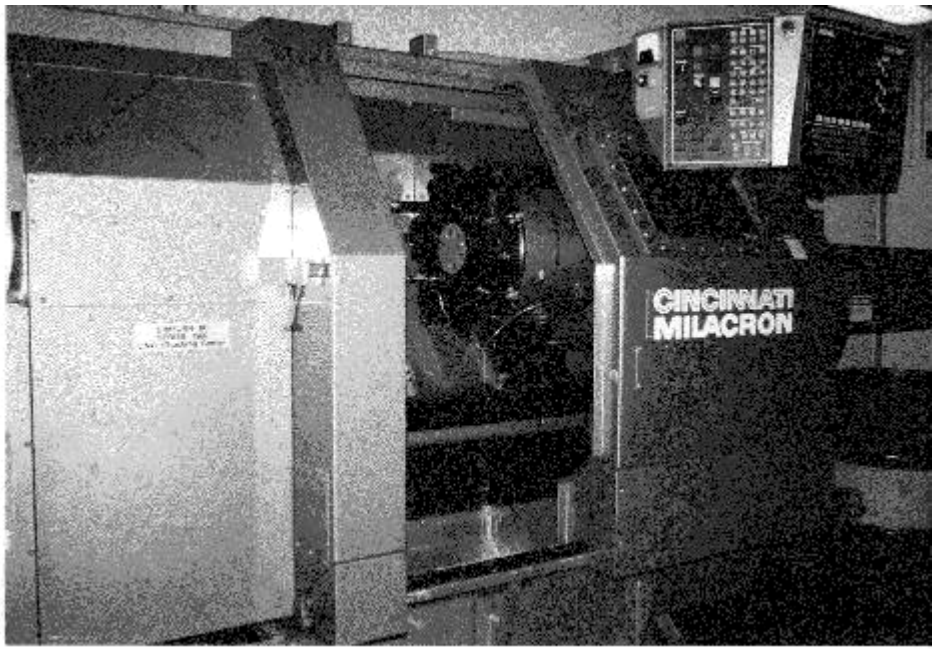

Figure 1.6: CNC lathe

CNC Machines:

Nowadays, more and more Computer Numerical Controlled (CNC) machines are being used in every kind of manufacturing processes. In a CNC machine, functions like program storage, tool offset and tool compensation, program-editing capability, various degree of computation, and the ability to send and receive data from a variety of sources, including remote locations can be easily realized through on board computer. The computer can store multiple-part programs, recalling them as needed for different parts. A CNC turret lathe in Michigan Technological University is shown in the following picture.

1.2 MATERIAL REMOVAL RATE (MRR)

The material removal rate (MRR) in turning operations is the volume of material/metal that is removed per unit time in mm^3/min. For each revolution of the work piece, a ring-shaped layer of material is removed. $MRR = (v.f.d \times 1000)\, in\, mm^3 / \min$

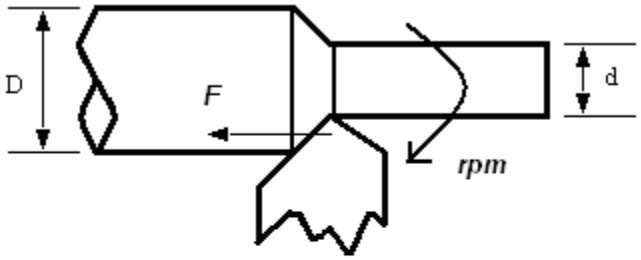

$$mrr = \left(\frac{\pi D^2}{4} - \frac{\pi d^2}{4}\right) \times F \times rpm$$

where,

D = diameter of workpiece before cutting
d = diameter of workpiece after cutting

Figure 1.7: MRR in turning

1.3 TOOL WEAR

Tool wear in machining is defined as the amount of volume loss of tool material on the contact surface due to the interactions between the tool and work piece. Specifically, tool wear is described by wear rate (volume loss per unit area per unit time) and is strongly

determined by temperature, stresses, and relative sliding velocity generated at the contact interface.

Metal cutting tools are subjected to extremely arduous conditions, high surface loads, and high surface temperatures arise because the chip slides at high speed along the tool rake face while exerting very high normal pressures (and friction force) on this face. The forces may be fluctuating due to the presence of hard particles in the component micro-structure, or more extremely, when interrupted cutting is being carried out. Hence cutting tools need:

- Strength at elevated temperatures
- High toughness
- High wear resistance
- High hardness

During the past 100 years there has been extensive research and development which has provided continuous improvement in the capability of cutting tool. A key factor in the wear rate of virtually all tool materials is the temperature reached during operation; unfortunately it is difficult to establish the values of the parameters needed for such calculations. However, experimental measurements have provided the basis for empirical approaches.

It is common to assume that all the energy used in cutting is converted to heat (a reasonable assumption) and that 80% of this is carried away in the chip (this will vary and depend upon several factors - particularly the cutting speed). This leaves about 20% of the heat generated going into the cutting tool. Even when cutting mild steel tool temperatures can exceed 550^{o}C, the maximum temperature high speed steel (HSS) can withstand without losing some hardness. Cutting hard steels with cubic boron nitride tools will result in tool and chip temperatures in excess of 1000^{o}C. During operation, one or more of the following wear modes may occur:

(a) Flank
(b) Notch
(c) Crater
(d) Edge rounding

(e) Edge chipping
(f) Edge cracking
(g) Catastrophic failure

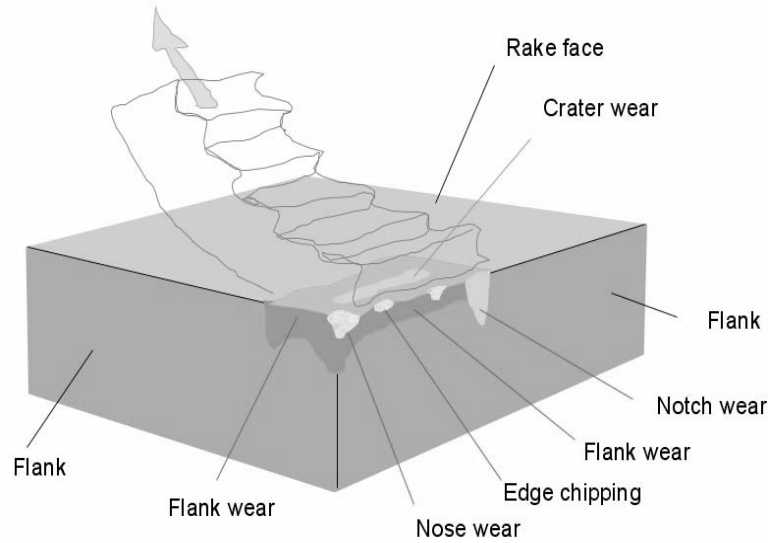

Figure 1.8.a: Different modes of wear

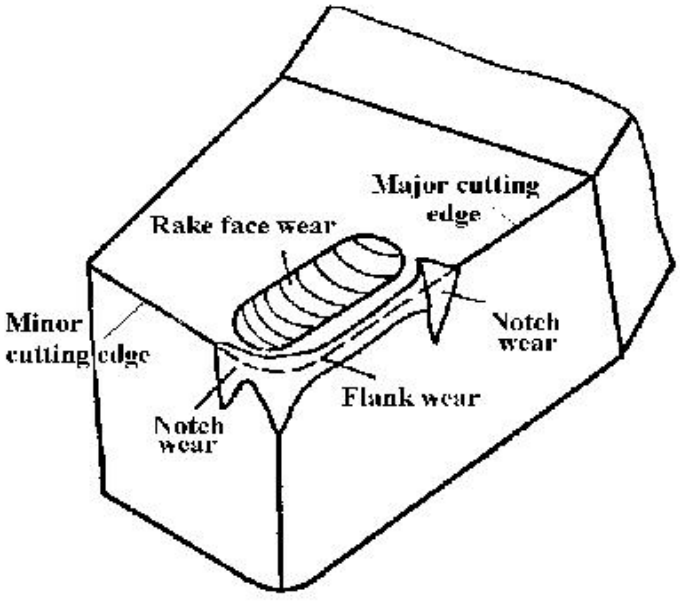

Figure 1.8.b Tool wear phenomena

Cutting tools are subjected to an extremely severe rubbing process. They are in metal-to-metal contact between the chip and work piece, under conditions of very high stress at high temperature. The situation is further aggravated (worsened) due to the existence of extreme stress and temperature gradients near the surface of the tool. During machining, cutting tools remove material from the component to achieve the required shape, dimension and surface roughness (finish). However, wear occurs during the cutting action, and it will ultimately result in the failure of the cutting tool. When the tool wear reaches a certain extent, the tool or active edge has to be replaced to guarantee the desired cutting action.

Rake face wear:

Crater wears:

The chip flows across the rake face, resulting in severe friction between the chip and rake face, and leaves a scar on the rake face which usually parallels to the major cutting edge. The crater wear can increase the working rake angle and reduce the cutting force, but it will also weaken the strength of the cutting edge. The parameters used to measure the crater wear can be seen in the diagram. The crater depth KT is the most commonly used parameter in evaluating the rake face wear.

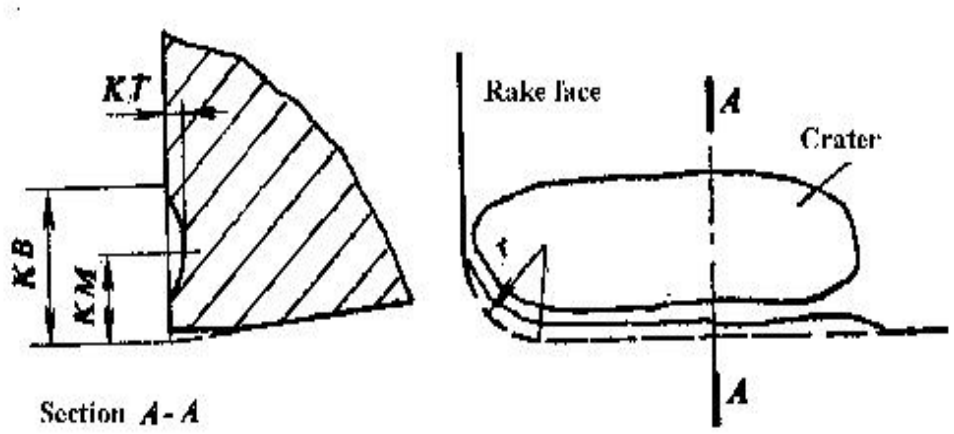

Figure 1.9: Crater wear

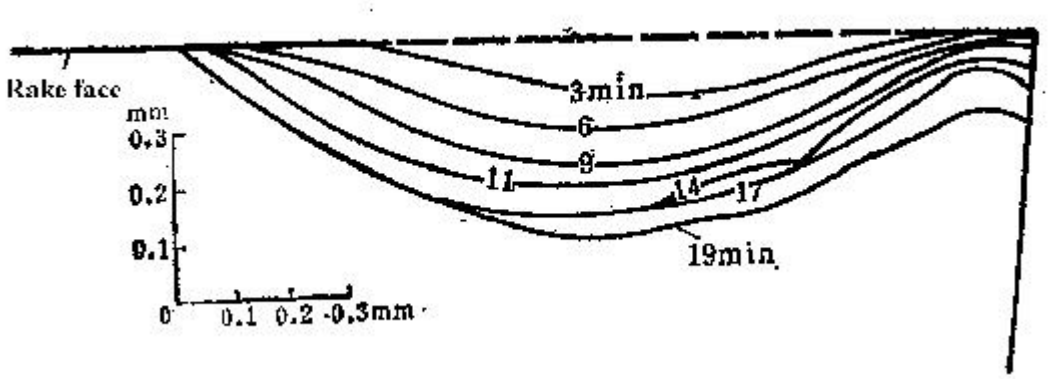

Figure 1.10: Crater wear and wear depth KT and width KB with cutting time

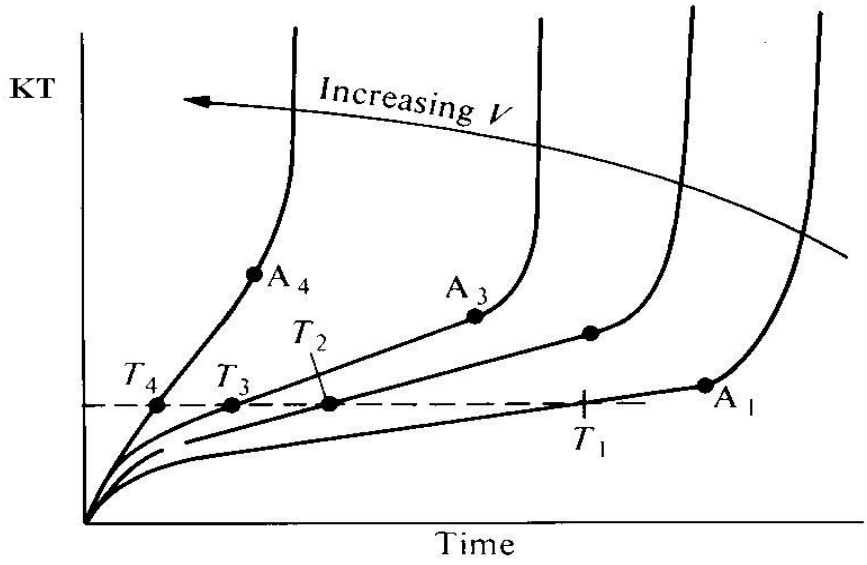

Figure 1.11: Effects of cutting speed V and cutting time T on crater wear depth KT

Flank wear (Clearance surface):

Wear on the flank (relief) face is called Flank wear and results in the formation of a wear land. Wear land formation is not always uniform along the major and minor cutting edges of the tool.

Flank wear most commonly results from abrasive wear of the cutting edge against the machined surface. Flank wear can be monitored in production by examining the tool or

by tracking the change in size of the tool or machined part. Flank wear can be measured by using the average and maximum wear land size VB and VBmax.

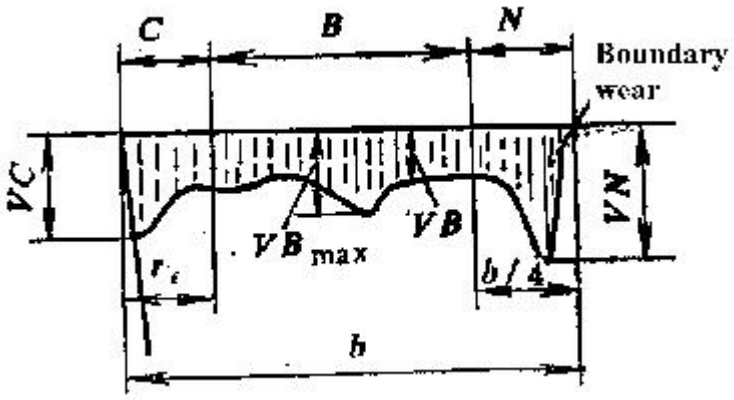

Figure 1.12: Flank wear

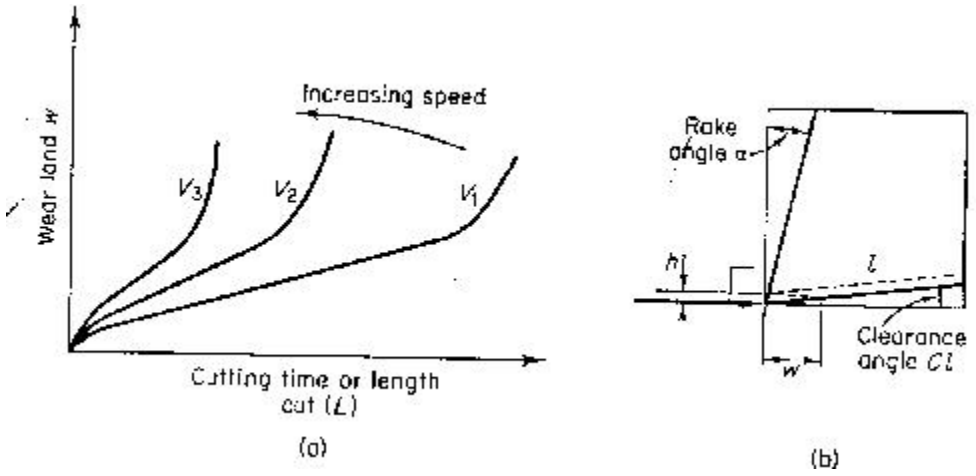

Figure 1.13: Typical stages of tool wear in normal cutting situation

Due to micro-cracking, surface oxidation and carbon loss layer, as well as micro-roughness at the cutting tool tip in tool grinding (manufacturing). For the new cutting edge, the small contact area and high contact pressure will result in high wear rate. The initial wear size is VB=0.05-0.1mm normally.

After the initial (or preliminary) wear (cutting edge rounding), the micro-roughness is improved, in this region the wear size is proportional to the cutting time. The wear rate is relatively constant.

When the wear size increases to a critical value, the surface roughness of the machined surface decreases, cutting force and temperature increase rapidly, and the wear rate increases. Then the tool loses its cutting ability. In practice, this region of wear should be avoided.

Flank wear and chipping will increase the friction, so that the total cutting force will increase. The component surface roughness will be increased, especially when chipping occurs.

Flank wear will also affect the component dimensional accuracy. When form tools are used, flank wear will also change the shape of the component produced.

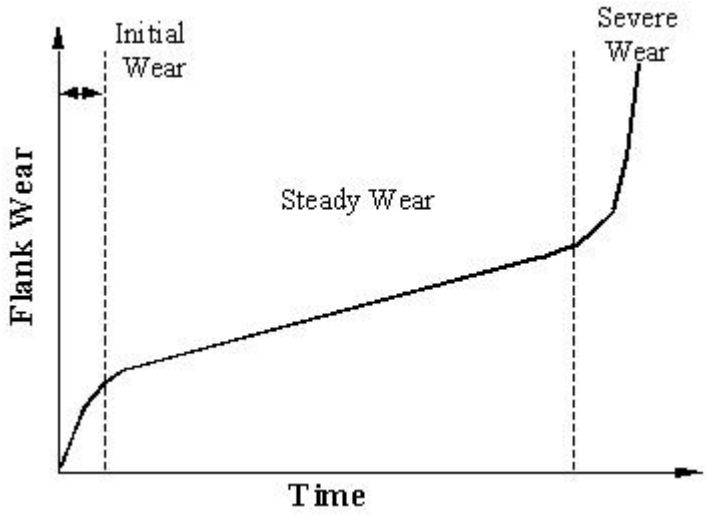

Figure 1.14: Different regions of wear

Table 1.1: Recommended wear land size for different tool material and operations.

Wear (in)	**Tool Material**	**Remarks**
0.030 (0.76 mm)	Carbide	Roughing passes
0.010-0.015 (0.25-0.38 mm)	Carbide	Finishing passes
0.060 or total destruction(1.25 mm)	H.S.S.	Roughing passes
0.010-0.015 (0.25-0.38 mm)	H.S.S.	Finishing passes
0.010-0.015 (0.25-0.38 mm)	Cemented oxides	Roughing and finishing passes

Notch Wear:

This is a special type of combined flank and rake face wear which occurs adjacent to the point where the major cutting edge intersects the work surface.

The gashing (or grooving, gouging) at the outer edge of the wear land is an indication of a hard or abrasive skin on the work material. Such a skin may develop during the first machine pass over a forging, casting or hot-rolled work piece. It is also common in machining of materials with high work-hardening characteristics, including many stainless steels and heat-resistant nickel or chromium alloys. In this case, the previous machining operation leaves a thin work-hardened skin.

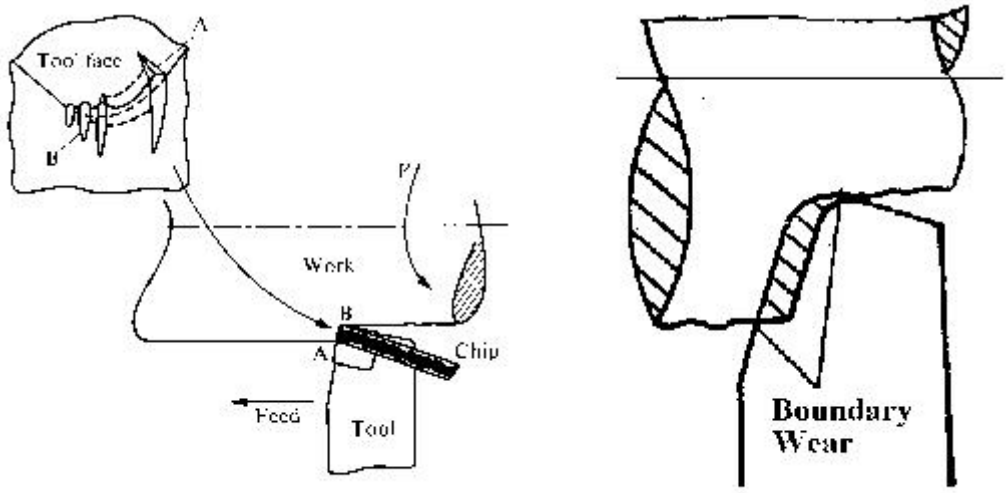

Figure 1.15: Notch wear

Chipping:

Chipping of the tool, as the name implies, involves removal of relatively large discrete particles of tool material. Tools subjected to discontinuous cutting conditions are particularly prone to chipping. Chipping of the cutting edge is more like micro-breakages rather than conventional wear. Built-up edge formation also has a tendency to promote tool chipping. A built-up edge is never completely stable, but it periodically breaks off. Each time some of the built-up material is removed it may take with it a lump (piece) of tool edge

Ultimate failure:

The final result of tool wear is the complete removal of the cutting point - ultimate failure of the tool. This may come about by temperature rise, which virtually causes the tool tip to soften until it flows plastically at very low shear stress. This melting process seems to start right at the cutting edge and because material flow blunts the edge, the melting process continues back into the tool; within a few seconds a piece of tool almost as large as the engaged depth of cut is removed.

An alternative mechanism of ultimate failure is the mechanical failure (usually a brittle fracture) of a relatively large portion of the cutting tip. This often results from a weakening of the tool by crater formation.

Ultimate failure by melting and plastic flow is most common in carbon and high-speed-steel tools, while fracture failures are most common in sintered carbide or ceramic tools.

1.3.1 CAUSES OF TOOL WEAR

- Hard particle wear (abrasive wear)
- Adhesive wear
- Diffusion wear
- Chemical wear
- Fracture wear

a) Hard particle wear (abrasive wear):

Abrasive wear is mainly caused by the impurities within the work piece material, such as carbon, nitride and oxide compounds, as well as the built-up fragments. This is a mechanical wear, and it is the main cause of the tool wear at low cutting speeds.

a) Adhesive wear mechanism:

The simple mechanism of friction and wear proposed by Bowden and Tabor is based on the concept of the formation of welded junctions and subsequent destruction of these. Due to the high pressure and temperature, welding occurs between the fresh surface of the chip and rake face (chip rubbing on the rake face results in a chemically clean

surface). [Process is used to advantage when Friction welding to produce twist drill and broaches and in tool manufacturing]. Severe wear is characterized by considerable welding and tearing of the softer rubbing surface at high wear rate, and the formation of relatively large wear particles. Under mild wear conditions, the surface finish of the sliding surfaces improves.

c) Diffusion wear:

Holm thought of wear as a process of atomic transfer at contacting asperities (Armarego and Brown). A number of workers have considered that the mechanism of tool wear must involve chemical action and diffusion. They have demonstrated welding and preferred chemical attack of tungsten carbide in tungsten-titanium carbides. They have shown the photo-micrograph evidence of the diffusion of tool constituents into the workpiece and chip. This diffusion results in changes of the tool and workpiece chemical composition. There are several ways in which the wear may be dependent on the diffusion mechanism.

1. Gross softening of the tool:

2. Diffusion of major tool constituents into the work (chemical element loss)

3. Diffusion of a work-material component into the tool

d) Chemical wear:

Corrosive wear (due to chemical attack of a surface)

e) Facture wear:

Fracture can be the catastrophic end of the cutting edge. The bulk breakage is the most harmful type of wear and should be avoided as far as possible.

Chipping of brittle surfaces

Other forms of tool wear:

Thermo-electric wear can be observed in high temperature region, and it reduces the tool wear. The high temperature results in the formation of thermal couple between the workpiece and the tool. Due to the heat related voltage established between the

workpiece and tool, it may cause an electric current between the two. However, the mechanism of thermo-electric wear has not been clearly developed. Major improvement (decrease) of tool wear has been seen through experimental tests with an isolated tool and component.

Thermal Cracking and Tool Fracture:

In milling, tools are subjected to cyclic thermal and mechanical loads. Teeth may fail by a mechanism not observed in continuous cutting. Two common failure mechanisms unique to milling are thermal cracking and entry failure.

The cyclic variations in temperature in milling induce cyclic thermal stress as the surface layer of the tool expands and contracts. This can lead to the formation of thermal fatigue cracks near the cutting edge. In most cases such cracks are perpendicular to the cutting edge and begin forming at the outer corner of the tool, spreading inward as cutting progresses. The growth of these cracks eventually leads to edge chipping or tool breakage.

Thermal cracking can be reduced by reducing the cutting speed or by using a tool material grade with a higher thermal shock resistance. In applications when coolant is supplied, adjusting the coolant volume can also reduce crack formation. An intermittent coolant supply or insufficient coolant can promote crack formation; if a steady, copious volume of coolant cannot be supplied, tool-life can often be increased by switching to dry cutting.

Edge chipping is common in milling. Chipping may occur when the tool first contacts the part (entry failure) or, more commonly, when it exits the part (exit failure). WC tool materials are especially prone to this.

Entry failure most commonly occurs when the outer corner of the insert strikes the part first. This is more likely to occur when the cutter rake angles are positive. Entry failure is therefore most easily prevented by switching from positive to negative rake cutters.

1.3.2 EFFECTS OF TOOL WEAR ON TECHNOLOGICAL PERFORMANCE MEASURES

Consequences of tool wear

1. Increase the cutting force;
2. Increase the surface roughness;
3. Decrease the dimensional accuracy;
4. Increase the temperature;
5. Vibration;
6. Lower the production efficiency, component quality;
7. Increase the cost.

Influence on cutting forces:

Crater wear, flank wear (or wear-land formation) and chipping of the cutting edge affect the performance of the cutting tool in various ways. The cutting forces are normally increased by wear of the tool. Crater wear may, however, under certain circumstances, reduce forces by effectively increasing the rake angle of the tool. Clearance-face (flank or wear-land) wear and chipping almost invariably increase the cutting forces due to increased rubbing forces.

Surface finish (roughness):

The surface finish produced in a machining operation usually deteriorates as the tool wears. This is particularly true for a tool worn by chipping and generally the case for a tool with flank-land wear; although there are circumstances in which a wear land may burnish (polish) the workpiece and produces a good finish.

Dimensional accuracy:

Flank wear influences the plan geometry of a tool; this may affect the dimensions of the component produced in a machine with set cutting tool position or it may influence the shape of the components produced in an operation utilizing a form tool. (If tool wear is rapid, cylindrical turning could result in a tapered workpiece)

Vibration or chatter:

Vibration or chatter is another aspect of the cutting process which may be influenced by tool wear. A wear land increases the tendency of a tool to dynamic instability. A cutting operation which is quite free of vibration when the tool is sharp may be subjected to an unacceptable chatter mode when the tool wears.

1.4 TOOL LIFE

There is no single universally accepted definition of tool life. The life needs to be specified with regard to the process aims. A common way of quantifying the end of a tool life is to put a limit on the maximum acceptable flank wear, VB or VB_{max}. Typical figures are:

HSS tools, roughing	1.5 mm
HSS tools, finishing	0.75 mm
Carbide tools	0.7 mm
Ceramic tools	0.6 mm

Mathematically the tool life can be expressed in the following equation (the Taylor equation): $VT^n = C$, Here

V	Cutting speed
T	Tool life
n, C	Constants

The constants n and C may be found for specific work piece and tool material and feed, f, either by experiment or from published data.

1.5 SURFACE STRUCTURE AND PROPERTIES

Surface roughness is an important measure of product quality since it greatly influences the performance of mechanical parts as well as production cost. Surface roughness has an impact on the mechanical properties like fatigue behavior, corrosion resistance, creep life,

etc. It also affects other functional attributes of parts like friction, wear, light reflection, heat transmission, lubrication, electrical conductivity, etc. Before surface roughness, it is also necessary to discuss about surface structure and properties, as they are closely related.

Upon close examination of the surface of a piece of metal, it can be found that it generally consists of several layers (Figure 1.16). The characteristics of these layers are briefly outlined here:

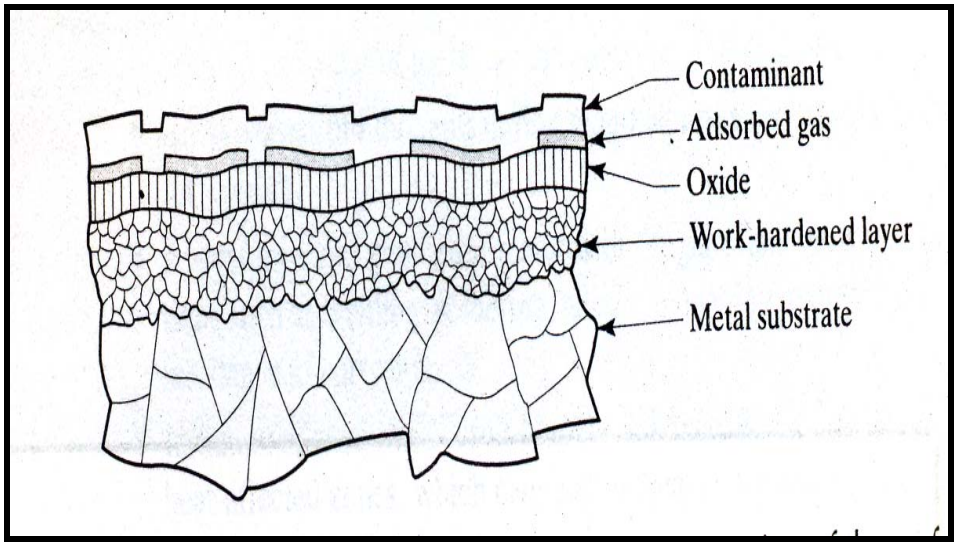

Figure 1.16: Schematic of a cross-section of the surface structure of metals

1. The bulk metal, also known as the metal substrate, has a structure that depends on the composition and processing history of the metal.
2. Above this bulk metal, there is a layer that usually has been plastically deformed and work-hardened to a greater extent during the manufacturing process. The depth and properties of the work-hardened layer (the Surface Structure) depend on such factors as the processing method used and how much frictional sliding the surface undergoes.

   The use of sharp tools and the selection of appropriate processing parameters result in surfaces with little or no disturbance. For example, if the surface is produced by machining using a dull and worn tool, or which takes place under poor cutting conditions, or if the surface is ground with a dull grinding wheel, the surface structure layer will be relatively thick. Also, non-uniform surface

deformation or severe temperature gradients during manufacturing operations usually cause residual stresses in the work-hardened layer.

3. Unless the metal is processed and kept in an inert (oxygen-free) environment, or is a noble metal such as gold or platinum, an oxide layer forms over the work-hardened layer.

    a. Iron has an oxide structure with FeO adjacent to the bulk metal, followed by a layer of Fe_3O_4 and then a layer of Fe_2O_3, which is exposed to the environment.
    b. Aluminum has a dense, amorphous (without crystalline structure) layer of Al_2O_3, with a thick, porous hydrated aluminum-oxide layer over it.

4. Under normal environmental conditions, surface oxide layers are generally covered with absorbed layers of gas and moisture. Finally, the outermost surface of the metal may be covered with contaminants such as dirt, dust, grease, lubricant residues, cleaning-compound residues, and pollutants from the environment.

Thus, surfaces have properties that generally are very difficult from those of the substrate. The oxide on a metal surface is generally much harder than the base metal. Consequently, oxides tend to be brittle and abrasive. This surface characteristic has several important effects on friction, wear, and lubrication in materials processing, and on products.

1.5.1 SURFACE INTEGRITY

Surface integrity is the sum of all the elements that describes all the conditions exiting on or at the surface of a work piece. Surface integrity has two aspects. The first is surface topography which describes the roughness, ‘lay’ or texture of this outermost layer of the work piece, i.e., its interface with the environment. The second is surface metallurgy

which describes the nature of the altered layers below the surface with respect to the base of the matrix material. This term assesses the effect of manufacturing processes on the properties of the work piece material. Figure 1.17 depicts a simulated section showing the various layers between the base material and the environment.

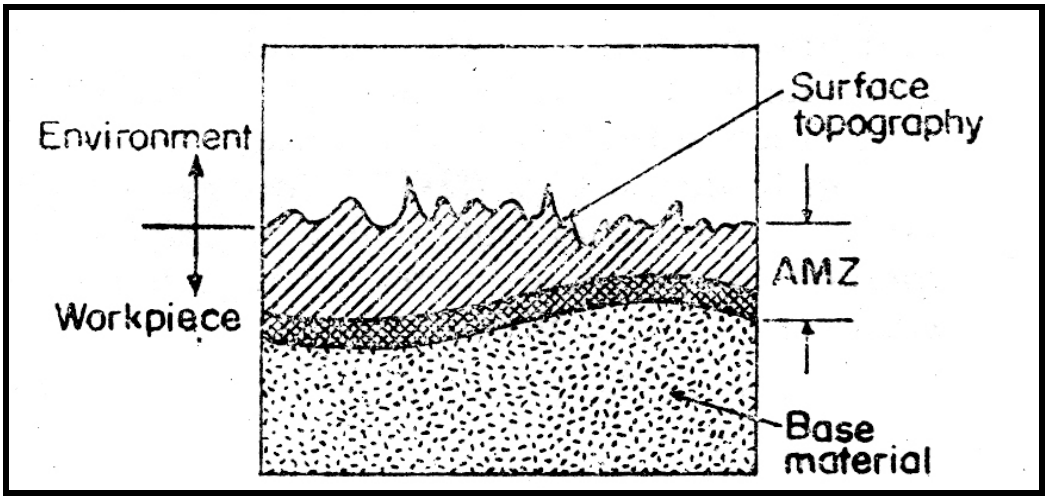

Figure 1.17: Various layers of a surface

Surface integrity describes not only the topological (geometric) features of surfaces and their physical and chemical properties, but their mechanical and metallurgical properties and characteristics as well. Surface integrity is an important consideration in manufacturing operations because it influences properties, such as fatigue strength, resistance to corrosion, and service life.

1.5.2 SURFACE TOPOGRAPHY

Outermost layers of all machined surfaces display a great number of both macro-geometrical and micro-geometrical deviations from the ideal geometrical surface. Surface roughness refers to deviation from the nominal surface of the third up to sixth order. Order of deviation is defined in international standards. First and second-order deviations refer to form, i.e. flatness, circularity, etc. and to waviness, respectively, and are due to machine tool errors, deformation of the work piece, erroneous setups and clamping, vibration and work piece material inhomogenities. Third and fourth-order deviations refer to periodic grooves, and to cracks and dilapidations, which are connected to the shape

and condition of the cutting edges, chip formation and process kinematics. Fifth and sixth-order deviations refer to work piece material structure, which is connected to physical-chemical mechanisms acting on a grain and lattice scale (slip, diffusion, oxidation, residual stress, etc.). Different order deviations are superimposed and form the surface roughness profile (Figure 1.18).

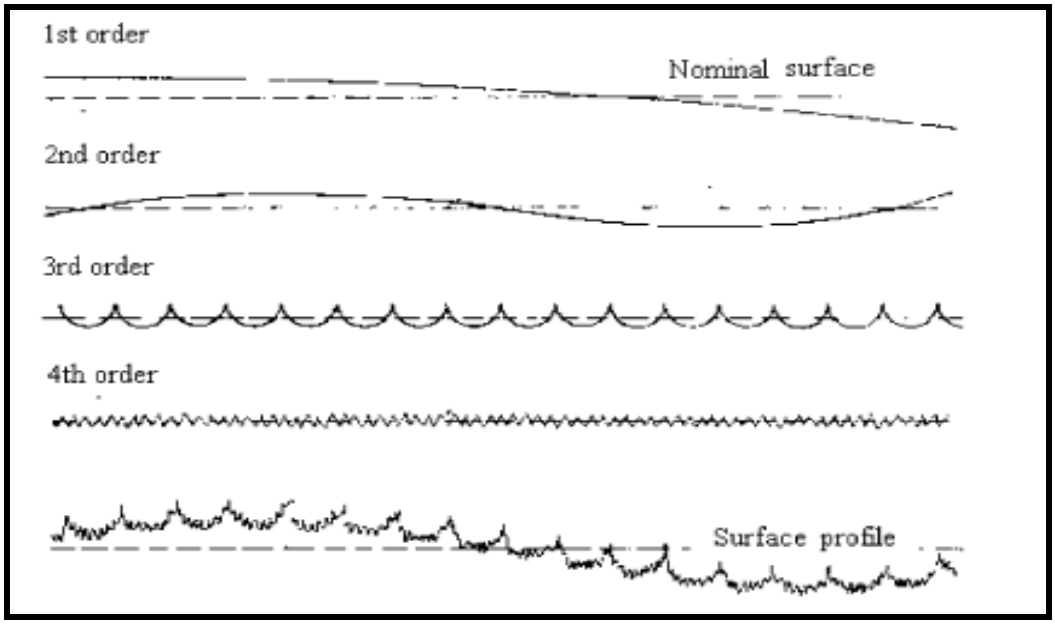

Figure 1.18: Surface form deviations

The principal elements of surfaces are discussed below:

a. **Surface:** The surface of an object is the boundary which separates that object from another substance. Its shape and extent are usually defined by a drawing or descriptive specifications.
b. **Profile:** It is the contour of any specified section through a surface.
c. **Roughness:** It is defined as closely spaced, irregular deviations on a scale smaller than that of waviness. Roughness may be superimposed on waviness. Roughness is expressed in terms of its height, its width, and its distance on the surface along which it is measured.
d. **Waviness:** It is a recurrent deviation from a flat surface, much like waves on the surface of water. It is measured and described in terms of the space between

adjacent crests of the waves (waviness width) and height between the crests and valleys of the waves (waviness height). Waviness can be caused by,

(i) Deflections of tools, dies, or the work piece,

(ii) Forces or temperature sufficient to cause warping,

(iii) Uneven lubrication,

(iv) Vibration, or

(v) Any periodic mechanical or thermal variations in the system during manufacturing operations.

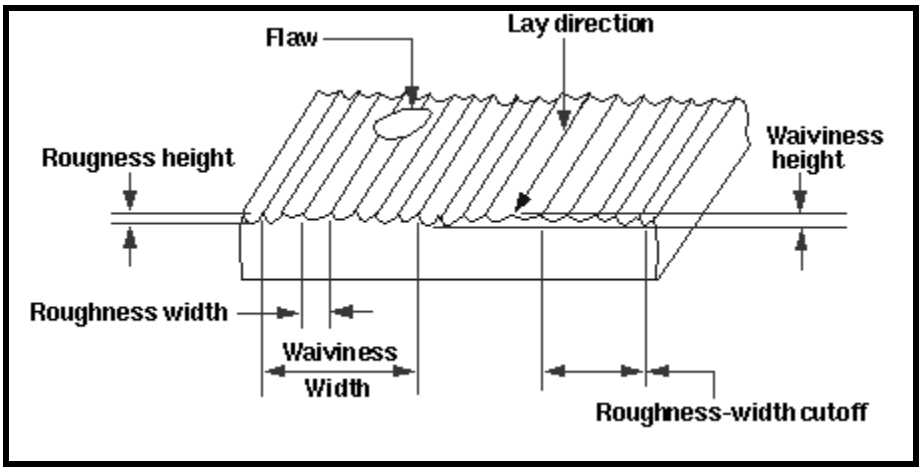

Figure 1.19: Surface characteristics (Courtesy, ANSI B46.1 - 1962)

e. **Flaws:** Flaws, or defects, are random irregularities, such as scratches, cracks, holes, depressions, seams, tears, or inclusions as shown in Figure 1.19.

f. **Lay:** Lay, or directionality, is the direction of the predominant surface pattern and is usually visible to the naked eye. Lay direction has been shown in Figure 1.19.

1.5.3 SURFACE FINISH IN MACHINING

The resultant roughness produced by a machining process can be thought of as the combination of two independent quantities:

a. Ideal roughness, and

b. Natural roughness.

a. Ideal roughness:

Ideal surface roughness is a function of feed and geometry of the tool. It represents the best possible finish which can be obtained for a given tool shape and feed. It can be achieved only if the built-up-edge, chatter and inaccuracies in the machine tool movements are eliminated completely. For a sharp tool without nose radius, the maximum height of unevenness is given by:

$$R_{\max} = \frac{f}{\cot\phi + \cot\beta}$$

Here f is feed rate, ϕ is major cutting edge angle and β is the minor cutting edge angle.

The surface roughness value is given by, $R_a = R_{max}/4$

Idealized model of surface roughness has been clearly shown in Figure 1.20.

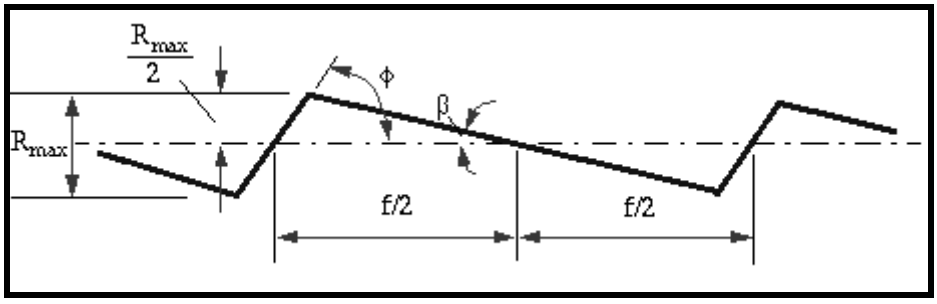

Figure 1.20: Idealized model of surface roughness

Practical cutting tools are usually provided with a rounded corner, and figure below shows the surface produced by such a tool under ideal conditions. It can be shown that the roughness value is closely related to the feed and corner radius by the following expression:

$$R_a = \frac{0.0321 f^2}{r}$$, where r is the corner radius.

b. Natural roughness:

In practice, it is not usually possible to achieve conditions such as those described above, and normally the natural surface roughness forms a large proportion of the actual roughness. One of the main factors contributing to natural roughness is the occurrence of a built-up edge and vibration of the machine tool. Thus, larger the built up edge, the

rougher would be the surface produced, and factors tending to reduce chip-tool friction and to eliminate or reduce the built-up edge would give improved surface finish.

1.5.4 FACTORS AFFECTING THE SURFACE FINISH

Whenever two machined surfaces come in contact with one another the quality of the mating parts plays an important role in the performance and wear of the mating parts. The height, shape, arrangement and direction of these surface irregularities on the work piece depend upon a number of factors such as:

A) The machining variables which include
   a) Cutting speed
   b) Feed, and
   c) Depth of cut.

B) The tool geometry

Some geometric factors which affect achieved surface finish include:

   a) Nose radius
   b) Rake angle
   c) Side cutting edge angle, and
   d) Cutting edge.

C) Work piece and tool material combination and their mechanical properties

D) Quality and type of the machine tool used,

E) Auxiliary tooling, and lubricant used, and

F) Vibrations between the work piece, machine tool and cutting tool.

1.5.5 ROUGNESS PARAMETERS

Each of the roughness parameters is calculated using a formula for describing the surface. There are many different roughness parameters in use, but R_a is the most common. Other common parameters include R_z, R_q, and R_{sk}. Some parameters are used only in certain

industries or within certain countries. For example, the R_k family of parameters is used mainly for cylinder bore linings.

Since these parameters reduce all of the information in a profile to a single number, great care must be taken in applying and interpreting them. Small changes in how the raw profile data is filtered, how the mean line is calculated, and the physics of the measurement can greatly affect the calculated parameter.

By convention every 2D roughness parameter is a capital R followed by additional characters in the subscript. The subscript identifies the formula that was used, and the R means that the formula was applied to a 2D roughness profile. Different capital letters imply that the formula was applied to a different profile. For example, R_a is the arithmetic average of the roughness profile.
Each of the formulas listed in the Table 2 assumes that the roughness profile has been filtered from the raw profile data and the mean line has been calculated. The roughness profile contains n ordered, equally spaced points along the trace, and y_i is the vertical distance from the mean line to the i^{th} data point. Height is assumed to be positive in the up direction, away from the bulk material.

1.5.6 AMPLITUDE PARAMETERS

Amplitude parameters characterize the surface based on the vertical deviations of the roughness profile from the mean line. Many of them are closely related to the parameters found in statistics for characterizing population samples. For example, R_a is the arithmetic average of the absolute values.

The amplitude parameters are by far the most common surface roughness parameters found in the United States on mechanical engineering drawings and in technical literature. Part of the reason for their popularity is that they are straightforward to calculate using a digital computer.

Table 1.2: Various surface roughness parameters and their formulae

Parameter	Description	Formula
R_a, R_{aa}, R_{yni}	Arithmetic average of absolute values	$R_a = \frac{1}{n}\sum_{i=1}^{n}\lvert y_i \rvert$
R_q, R_{RMS}	Root mean squared	$R_q = \sqrt{\frac{1}{n}\sum_{i=1}^{n} y_i^{\,2}}$
R_v	Maximum valley depth	$R_v = \min_i y_i$
R_p	Maximum peak height	$R_p = \max_i y_i$
R_t	Maximum Height of the Profile	$R_t = R_p - R_v$
R_{sk}	Skew ness	$R_{sk} = \frac{1}{nR_q^{\,3}}\sum_{i=1}^{n} y_i^{\,3}$
R_{ku}	Kurtosis	$R_{ku} = \frac{1}{nR_q^{\,4}}\sum_{i=1}^{n} y_i^{\,4}$
R_{zDIN}, R_{tm}	average distance between the highest peak and lowest valley in each sampling length, ASME Y14.36M - 1996 Surface Texture Symbols	$R_{zDIN} = \frac{1}{s}\sum_{i=1}^{s} R_{ti}$, where s is the number of sampling lengths, and R_{ti} is R_t for the i^{th} sampling length.
R_{zJIS}	Japanese Industrial Standard for R_z, based on the five highest peaks and lowest valleys over the entire sampling length.	$R_{zJIS} = \frac{1}{5}\sum_{i=1}^{5} R_{pi} - R_{vi}$, where R_{pi} & R_{vi} are the i^{th} highest peak, and lowest valley respectively.

1.5.7 MEASUREMENT OF SURFACE ROUGHNESS

Inspection and assessment of surface roughness of machined work pieces can be carried out by means of different measurement techniques. These methods can be ranked into the following classes:

1. *Direct measurement methods*
2. *Comparison based techniques*
3. *Non contact methods*
4. *On-process measurement*

1. Direct measurement methods

Direct methods assess surface finish by means of stylus type devices. Measurements are obtained using a stylus drawn along the surface to be measured. The stylus motion perpendicular to the surface is registered. This registered profile is then used to calculate the roughness parameters. This method requires interruption of the machine process, and the sharp diamond stylus can make micro-scratches on surfaces.

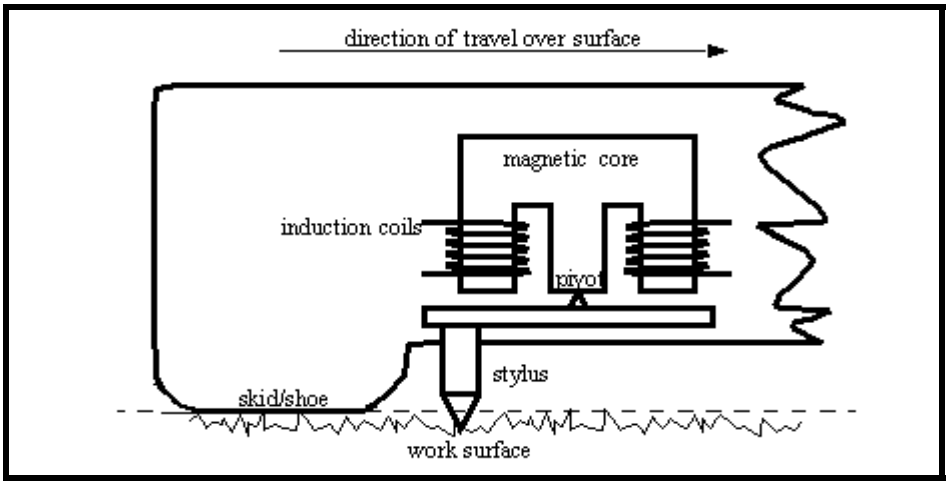

Figure 1.21: Schematic diagram of surface roughness measurement technique by stylus equipment

Stylus equipment

- One example of this is the Brown and Sharpe Surfcom unit.

- Basically, this technique uses a stylus that tracks small changes in surface height, and a skid that follows large changes in surface height. The use of the two together reduces the effects of non-flat surfaces on the surface roughness measurement. The relative motion between the skid and the stylus is measured with a magnetic circuit and induction coils. Schematic diagram of surface roughness measurement technique by stylus equipment has been shown in Figure 1.21.
- The actual apparatus uses the apparatus hooked to other instrumentation. The induction coils drive amplifiers, and other signal conditioning hardware. The then amplified signal is used to drive a recorder that shows stylus position, and a digital readout that displays the CLA/R_a value.

- The paper chart that is recorded is magnified in height by 100000: 1, and in length by 82: 1 to make the scale suitable to the human eye.

- The datum that the stylus position should be compared to can be one of three,
  a. Skid - can be used for regular frequency roughness (Figure 1.22)
  b. Shoe - can be used for irregular frequency roughness (Figure 1.23)
  c. Independent - can use an optical flat (Figure 1.24)

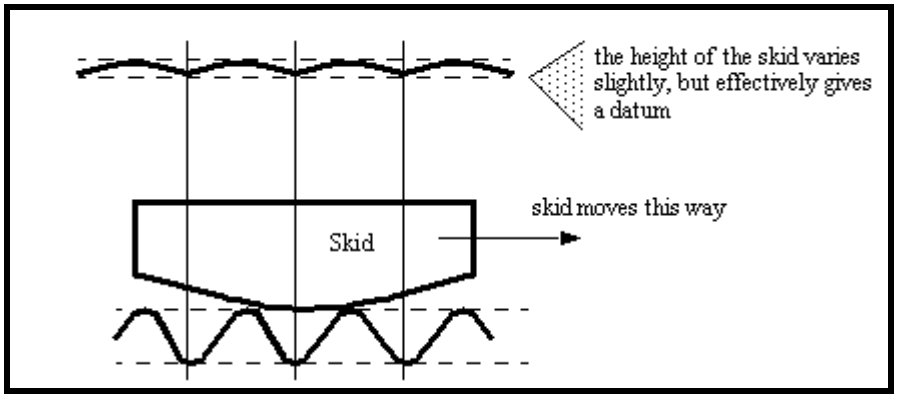

Figure 1.22: Skid – used for regular frequencies

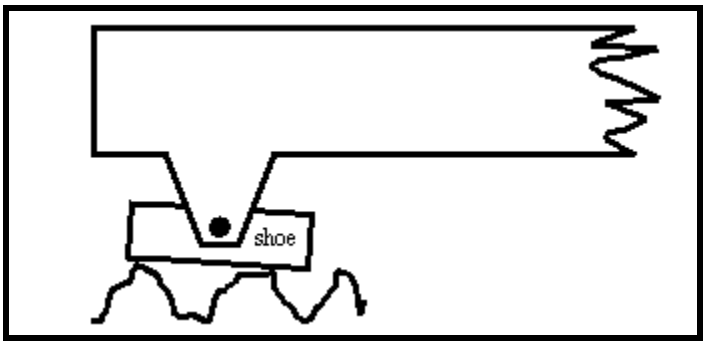

Figure 1.23: Flat shoe – used for surfaces with irregular frequencies

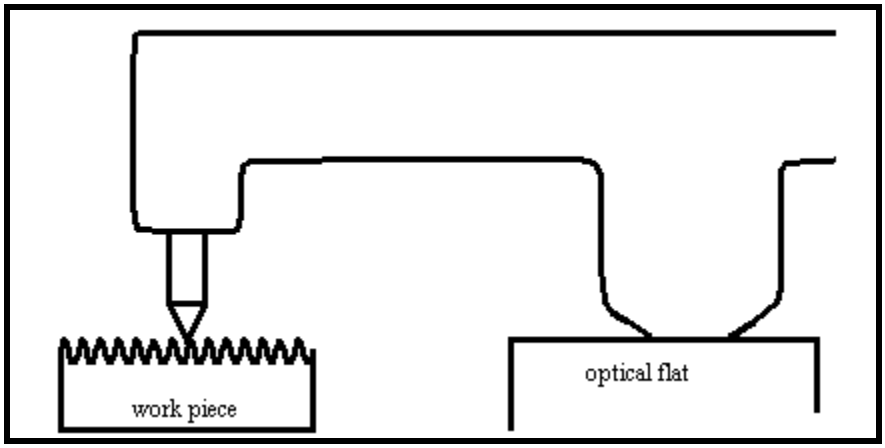

Figure 1.24: Independent datum

2. Comparison based techniques

Comparison techniques use specimens of surface roughness produced by the same process, material and machining parameters as the surface to be compared. Visual and tactile sensors are used to compare a specimen with a surface of known surface finish. Because of the subjective judgment involved, this method is useful for surface roughness R_q >1.6 micron.

3. Non contact methods

There have been some works done to attempt to measure surface roughness using non contact technique. Here is an electronic speckle correlation method given as an example. When coherent light illuminates a rough surface, the diffracted waves from each point of the surface mutually interfere to form a pattern which appears as a grain pattern of bright and dark regions. The spatial statistical properties of this speckle image can be related to

the surface characteristics. The degree of correlation of two speckle patterns produced from the same surface by two different illumination beams can be used as a roughness parameter.

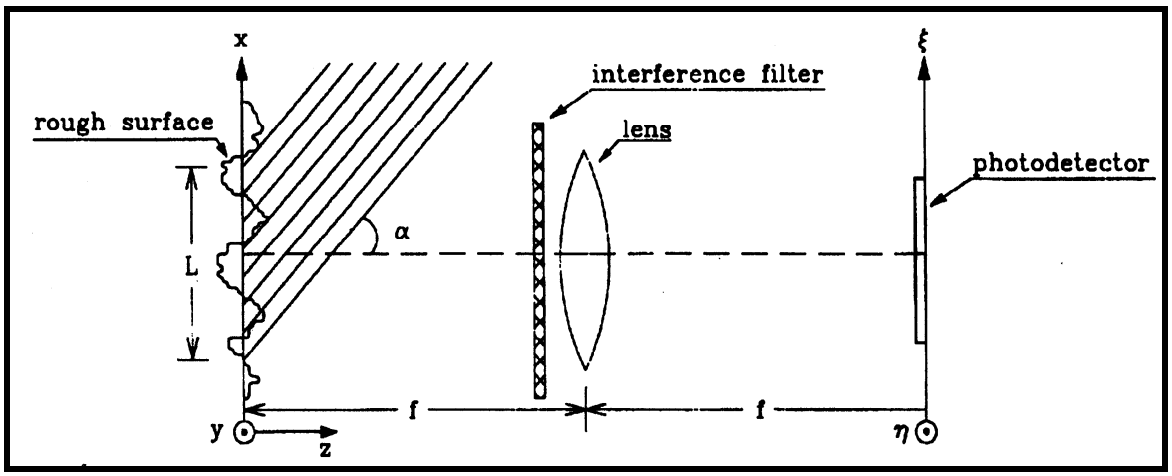

Figure 1.25: Surface roughness measurement principle by non-contact method

The Figure 1.25 shows the measurement principle. A rough surface is illuminated by a monochromatic plane wave with an angle of incidence with respect to the normal to the surface; multi-scattering and shadowing effects are neglected. The photo-sensor of a CCD camera placed in the focal plane of a Fourier lens is used for recording speckle patterns. Assuming Cartesian coordinates x,y,z, a rough surface can be represented by its ordinates Z(x,y) with respect to an arbitrary datum plane having transverse coordinates (x,y). Then the rms value of surface roughness can be defined and calculated.

4. On-process measurement

Many methods have been used to measure surface roughness in process. For example:

a. Machine vision: In this technique, a light source is used to illuminate the surface with a digital system to viewing the surface and the data being sent to a computer for analysis. The digitized data is then used with a correlation chart to get actual roughness values.

b. Inductance method: An inductance pickup is used to measure the distance between the surface and the pickup. This measurement gives a parametric value that

may be used to give a comparative roughness. However, this method is limited to measuring magnetic materials.

c. Ultrasound: A spherically focused ultrasonic sensor is positioned with a non normal incidence angle above the surface. The sensor sends out an ultrasonic pulse to the personal computer for analysis and calculation of roughness parameters.

1.5.8 FACTORS INFLUENCING SURFACE ROUGHNESS IN TURNING

Generally, it is found that the factors influencing surface roughness in turning are:

(i) Depth of cut:

Increasing the depth of cut increases the cutting resistance and the amplitude of vibrations. As a result, cutting temperature also rises. Therefore, it is expected that surface quality will deteriorate.

(ii) Feed:

Experiments show that as feed rate increases surface roughness also increases due to the increase in cutting force and vibration.

(iii) Cutting speed:

It is found that an increase of cutting speed generally improves surface quality.

(iv)Engagement of the cutting tool:

This factor acts in the same way as the depth of cut.

(v) Cutting tool wears:

The irregularities of the cutting edge due to wear are reproduced on the machined surface. Apart from that, as tool wear increases, other dynamic phenomena such as excessive vibrations will occur, thus further deteriorating surface quality.

(vi) Use of cutting fluid:

The cutting fluid is generally advantageous in regard to surface roughness because it affects the cutting process in three different ways. Firstly, it absorbs the heat that is generated during cutting by cooling mainly the tool point and the work surface. In addition to this, the cutting fluid is able to reduce the friction between the rake face and the chip as well as between the flank and the machined surface. Lastly, the washing action of the cutting fluid is considerable, as it consists in removing chip fragments and wear particles. Therefore, the quality of a surface machined with the presence of cutting fluid is expected to be better than that obtained from dry cutting.

(vii) Three components of the cutting force:

It should be noted that force values can not be set a priori, but are related to other factors of the experiment as well as to factors possibly not included in the experiment, i.e. force is not an input factor and is used as an indicator of the dynamic characteristics of the work piece—cutting tool—machine system.

Finally, the set of parameters including the above mentioned parameters that are thought to influence surface roughness, have been investigated from the various researchers.

1.6 QUALITY AND PRODUCTIVITY

- Importance of productivity:
  - Keeps costs down to improve profits and/or reduce prices.
  - Enables firms to spend more on improving customer service and supplementary services.
- Importance of quality:
  - Increase repeat purchases from loyal customers.
  - Enables a firm to differentiate its offerings.

For years, quality and productivity have been viewed as two important indexes of company performance, especially in manufacturing industries. However, they are always

emphasized separately. The main reason that quality and productivity are not emphasized simultaneously is that the objectives of quality management and productivity management are traditionally viewed as contradictory and indicates that quality and productivity should have a positive relationship.

Managing quality effectively has been a key determinant in an organizations' pursuit of lower total costs and increased customer satisfaction. In earlier days, quality challenges were pre-dominantly specification or process led and linked to equipment being unable to produce components and products of quality desired by customers to a desired specification in a reliable fashion. This was largely an enterprise challenge and was tackled as such. Today's challenges are very different. The quality of a product today depends not only on the activities carried out on it within the enterprise but also at every stage in the value chain.

Every manufacturing organization is concerned with the quality of its product. While it is important the quantity requirements be satisfied and production schedule met, it is equally important that the finished product meet established specifications. It is because customer's satisfaction is derived from quality products and services. Stiff competition in the national and international level and customer's awareness require production of quality goods and services for survival and growth of the company. Quality and productivity are more likely to bring prosperity into the country and improve quality of work life.
However, the management looks to achieve customer satisfaction by running its business at the desired economic level. Both these can be attained by prosperity integrity quality development, quality maintenance and quality improvement of the products.

Productivity is a measure of output resulting from a given input.
Productivity = (Output) / (Input).

Productivity may be designated in many ways such as output per workers, direct labor or group of workers, or unit of material or unit of energy or Rupee of capital investment etc.

One must keep in mind that productivity is influenced by many factors such as worker skill, motivation and effort, job methods used, quality of workmanship, employee innovation, the machines used and effectiveness of management. Productivity is the backbone of economic progress of any nation. Higher productivity leads to higher standard of living. Higher productivity results if more output can be got from same input or same output can be got from less input or more increase in output with correspondingly lesser increase in input.

Higher productivity results in reduction of costs as well as increased sales potential, more responsive customer service, increased cash flow and profits. Greater success in existing business can lead to expansion of operations and increase in number of jobs. If wage increases without accompanying productivity increase, then it will lead to increased product cost and contribute to inflation.

Is has been established that an increase in productivity can be caused by five different relationships of input and output:

• Output and input increases, but the increase in input is proportionally less than increase in output;

• Output increases while input stays the same;

• Output increases while input is reduced;

• Output stays the same while input decreases;

• Output decreases while input decreases even more.

1.7 REVIEW OF PAST RESEARCH

Zhou et al. (1995) investigated on tool life criteria in raw turning. A new tool-life criterion depending on a pattern-recognition technique was proposed and neural network and wavelet techniques were used to realize the new criterion. The experimental results showed that this criterion was applicable to tool condition monitoring in a wide range of cutting conditions.

Lin et al. (2001) adopted an abdicative network to construct a prediction model for surface roughness and cutting force. Once the process parameters: cutting speed, feed rate

and depth of cut were given; the surface roughness and cutting force could be predicted by this network. Regression analysis was also adopted as second prediction model for surface roughness and cutting force. Comparison was made on the results of both models indicating that adductive network was found more accurate than that by regression analysis.

Feng and Wang (2002) investigated for the prediction of surface roughness in finish turning operation by developing an empirical model through considering working parameters: work piece hardness (material), feed, cutting tool point angle, depth of cut, spindle speed, and cutting time. Data mining techniques, nonlinear regression analysis with logarithmic data transformation were employed for developing the empirical model to predict the surface roughness.

Suresh et al. (2002) focused on machining mild steel by TiN-coated tungsten carbide (CNMG) cutting tools for developing a surface roughness prediction model by using Response Surface Methodology (RSM). Genetic Algorithms (GA) used to optimize the objective function and compared with RSM results. It was observed that GA program provided minimum and maximum values of surface roughness and their respective optimal machining conditions.

Lee and Chen (2003) highlighted on artificial neural networks (OSRR-ANN) using a sensing technique to monitor the effect of vibration produced by the motions of the cutting tool and work piece during the cutting process developed an on-line surface recognition system. The authors employed tri-axial accelerometer for determining the direction of vibration that significantly affected surface roughness then analyzed by using a statistical method and compared prediction accuracy of both the ANN and SMR.

Choudhury and Bartarya (2003) focused on design of experiments and the neural network for prediction of tool wear. The input parameters were cutting speed, feed and depth of cut; flank wear, surface finish and cutting zone temperature were selected as outputs. Empirical relation between different responses and input variables and also through neural network (NN) program helped in predictions for all the three response variables and compared which method was best for the prediction.

Chien and Tsai (2003) developed a model for the prediction of tool flank wear followed by an optimization model for the determination of optimal cutting conditions in

machining 17-4PH stainless steel. The back-propagation neural network (BPN) was used to construct the predictive model. The genetic algorithm (GA) was used for model optimization.

Kirby et al. (2004) developed the prediction model for surface roughness in turning operation. The regression model was developed by a single cutting parameter and vibrations along three axes were chosen for in-process surface roughness prediction system. By using multiple regression and Analysis of Variance (ANOVA) a strong linear relationship among the parameters (feed rate and vibration measured in three axes) and the response (surface roughness) was found. The authors demonstrated that spindle speed and depth of cut might not necessarily have to be fixed for an effective surface roughness prediction model.

Őzel and Karpat (2005) studied for prediction of surface roughness and tool flank wear by utilizing the neural network model in comparison with regression model. The data set from measured surface roughness and tool flank wear were employed to train the neural network models. Predictive neural network models were found to be capable of better predictions for surface roughness and tool flank wear within the range in between they were trained.

Luo et al. (2005) carried out theoretical and experimental studies to investigate the intrinsic relationship between tool flank wear and operational conditions in metal cutting processes using carbide cutting inserts. The authors developed the model to predict tool flank wear land width which combined cutting mechanics simulation and an empirical model. The study revealed that cutting speed had more dramatic effect on tool life than feed rate.

Kohli and Dixit (2005) proposed a neural-network-based methodology with the acceleration of the radial vibration of the tool holder as feedback. For the surface roughness prediction in turning process the back-propagation algorithm was used for training the network model. The methodology was validated for dry and wet turning of steel using high speed steel and carbide tool and observed that the proposed methodology was able to make accurate prediction of surface roughness by utilizing small sized training and testing datasets.

Pal and Chakraborty (2005) studied on development of a back propagation neural network model for prediction of surface roughness in turning operation and used mild steel work-pieces with high speed steel as the cutting tool for performing a large number of experiments. The authors used speed, feed, depth of cut and the cutting forces as inputs to the neural network model for prediction of the surface roughness. The work resulted that predicted surface roughness was very close to the experimental value.

Őzel and Karpat (2005) developed models based on feed forward neural networks in predicting accurately both surface roughness and tool flank wear in finish dry hard turning.

Sing and Kumar (2006) studied on optimization of feed force through setting of optimal value of process parameters namely speed, feed and depth of cut in turning of EN24 steel with TiC coated tungsten carbide inserts. The authors used Taguchi's parameter design approach and concluded that the effect of depth of cut and feed in variation of feed force were affected more as compare to speed.

Ahmed (2006) developed the methodology required for obtaining optimal process parameters for prediction of surface roughness in Al turning. For development of empirical model nonlinear regression analysis with logarithmic data transformation was applied. The developed model showed small errors and satisfactory results. The study concluded that low feed rate was good to produce reduced surface roughness and also the high speed could produce high surface quality within the experimental domain.

Abburi and Dixit (2006) developed a knowledge-based system for the prediction of surface roughness in turning process. Fuzzy set theory and neural networks were utilized for this purpose. The authors developed rule for predicting the surface roughness for given process variables as well as for the prediction of process variables for a given surface roughness.

Zhong et al. (2006) predicted the surface roughness of turned surfaces using networks with seven inputs namely tool insert grade, work piece material, tool nose radius, rake angle, depth of cut, spindle rate, and feed rate.

Kumanan et al. (2006) proposed the methodology for prediction of machining forces using multi-layered perceptron trained by genetic algorithm (GA). The data obtained from experimental results of a turning process were explored to train the proposed

artificial neural networks (ANNs) with three inputs to get machining forces as output. The optimal ANN weights were obtained using GA search. This function-replacing hybrid made of GA and ANN was found computationally efficient as well as accurate to predict the machining forces for the input machining conditions.

Mahmoud and Abdelkarim (2006) studied on turning operation using High-Speed Steel (HSS) cutting tool with 45^0 approach angle. This tool showed that it could perform cutting operation at higher speed and longer tool life than traditional tool with 90^0 approach angle. The study finally determined optimal cutting speed for high production rate and minimum cost, tool like, production time and operation costs.

Doniavi et al. (2007) used response surface methodology (RSM) in order to develop empirical model for the prediction of surface roughness by deciding the optimum cutting condition in turning. The authors showed that the feed rate influenced surface roughness remarkably. With increase in feed rate surface roughness was found to be increased. With increase in cutting speed the surface roughness decreased. The analysis of variance was applied which showed that the influence of feed and speed were more in surface roughness than depth of cut.

Kassab and Khoshnaw (2007) examined the correlation between surface roughness and cutting tool vibration for turning operation. The process parameters were cutting speed, depth of cut, feed rate and tool overhanging. The experiments were carried out on lathe using dry turning (no cutting fluid) operation of medium carbon steel with different level of aforesaid process parameters. Dry turning was helpful for good correlation between surface roughness and cutting tool vibration because of clean environment. The authors developed good correlation between the cutting tool vibration and surface roughness for controlling the surface finish of the work pieces during mass production. The study concluded that the surface roughness of work piece was observed to be affected more by cutting tool acceleration; acceleration increased with overhang of cutting tool. Surface roughness was found to be increased with increase in feed rate.

Al-Ahmari (2007) developed empirical models for tool life, surface roughness and cutting force for turning operation. The process parameters used in the study were speed, feed, depth of cut and nose radius to develop the machinability model. The methods used

for developing aforesaid models were Response Surface Methodology (RSM) and neural networks (NN).

Thamizhmanii et al. (2007) applied Taguchi method for finding out the optimal value of surface roughness under optimum cutting condition in turning SCM 440 alloy steel. The experiment was designed by using Taguchi method and experiments were conducted and results thereof were analyzed with the help of ANOVA (Analysis of Variance) method. The causes of poor surface finish as detected were machine tool vibrations, tool chattering whose effects were ignored for analyses. The authors concluded that the results obtained by this method would be useful to other researches for similar type of study on tool vibrations, cutting forces etc. The work concluded that depth of cut was the only significant factor which contributed to the surface roughness.

Natarajan et al. (2007) presented the on-line tool wear monitoring technique in turning operation. Spindle speed, feed, depth of cut, cutting force, spindle-motor power and temperature were selected as the input parameters for the monitoring technique. For finding out the extent of tool wear; two methods of Hidden Markov Model (HMM) such as the Bar-graph Method and the Multiple Modeling Methods were used. A decision fusion centre algorithm (DFCA) was used for increasing the reliability of this output which combined the outputs of the individual methods to make a global decision about the wear status of the tool. Finally, all the proposed methods were combined in a DFCA to determine the wear status of the tool during the turning operations.

Ozel et al. (2007) carried out finish turning of AISI D2 steels (60 HRC) using ceramic wiper (multi-radii) design inserts for surface finish and tool flank wear investigation. For prediction of surface roughness and tool flank wear multiple linear regression models and neural network models were developed. Neural network based predictions of surface roughness and tool flank wear were carried out, compared with a non-training experimental data and the results thereof showed that the proposed neural network models were efficient to predict tool wear and surface roughness patterns for a range of cutting conditions. The study concluded that best tool life was obtained in lowest feed rate and lowest cutting speed combination.

Wang and Lan (2008) used Orthogonal Array of Taguchi method coupled with grey relational analysis considering four parameters viz. speed, cutting depth, feed rate, tool

nose run off etc. for optimizing three responses: surface roughness, tool wear and material removal rate in precision turning on an ECOCA-3807 CNC Lathe. The MINITAB software was explored to analyze the mean effect of Signal-to-Noise (S/N) ratio to achieve the multi-objective features. This study not only proposed an optimization approaches using Orthogonal Array and grey relational analysis but also contributed a satisfactory technique for improving the multiple machining performances in precision CNC turning with profound insight.

Srikanth and Kamala (2008) evaluated optimal values of cutting parameters by using a Real Coded Genetic Algorithm (RCGA) and explained various issues of RCGA and its advantages over the existing approach of Binary Coded Genetic Algorithm (BCGA). They concluded that RCGA was reliable and accurate for solving the cutting parameter optimization and construct optimization problem with multiple decision variables. These decision variables were cutting speed, feed, depth of cut and nose radius. The authors highlighted that the faster solution can be obtain with RCGA with relatively high rate of success, with selected machining conditions thereby providing overall improvement of the product quality by reduction in production cost, reduction in production time, flexibility in machining parameter selection.

Sahoo et al. (2008) studied for optimization of machining parameters combinations emphasizing on fractal characteristics of surface profile generated in CNC turning operation. The authors used L_{27} Taguchi Orthogonal Array design with machining parameters: speed, feed and depth of cut on three different work piece materials viz. aluminum, mild steel and brass. It was concluded that feed rate was more significant influencing surface finish in all three materials. It was observed that in case of mild steel and aluminum feed showed some influences while in case of brass depth of cut was noticed to impose some influences on surface finish. The factorial interaction was responsible for controlling the fractal dimensions of surface profile produced in CNC turning.

Reddy et al. (2008) adopted multiple regression model and artificial neural network to deal with surface roughness prediction model for machining of aluminium alloys by CNC turning. For judging the efficiency and ability of the model in surface roughness prediction the authors used the percentage deviation and average percentage deviation.

The study of experimental results showed that the artificial neural network was efficient as compared to multiple regression models for the prediction of surface roughness.

Wannas (2008) carried out experiments for hard turning of graphitic cast iron for the prediction of status of tool wear by using radial basis function neural network (RBFNN) model. The RBFNN had three inputs: speed, feed and depth of cut and one output: state variable node. The error was less as obtained from neural network model than the regression model.

Lan et al. (2008) considered four cutting parameters: speed, feed, depth of cut, and nose runoff varied in three levels for predicting the surface roughness of CNC turned product.

Thamma (2008) constructed the regression model to find out the optimal combination of process parameters in turning operation for Aluminium 6061 work pieces. The study highlighted that cutting speed, feed rate, and nose radius had a major impact on surface roughness. Smoother surfaces could be produced when machined with a higher cutting speed, smaller feed rate, and smaller nose radius.

Fnides et al. (2008) studied on machining of slide-lathing grade X38CrMoV5-1 steel treated at 50 HRC by a mixed ceramic tool (insert CC650) to reveal the influences of cutting parameters: feed rate, cutting speed, depth of cut and flank wear on cutting forces as well as on surface roughness. The authors found that tangential cutting force was very sensitive to the variation of cutting depth. It was observed that surface roughness was very sensitive to the variation of feed rate and that flank wear had a great influence on the evolution of cutting force components and on the criteria of surface roughness.

Biswas et al. (2008) studied that on-line flank wear directly influenced the power consumption, quality of the surface finish, tool life, productivity etc. The authors developed a Neuro-Fuzzy model for prediction of the tool wear. From the orthogonal machining of aluminium with high-speed steel tool for various rake angles, feed and velocity the experimental data were obtained and input along with other machining parameters ratio between cutting force and tangential forces was collected. These were used to predict the tool wear. The final parameters of the model were obtained by tuning the crude values obtained from mountain clustering method by using back-propagation learning algorithm and finally the present Neuro-Fuzzy system which predicted the flank

wear with reasonable accuracy and proved it to be a potent tool in estimating flank wears on-line.

Fu and Hope (2008) established an intelligent tool condition monitoring system by applying a unique fuzzy neural hybrid pattern recognition system. The study concluded that armed with the advanced pattern recognition methodology, the established intelligent tool condition monitoring system had the advantages of being suitable for different machining conditions, robust to noise and tolerant to faults.

Wang et al. (2008) studied on Hybrid Neural Network-based modeling approach integrated with an analytical tool wear model and an artificial neural network that was used to predict CBN tool flank wear in turning of hardened 52100 bearing steel. Experimental results showed that the proposed Hybrid Neural Network excelled the analytical tool wear model approach and the general neural network-based modeling approach.

Shetty et al. (2008) discussed the use of Taguchi and response surface methodologies for minimizing the surface roughness in turning of discontinuously reinforced aluminum composites (DRACs) having aluminum alloy 6061 as the matrix and containing 15 vol. % of silicon carbide particles of mean diameter 25μm under pressured steam jet approach. The measured results were then collected and analyzed with the help of the commercial software package MINITAB15. The experiments were conducted using Taguchi's experimental design technique. The matrix of test conditions included cutting speeds of 45, 73 and 101 m/min, feed rates of 0.11, 0.18 and 0.25 mm/rev and steam pressure 4, 7, 10 bar while the depth of cut was kept constant at 0.5 mm. The effect of cutting parameters on surface roughness was evaluated and the optimum cutting condition for minimizing the surface roughness was also determined finally. A second-order model was established between the cutting parameters and surface roughness using response surface methodology. The experimental results revealed that the most significant machining parameter for surface roughness was steam pressure followed by feed. The predicted values and measured values were fairly close, which indicated that the developed model could be effectively used to predict the surface roughness in the machining of DRACs.

1.7 OBJECTIVE AND SCOPE OF THE PRESENT WORK

Literature depicts that a considerable amount of work has been carried out by previous investigators for modeling, simulation and parametric optimization of surface properties of the product in turning operation. Issues related to tool life, tool wear, cutting forces have been addressed to. Apart from optimizing a single response (process output), multi-objective optimization problems have also been solved using Taguchi method followed by grey relation theory. However, this approach is based on the assumption that quality indices being uncorrelated or independent [Datta et al. (2009)]. But it is felt that, in practice, there may be some correlation among various quality indices (responses) under consideration. To overcome this limitation of grey based Taguchi approach, the present study proposes application of Principal Component Analysis (PCA) to convert correlated responses into uncorrelated quality indices called principal components. Finally based on grey relation theory and utility concept, Taguchi method has been applied to solve this optimization problem. The study demonstrates detailed methodology of the proposed optimization technique which integrates PCA, grey relational analysis and utility based extended Taguchi method; and validates its effectiveness through case studies in which correlated multiple surface roughness characteristics, MRR of a turned product along with depth of flank wear of the cutting tool have been optimized.

CHAPTER 2

CHAPTER 2: EXPERIMENTATION

The scope and objectives of the present work have already been mentioned in the forgoing chapter. Accordingly the present study has been done through the following plan of experiment.

a) Checking and preparing the Centre Lathe ready for performing the machining operation.

b) Cutting MS bars by power saw and performing initial turning operation in Lathe to get desired dimension of the work pieces.

c) Calculating weight of each specimen by the high precision digital balance meter before machining.

d) Performing straight turning operation on specimens in various cutting environments involving various combinations of process control parameters like: spindle speed, feed and depth of cut.

e) Calculating weight of each machined plate again by the digital balance meter.

f) Measuring surface roughness and surface profile with the help of a portable stylus-type profilometer, *Talysurf* (Taylor Hobson, Surtronic 3+, UK)

g) Measuring cutting tool flank wear in tool makers microscope.

2.1 PROCESS VARIABLES AND THEIR LIMITS

The working ranges of the parameters for subsequent design of experiment, based on Taguchi's L_9 Orthogonal Array (OA) design have been selected. In the present experimental study, spindle speed, feed rate and depth of cut have been considered as process variables. The process variables with their units (and notations) are listed in Table 2.1.

Table 2.1: Process variables and their limits

	Process variables		
Values in coded form	Spindle Speed (N) (RPM)	Feed (f) (mm/rev)	Depth of cut (d) (mm)
-1	220	0.044	0.4
0	530	0.088	0.8
+1	860	0.132	1.2

2.1.1 DESIGN OF EXPERIMENT

Experiments have been carried out using Taguchi's L_9 Orthogonal Array (OA) experimental design which consists of 9 combinations of spindle speed, longitudinal feed rate and depth of cut. According to the design catalogue [Peace, G., S., (1993)] prepared by Taguchi, L_9 Orthogonal Array design of experiment has been found suitable in the present work. It considers three process parameters (without interaction) to be varied in three discrete levels. The experimental design has been shown in Table 2.2 (all factors are in coded form). The coded number for variables used in Table 2.1 and 2.2 are obtained from the following transformation equations:

Spindle speed: $$A = \frac{N - N_0}{\Delta N} \quad (1)$$

Feed rate: $$B = \frac{f - f_0}{\Delta f} \quad (2)$$

Depth of cut: $$C = \frac{d - d_0}{\Delta d} \quad (3)$$

Here A, B and C are the coded values of the variables N, f and d respectively; N_0, f_0 and d_0 are the values of spindle speed, feed rate and depth of cut at zero level; $\Delta N, \Delta f$ and Δd are the units or intervals of variation in N, f and d respectively.

Table 2.2: Taguchi's L_9 Orthogonal Array

Sl. No.	Factorial combination		
	(N)	(f)	(d)
1	-1	-1	-1
2	-1	0	0
3	-1	1	1
4	0	-1	0
5	0	0	1
6	0	1	-1
7	1	-1	1
8	1	0	-1
9	1	1	0

2.2 EQUIPMENTS USED

2.2.1 CENTRE LATHE

Machine no in machine shop is -01
Manufactured by - Tussor machine tool India (p) LTD Coimbatore-29' India
Model-180*750
Serial no-700002
Manufacturing date-23/10/2007

Figure 2.1: Experimental setup (lathe)

Table 2.3: Specifications of the lathe

CAPACITY	SP/200	
	mm	inches
center height	200	7 7/8``
center distance	750-1000	30''-40''
swing over bed	400	15 3/8''
swing over gap	560	22''
swing over carriage	375	14 3/4''
swing over cross slide	245	9 5/8''
bed width	250	10``
gap length in front of face plate	120	4 3/4''
HEAD STOCK		
main spindle bore	42	1 5/8''
main spindle nose	DIN 55027-5	cam lock no 5
main spindle morse taper	4	4
9 speed range	60-2000	60-2000
THREAD AND FEED BOX		
44 longitudinal feeds	0,05-0.75	0.0018-0,026''
44 cross feeds	0,025-0,375	0,0005-0,0076''
44 metric threads	0,5-7,5	0,5-0,7
44 withworth thread in T.P.1	60-4	60-4
44 modular threads	0,25-3,75	0,25-3,75
44 pitch diametral thread	120-8	120-8
thread oflead screw	6	4h/1h''
SLIDE AND CARRIAGE		
cross slide travel	245	9 5/8''
tool post slide travel	120	4 3/4''
maximum tool dimensions	20*20	3/4''-3/4''
TAILSTOCK		
tailstock barrel diameter	58	2 9/32''
tailstock barrel travel	200	7 7/8''
tailstock taper	4	4
MOTORS		
main motor power in kW	4	4
pump motor power in kW	0,06	0,06
STEALDIES		
max~min capacity of fixed steady	10-130	3/8''-5''
max~min capacityof traveling steady	Oct-80	3/8''-3'' 3/16''

2.2.2 CUTTING TOOL USED

Tool material-HSS
MIRANDA S-400
STS (5/8''*6'') 15.88*152.80 mm

2.2.3 WORK PIECE USED

AISI 1040 MS bars (of diameter 32mm and length 40mm)

2.2.4 ROUGHNESS MEASUREMENT

Roughness measurement has been done using a portable stylus-type profilometer, *Talysurf* (Taylor Hobson, Surtronic 3+, UK) shown in Figure 2.2. The Talysurf instrument (Surtronic 3+) is a portable, self-contained instrument for the measurement of surface texture. The parameter evaluations are microprocessor based. The measurement results are displayed on an LCD screen and can be output to an optional printer or another computer for further evaluation. The instrument is powered by non-rechargeable alkaline battery (9V). It is equipped with a diamond stylus having a tip radius 5 μm. The measuring stroke always starts from the extreme outward position. At the end of the measurement the pickup returns to the position ready for the next measurement. The selection of cut-off length determines the traverse length. Usually as a default, the traverse length is five times the cut-off length though the magnification factor can be changed. The profilometer has been set to a cut-off length of 0.8 mm, filter 2CR, traverse speed 1 mm/sec and 4 mm traverse length. Roughness measurements, in the transverse direction, on the work pieces have been repeated four times and average of four measurements of surface roughness parameter values has been recorded. The measured profile has been digitized and processed through the dedicated advanced surface finish analysis software *Talyprofile* for evaluation of the roughness parameters. Surface roughness measurement with the help of stylus has been shown in Figure 2.3. Some typical surface roughness and waviness profile curves have been shown in Appendix.

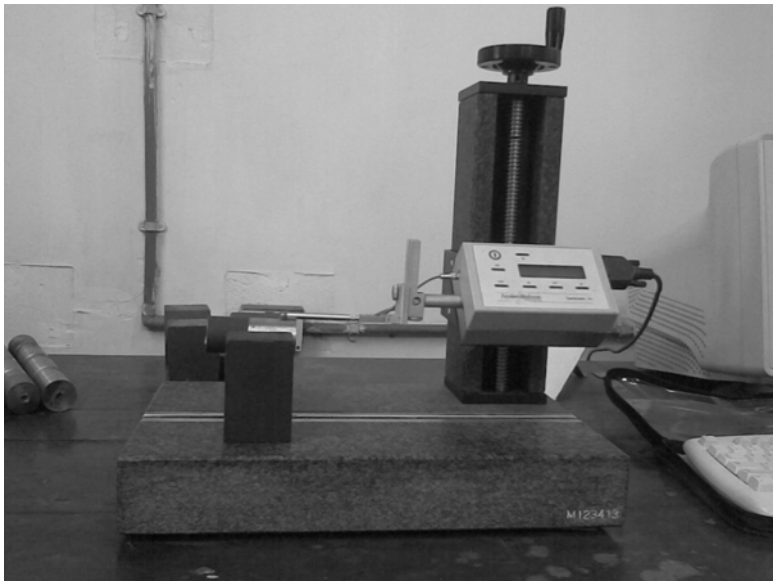

Figure 2.2: Stylus-type profilometer, Talysurf (Taylor Hobson, Surtronic 3+)

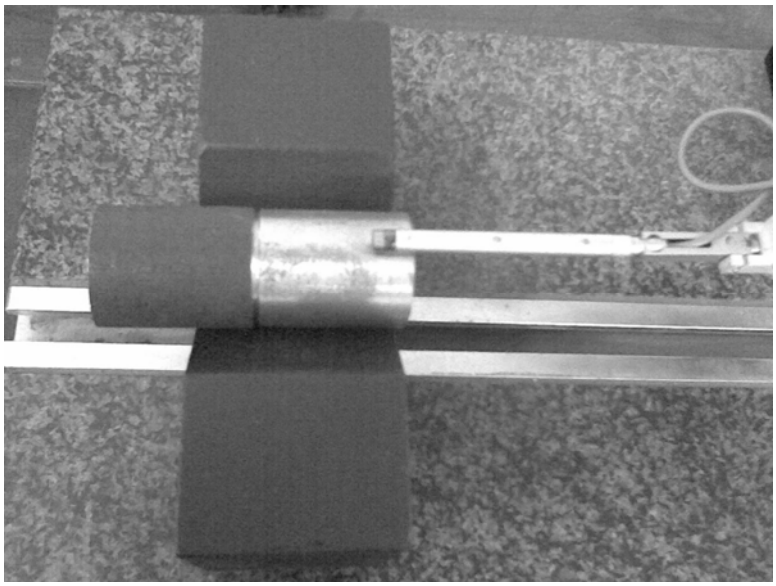

Figure 2.3: Photographic view of stylus during surface roughness measurement

2.2.5 MATERIAL REMOVAL RATE MEASUREMENT

Material removal rate (MRR) has been calculated from the difference of weight of work piece before and after experiment.

$$MRR = \frac{W_i - W_f}{\rho_s t} mm^3 / \min \quad (4)$$

Where, W_i is the initial weight of work piece in g; W_f is the final weight of work piece in g; t is the machining time in minutes; ρ_s is the density of mild steel (7.8 x 10^{-3} g/mm^3).

The weight of the work piece has been measured in a high precision digital balance meter (Model: DHD – 200 Macro single pan DIGITAL reading electrically operated analytical balance made by Dhona Instruments), which can measure up to the accuracy of 10^{-4} g and thus eliminates the possibility of large error while calculating material removal rate (MRR) in straight turning operation.

2.2.6 MEASUREMENT OF CUTTING TOOL FLANK WEAR

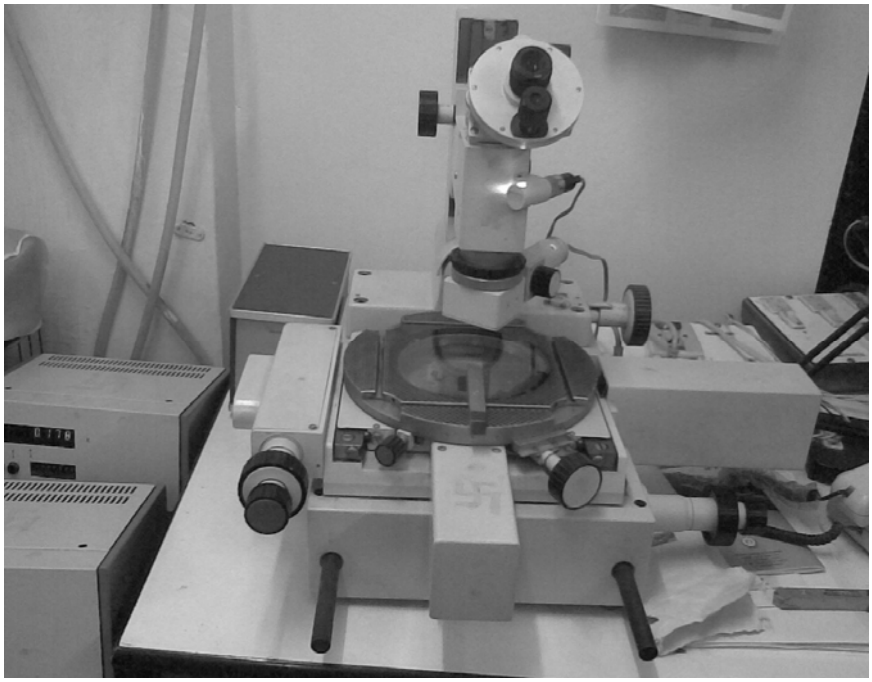

Figure 2.4: Tool maker's microscope

Depth of flank wear has been measured by tool maker's microscope. Specification given below:

1.1	Nr	14832
DDR	Made in the CDR	
1554	Achsenhohe 42.52 mm	

2.3 DATA COLLECTION

MS bars (of diameter 32mm and length 40mm) required for conducting the experiment have been prepared first. Nine numbers of samples of same material and same dimensions have been made. After that, the weight of each samples have been measured accurately with the help of a high precision digital balance meter. Then, using different levels of the process parameters nine specimens have been turned in lathe accordingly. Machining time for each sample has been calculated accordingly.

After machining, weight of each machined parts have been again measured precisely with the help of the digital balance meter. Then surface roughness and surface profile have been measured precisely with the help of a portable stylus-type profilometer, *Talysurf* (Taylor Hobson, Surtronic 3+, UK).

The results of the experiments have been shown in Table 2.4 (a) to (c). Analysis has been made based on those experimental data in the following chapter. Optimization of surface roughness, material removal rate and depth of flank wear of the cutting tool has been made by PCA and Taguchi method coupled with grey relational analysis as well as utility concept. Confirmatory tests have also been conducted finally to validate optimal results.

Table 2.4.a: Depth of flank wear

Sample Number	Depth of flank wear (mm)
1	0.151
2	0.101
3	0.178
4	0.07
5	0.104
6	0.059
7	0.224
8	0.079
9	0.019

Table 2.4.b: Experimental Data Related to Surface Roughness Characteristics

Sl. No.	R_a			R_q			R_{sk}			R_{ku}			R_{sm}		
	Run 1	Run 2	Run 3	Run 1	Run 2	Run 3	Run 1	Run 2	Run 3	Run 1	Run 2	Run 3	Run 1	Run 2	Run 3
1	3.12	3.29	3.05	3.96	4.09	3.73	-0.157	-0.152	0.577	3.60	3.53	4.98	0.115	0.114	0.104
2	4.05	4.76	5.35	5.11	6.05	6.56	0.197	-0.403	-0.245	3.71	3.97	2.72	0.130	0.164	0.190
3	3.84	4.04	3.83	4.71	4.93	4.69	0.0576	0.363	-0.0483	2.76	2.98	3.09	0.124	0.122	0.131
4	6.56	5.61	5.10	7.90	6.67	6.23	0.398	-0.396	0.439	3.01	3.13	2.76	0.201	0.183	0.160
5	3.75	4.24	3.11	4.62	5.22	3.89	0.414	0.143	-0.192	3.16	4.30	4.09	0.138	0.138	0.138
6	3.23	4.15	4.24	3.97	4.93	5.25	0.131	0.283	0.094	2.90	2.68	2.67	0.145	0.151	0.156
7	1.30	1.46	1.43	1.54	1.85	1.77	-0.184	0.811	0.621	2.76	5.36	3.51	0.0784	0.101	0.0898
8	4.05	3.89	3.29	4.85	4.54	3.95	0.18	0.233	0.280	2.51	2.05	2.36	0.129	0.145	0.136
9	3.67	4.10	3.88	4.66	4.87	4.75	-0.184	0.160	0.109	3.92	2.69	3.58	0.110	0.176	0.116

Table 2.4.c: Measurement of Material Removal Rate (MRR)

Sample Number	Weight before turning (kg)	Weight after turning (kg)	Machining time (min)	Material removal rate mm^3/min
1	0.472	0.468	4.1322	124.1
2	0.494	0.48	2.0661	868.7
3	0.656	0.63	1.3774	2420.0
4	0.488	0.476	1.7153	896.9
5	0.482	0.47	0.8576	1793.8
6	0.516	0.506	0.5718	2242.3
7	0.504	0.484	1.0571	2425.6
8	0.49	0.48	0.5285	2425.6
9	0.516	0.502	0.3781	4746.5

CHAPTER 3

CHAPTER 3: DATA ANALYSES AND CONCLUSIONS

3.1 PRINCIPAL COMPONENT ANALYSIS (PCA)

Principal Component Analysis (PCA), [Su and Tong (1997)] is a way of identifying patterns in the correlated data, and expressing the data in such a way so as to highlight their similarities and differences. The main advantage of PCA is that once the patterns in data have been identified, the data can be compressed, i.e. by reducing the number of dimensions, without much loss of information. The methods involved in PCA are discussed below:

1. Getting some data
2. Normalization of data
3. Calculation of covariance matrix.
4. Interpretation of covariance matrix.

   The normalized data have then been utilized to construct a variance-covariance matrix M , which is illustrated as below:

$$M = \begin{bmatrix} N_{1,1} & N_{1,2} & . & . & . & N_{1,u} \\ N_{2,1} & N_{2,2} & . & . & . & N_{2,p} \\ . & . & . & . & . & . \\ . & . & . & . & . & . \\ N_{q,1} & N_{q,2} & . & . & . & N_{q,p} \end{bmatrix} \tag{5}$$

$$\text{where } N_{k,l} = \frac{Cov(Y^*_{i,k}, Y^*_{i,l})}{\sqrt{Var(Y^*_{i,k})Var(Y^*_{i,l})}} \tag{6}$$

In which u stands for the number of quality characteristics and p stands for the number of experimental runs. Then, eigenvectors and Eigenvalues of matrix M can be computed, which are denoted by $\vec{V}_j$ and λ_j respectively.

In PCA the eigenvector $\vec{V}_j$ represents the weighting factor of j number of quality characteristics of the jth principal component. For example, if Q_j represents the jth quality characteristic, the jth principal component ψ_j can be treated as a quality indicator with the required quality characteristic.

$$\psi_j = V_{1j}Q_1 + V_{2j}Q_2 + ... + V_{jj}Q_j = \vec{V}_j.\vec{Q} \quad (7)$$

It is to be noted that every principal component ψ_j represents a certain degree of explanation of the variation of quality characteristics, namely the accountability proportion (AP). When several principal components are accumulated, it increases the accountability proportion of quality characteristics. This is denoted as cumulative accountability proportion (CAP). In the present work, the composite principal component ψ has been defined as the combination of principal components with their individual Eigenvalues. This composite principal component ψ serves as the representative of multi-quality responses, called multi/composite quality indicator.

If a quality characteristic Q_j strongly dominates in the jth principal component, this principal component becomes the major indicator of such a quality characteristic. It should be noted that one quality indicator may often represent all the multi-quality characteristics. Selection of individual principal components (ψ_j), those to be included in the composite quality indicator ψ, depends on their individual accountability proportion.

3.2 GREY RELATIONAL ANALYSIS

In grey relational analysis, experimental data i.e. measured features of quality characteristics of the product are first normalized ranging from zero to one. This process is known as grey relational generation. Next, based on normalized experimental data, grey relational coefficient is calculated to represent the correlation between the desired and actual experimental data. Then overall grey relational grade is determined by averaging the grey relational coefficient corresponding to selected responses. The overall

performance characteristic of the multiple response process depends on the calculated grey relational grade. This approach converts a multiple- response- process optimization problem into a single response optimization situation, with the objective function is overall grey relational grade. The optimal parametric combination is then evaluated by maximizing the overall grey relational grade.

In grey relational generation, the normalized data corresponding to Lower-the-Better (LB) criterion can be expressed as:

$$x_i(k) = \frac{\max y_i(k) - y_i(k)}{\max y_i(k) - \min y_i(k)} \tag{8}$$

For Higher-the-Better (HB) criterion, the normalized data can be expressed as:

$$x_i(k) = \frac{y_i(k) - \min y_i(k)}{\max y_i(k) - \min y_i(k)} \tag{9}$$

where $x_i(k)$ is the value after the grey relational generation, $\min y_i(k)$ is the smallest value of $y_i(k)$ for the *kth* response, and $\max y_i(k)$ is the largest value of $y_i(k)$ for the *kth* response. An ideal sequence is $x_0(k)$ for the responses. The purpose of grey relational grade is to reveal the degrees of relation between the sequences say, $[x_0(k)\ and\ x_i(k),\ i = 1, 2, 3.....,9]$. The grey relational coefficient $\xi_i(k)$ can be calculated as

$$\xi_i(k) = \frac{\Delta_{\min} + \theta \Delta_{\max}}{\Delta_{0i}(k) + \theta \Delta_{\max}} \tag{10}$$

where $\Delta_{0i} = \left\| x_0(k) - x_i(k) \right\|$ = difference of the absolute value $x_0(k)$ and $x_i(k)$; θ is the distinguishing coefficient $0 \le \theta \le 1$; $\Delta_{\min} = \forall j^{\min} \in i \forall k^{\min} \left\| x_0(k) - xj(k) \right\|$ = the smallest value of Δ_{0i}; and $\Delta_{\max} = \forall j^{\max} \in i \forall k^{\max} \left\| x_0(k) - xj(k) \right\|$ = largest value of Δ_{0i}. After

averaging the grey relational coefficients, the grey relational grade γ_i can be computed as:

$$\gamma_i = \frac{1}{n}\sum_{k=1}^{n}\xi_i(k) \tag{11}$$

where n = number of process responses. The higher value of grey relational grade corresponds to intense relational degree between the reference sequence $x_0(k)$ and the given sequence $x_i(k)$. The reference sequence $x_0(k)$ represents the best process sequence. Therefore, higher grey relational grade means that the corresponding parameter combination is closer to the optimal.

However, Equation (11) assumes that all response features are equally important. But, in practical case, it may not be so. Therefore, different weightages have been assigned to different response features according to their relative priority. In that case, the equation for calculating overall grey relational grade (with different weightages for different responses) is modified as shown below:

$$\gamma_i = \frac{\sum_{k=1}^{n} w_k \xi_i(k)}{\sum_{k=1}^{n} w_k} \tag{12}$$

Here, γ_i is the overall grey relational grade for *ith* experiment. $\xi_i(k)$ is the grey relational coefficient of *kth* response in *ith* experiment and w_k is the weightage assigned to the *kth* response.

3.3 UTILITY CONCEPT

According to the utility theory, if X_i is the measure of effectiveness of an attribute (or quality characteristics) i and there are n attributes evaluating the outcome space, then the joint utility function can be expressed as:

$$U\left(X_1, X_2, ..., X_n\right) = f\left(U_1\left(X_1\right).U_2\left(X_2\right).....U_n\left(X_n\right)\right) \quad (13)$$

Here $U_i\left(X_i\right)$ is the utility of the i_{th} attribute.

The overall utility function is the sum of individual utilities if the attributes are independent, and is given as follows:

$$U\left(X_1, X_2, ..., X_n\right) = \sum_{i=1}^{n} U_i\left(X_i\right) \quad (14)$$

The attributes may be assigned weights depending upon the relative importance or priorities of the characteristics. The overall utility function after assigning weights to the attributes can be expressed as:

$$U\left(X_1, X_2, ..., X_n\right) = \sum_{i=1}^{n} W_i.U_i\left(X_i\right) \quad (15)$$

Here W_i is the weight assigned to the attribute i. The sum of the weights for all the attributes must be equal to 1.

A preference scale for each quality characteristic is constructed for determining its utility value. Two arbitrary numerical values (preference number) 0 and 9 are assigned to the just acceptable and the best value of the quality characteristic respectively. The preference number P_i can be expressed on a logarithmic scale as follows:

$$P_i = A \times \log\left(\frac{X_i}{X_i^{'}}\right) \quad (16)$$

Here X_i is the value of any quality characteristic or attribute i , $X_i^{'}$ is just acceptable value of quality characteristic or attribute i and A is a constant. The value A can be found by the condition that if $X_i = X^*$ (where X^* is the optimal or best value), then $P_i = 9$.

Therefore,

$$A = \frac{9}{\log \frac{X^*}{X_i'}} \tag{17}$$

The overall utility can be expressed as follows:

$$U = \sum_{i=1}^{n} W_i . P_i \tag{18}$$

Subject to the condition: $\sum_{i=1}^{n} W_i = 1$ (19)

Among various quality characteristics types, viz. Lower-the-Better, Higher-the-Better, and Nominal-the-Best suggested by Taguchi, the utility function would be Higher-the-Better type. Therefore, if the quality function is maximized, the quality characteristics considered for its evaluation will automatically be optimized (maximized or minimized as the case may be).

In the proposed approach based on quality loss (of principal components) utility values are calculated. Utility values of individual principal components are accumulated to calculate overall utility index. Overall utility index servers as the single objective function for optimization.

3.4 TAGUCHI METHOD

Taguchi Method is developed by Dr. Genichi Taguchi, a Japanese quality management consultant. The method explores the concept of quadratic quality loss function (Figure 3.1) and uses a statistical measure of performance called Signal-to-Noise (S/N) ratio. The S/N ratio takes both the mean and the variability into account. The S/N ratio is the ratio of the mean (Signal) to the standard deviation (Noise). The ratio depends on the quality characteristics of the product/process to be optimized. The standard S/N ratios generally used are as follows: - Nominal is Best (NB), Lower the Better (LB) and Higher the Better

(HB), (Equations 10 to l2). The optimal setting is the parameter combination, which has the highest S/N ratio.

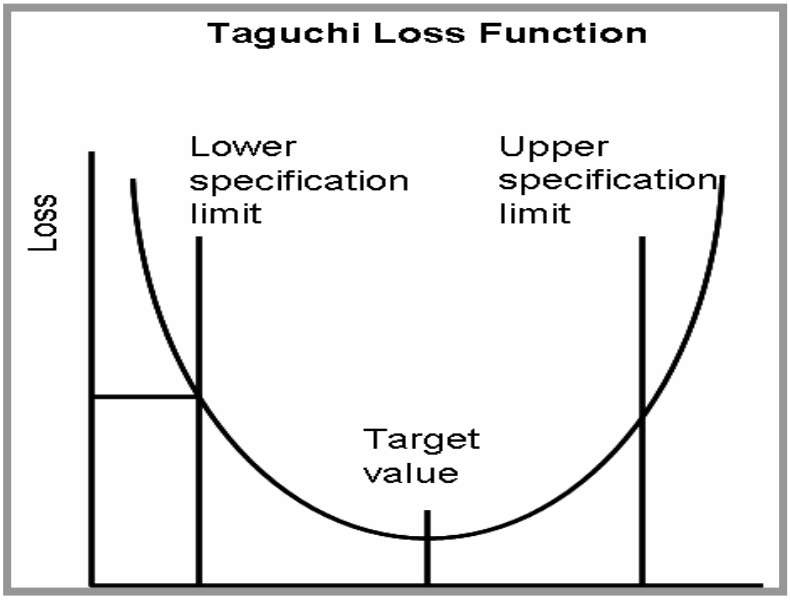

Figure 3.1: Taguchi's quadratic loss function

- ✓ **Taguchi's S/N Ratio for (NB) Nominal-the-best**

  (Quality characteristics is usually a nominal output, say *Diameter)*

$$\eta = 10\ln_{10}\frac{1}{n}\sum_{i=1}^{n}\frac{\mu^2}{\sigma^2} \tag{20}$$

- ✓ **Taguchi's S/N Ratio for (LB) Lower-the-better**

  (Quality characteristics is usually a nominal output, say *Defects)*

$$\eta = -10\ln_{10}\frac{1}{n}\sum_{i=1}^{n}y_i^2 \tag{21}$$

- ✓ **Taguchi's S/N Ratio for (HB) Higher-the-better**

  (Quality characteristics is usually a nominal output, say *Current)*

$$\eta = -10\ln_{10}\frac{1}{n}\sum_{i=1}^{n}\frac{1}{y_i^2} \tag{22}$$

(All notations carry their usual meanings)

3.5 CASE STUDY 1

OPTIMIZATION OF SURFACE ROUGHNESS PARAMETERS AND MRR USING PINCIPAL COMPONENT ANALYSIS (PCA), UTILITY THEORY AND TAGUCHI METHOD

3.5.1 PROCEDURE ADAPTED FOR OPTIMIZATION

The proposed optimization methodology combines Principal Component Analysis (PCA) [Antony (2000), Datta et al. (2009)], utility concept [Walia et al. (2006)] and Taguchi method [Datta et al. (2008)] based on selected Taguchi's Orthogonal Array (OA) Design of Experiment (DOE). The detailed methodology is described below.

Assuming, the number of experimental runs in Taguchi's OA design is m, and the number of quality characteristics is n. The experimental results can be expressed by the following series: $X_1, X_2, X_3, ..., X_i, ..., X_m$

Here,

$X_1 = \{X_1(1), X_1(2).....X_1(k).....X_1(n)\}$

.

.

.

.

$X_i = \{X_i(1), X_i(2).....X_i(k).....X_i(n)\}$

.

.

.

.

$X_m = \{X_m(1), X_m(2).....X_m(k).....X_m(n)\}$

Here, X_i represents the $i\,th$ experimental results and is called the comparative sequence.

Let, X_0 be the reference sequence:

Let, $X_0 = \{X_0(1), X_0(2).....X_0(k).....X_0(n)\}$

The value of the elements in the reference sequence means the optimal value (ideal or desired value) of the corresponding quality characteristic. X_0 and X_i both includes n elements, and $X_0(k)$ and $X_i(k)$ represent the numeric value of $k\,th$ element in the reference sequence and the comparative sequence, respectively, $k = 1, 2, ..., n$.

Step 1: Normalization of the responses (quality characteristics)

When the range of the series is too large or the optimal value of a quality characteristic is too enormous, it will cause the influence of some factors to be ignored. The original experimental data must be normalized to eliminate such effect. There are three different types of data normalization according to whether we require the LB (Lower-the-Better), the HB (Higher-the-Better) and NB (Nominal-the-Best). The normalization is taken by the following equations.

(a) LB (Lower-the-Better)

$$X_i^*(k) = \frac{\min X_i(k)}{X_i(k)} \tag{23}$$

(b) HB (Higher-the-Better)

$$X_i^*(k) = \frac{X_i(k)}{\max X_i(k)} \tag{24}$$

(c) NB (Nominal-the-Best)

$$X_i^*(k) = \frac{\min\{X_i(k), X_{0b}(k)\}}{\max\{X_i(k), X_{0b}(k)\}} \tag{25}$$

Here, $i = 1, 2, ..., m;$
$k = 1, 2, ..., n$

$X_i^*(k)$ is the normalized data of the $k\,th$ element in the $i\,th$ sequence.

$X_{0b}(k)$ is the desired value of the $k\,th$ quality characteristic. After data normalization, the value of $X_i^*(k)$ will be between 0 and 1. The series $X_i^*, i = 1, 2, 3, ..., m.$ can be viewed as the comparative sequence used in the present case.

Step 2: Checking for correlation between two quality characteristics

Let,
$$Q_i = \{X_0^*(i), X_1^*(i), X_2^*(i), ..., X_m^*(i)\} \quad (26)$$
$$where,\ i = 1, 2, ..., n.$$

It is the normalized series of the $i\,th$ quality characteristic. The correlation coefficient between two quality characteristics is calculated by the following equation:

$$\rho_{jk} = \frac{Cov(Q_j, Q_k)}{\sigma_{Q_j} \times \sigma_{Q_k}}, \quad (27)$$

here, $j = 1, 2, 3....., n.$
$k = 1, 2, 3, ..., n.,$
$j \neq k$

Here, ρ_{jk} is the correlation coefficient between quality characteristic j and quality characteristic k; $Cov(Q_j, Q_k)$ is the covariance of quality characteristic j and quality characteristic k; σ_{Q_j} *and* σ_{Q_k} are the standard deviation of quality characteristic j and quality characteristic k, respectively.

The correlation is checked by testing the following hypothesis:

$$\begin{cases} H_0 : \rho_{jk} = 0 & (There\ is\ no\ correlation) \\ H_1 : \rho_{jk} \neq 0 & (There\ is\ correlation) \end{cases} \quad (28)$$

Step 3: Calculation of the principal component score

(a) Calculate the Eigenvalue λ_k and the corresponding eigenvector $\beta_k\ (k = 1, 2, ..., n)$ from the correlation matrix formed by all quality characteristics.

(b) Calculate the principal component scores of the normalized reference sequence and comparative sequences using the equation shown below:

$$Y_i(k) = \sum_{j=1}^{n} X_i^*(j)\beta_{kj}, \quad i = 0, 1, 2, ..., m; k = 1, 2, ..., n. \quad (29)$$

Here, $Y_i(k)$ is the principal component score of the $k\,th$ element in the $i\,th$ series. $X_i^*(j)$ is the normalized value of the $j\,th$ element in the $i\,th$ sequence, and β_{kj} is the $j\,th$ element of eigenvector β_k.

Step 4: Estimation of quality loss $\Delta_{0,i}(k)$

$\Delta_{0,i}(k)$ is the absolute value of difference between $X_0(k)$ and $X_i(k)$ (difference between desired value and ith experimental value for kth response. If responses are correlated then instead of using $X_0(k)$ and $X_i(k)$, $Y_0(k)$ and $Y_i(k)$ should be used.

$$\Delta_{0,i}(k) = \begin{cases} \left| X_0^*(k) - X_i^*(k) \right|, & no\ significant\ correlation\ between\ quality\ characteristics \\ \left| Y_0(k) - Y_i(k) \right|, & Significant\ correlation\ between\ quality\ characteristics \end{cases} \quad (30)$$

Step 5: Adaptation of utility theory: Calculation of overall utility index

According to the utility theory, if X_i is the measure of effectiveness of an attribute (or quality characteristics) i and there are n attributes evaluating the outcome space, then the joint utility function can be expressed as:

$$U\left(X_1, X_2, ..., X_n\right) = f\left(U_1\left(X_1\right).U_2\left(X_2\right).....U_n\left(X_n\right)\right) \quad (31)$$

Here $U_i\left(X_i\right)$ is the utility of the i_{th} attribute.

The overall utility function is the sum of individual utilities if the attributes are independent, and is given as follows:

$$U\left(X_1, X_2, ..., X_n\right) = \sum_{i=1}^{n} U_i\left(X_i\right) \quad (32)$$

The attributes may be assigned weights depending upon the relative importance or priorities of the characteristics. The overall utility function after assigning weights to the attributes can be expressed as:

$$U\left(X_1, X_2, ..., X_n\right) = \sum_{i=1}^{n} W_i.U_i\left(X_i\right) \quad (33)$$

Here W_i is the weight assigned to the attribute i. The sum of the weights for all the attributes must be equal to 1.

A preference scale for each quality characteristic is constructed for determining its utility value. Two arbitrary numerical values (preference number) 0 and 9 are assigned to the just acceptable and the best value of the quality characteristic respectively. The preference number P_i can be expressed on a logarithmic scale as follows:

$$P_i = A \times \log\left(\frac{X_i}{X_i^{'}}\right) \tag{34}$$

Here X_i is the value of any quality characteristic or attribute i , $X_i^{'}$ is just acceptable value of quality characteristic or attribute i and A is a constant. The value A can be found by the condition that if $X_i = X^*$ (where X^* is the optimal or best value), then $P_i = 9$. Therefore,

$$A = \frac{9}{\log\frac{X^*}{X_i^{'}}} \tag{35}$$

The overall utility can be expressed as follows:

$$U = \sum_{i=1}^{n} W_i.P_i \tag{36}$$

Subject to the condition: $\sum_{i=1}^{n} W_i = 1$ (37)

Among various quality characteristics types, viz. Lower-the-Better, Higher-the-Better, and Nominal-the-Best suggested by Taguchi, the utility function would be Higher-the-Better type. Therefore, if the quality function is maximized, the quality characteristics considered for its evaluation will automatically be optimized (maximized or minimized as the case may be).

In the proposed approach based on quality loss (of principal components) utility values are calculated. Utility values of individual principal components are accumulated to calculate overall utility index. Overall utility index servers as the single objective function for optimization.

Step 6: Optimization of overall utility index using Taguchi method

Finally overall utility index is optimized (maximized) using Taguchi method. For calculating S/N ratio; HB criterion is selected.

3.5.2 DATA ANALYSIS

Experimental data (Table 3.1) have been normalized first. For all surface roughness parameters LB criterion (Equation 23) and for material removal rate HB criterion (Equation 24) has been selected. Normalized experimental data are shown in Table 3.2.

The correlation coefficients between individual responses have been computed using Equation 27. Table 3.3 represents Pearson's correlation coefficients. It has been observed that all the responses are correlated (coefficient of correlation having non-zero value). Table 3.4 presents Eigenvalues, eigenvectors, accountability proportion (AP) and cumulative accountability proportion (CAP) computed for the five major quality indicators (ψ). It has been found that first three principal components; ψ_1, ψ_2, ψ_3 can take care of 64.6%, 24.9% and 9% variability in data respectively. The contribution of third and forth principal components: ψ_3, ψ_4 have been found negligible to interpret variability into data. Moreover, cumulative accountability proportion (CAP) for first three principal components has been found 98.5%. Therefore, these two principal components can be ignored and the first three principal components can be treated as independent or uncorrelated quality indices instead of five correlated quality indices. Correlated responses have been transformed into three independent quality indices (major principal components) using Equation 29. These have been furnished in Table 3.5. Quality loss estimates (difference between ideal and actual gain) for aforesaid major principal components have been calculated (Equation 30) and presented in Table 3.6. Based on quality loss, utility values corresponding to the four principal components have been computed using Equations 34, 35.

In all the cases minimum observed value of the quality loss (from Table 3.6) has been considered as its optimal value or most expected value; whereas maximum observed value for the quality loss has been treated as the just acceptable value. Individual utility

measures corresponding to three major principal components have been furnished in Table 3.7. The overall utility index has been computed using Equation 36; tabulated in Table 3.8 with their corresponding (Signal-to-Noise) S/N ratio. In this computation it has been assumed that all quality indices are equally important (same priority weightage, 33.33%). Figure 3.2 reflects S/N ratio plot for overall utility index; S/N ratio being computed using Equation (38).

$$SN\,(Higher-the-better) = -10\log\left[\frac{1}{t}\sum_{i=1}^{t}\frac{1}{y_i^2}\right] \tag{38}$$

Here t is the number of measurements, and y_i the measured ith characteristic value i.e. ith quality indicator. Optimal parameter setting has been evaluated from Figure 3.2. The optimal setting should confirm highest utility index (HB criterion).

The predicted optimal setting becomes $A_1B_1C_1$.

After evaluating the optimal parameter settings, the next step is to predict and verify the optimal result using the confirmatory test. Table 3.9 reflects the satisfactory result of confirmatory experiment.

Table 3.1: Surface Roughness Characteristics (Average values) and MRR

Sl. No.	R_a (μm)	R_q (μm)	R_{ku}	R_{sm} (mm)	MRR $\left(\frac{mm^3}{\min}\right)$
1	3.153	3.927	4.037	0.111	124.1
2	4.720	5.907	3.467	0.161	868.7
3	3.903	4.777	2.943	0.126	2420.0
4	5.757	6.933	2.967	0.181	896.9
5	3.700	4.577	3.850	0.138	1793.8
6	3.873	4.717	2.750	0.151	2242.3
7	1.397	1.720	3.877	0.090	2425.6
8	3.743	4.447	2.307	0.137	2425.6
9	3.883	4.760	3.397	0.134	4746.5

Table 3.2: Normalized response data

Sl. No.	R_a	R_q	R_{ku}	R_{sm}	MRR
Ideal sequence	1.0000	1.0000	1.0000	1.0000	1.0000
1	0.4431	0.4380	0.5715	0.8108	0.0261
2	0.2960	0.2912	0.6654	0.5590	0.1830
3	0.3579	0.3601	0.7839	0.7143	0.5098
4	0.2427	0.2481	0.7776	0.4972	0.1890
5	0.3776	0.3758	0.5992	0.6522	0.3779
6	0.3607	0.3646	0.8389	0.5960	0.4724
7	1.0000	1.0000	0.5950	1.0000	0.5110
8	0.3732	0.3868	1.0000	0.6569	0.5110
9	0.3598	0.3613	0.6791	0.6716	1.0000

Table 3.3: Correlation among quality characteristics

Sl. No.	Correlation between responses	Pearson correlation coefficient	Comment
1	R_a and R_q	1.000	Both are correlated
2	R_a and R_{ku}	0.120	Both are correlated
3	R_a and R_{sm}	0.940	Both are correlated
4	R_a and MRR	0.457	Both are correlated
5	R_q and R_{ku}	0.134	Both are correlated
6	R_q and R_{sm}	0.938	Both are correlated
7	R_q and MRR	0.463	Both are correlated
8	R_{ku} and R_{sm}	0.019	Both are correlated
9	R_{ku} and MRR	0.458	Both are correlated
10	R_{sm} and MRR	0.413	Both are correlated

Table 3.4: Eigenvalues, eigenvectors, accountability proportion (AP) and cumulative accountability proportion (CAP) computed for the five major quality indicators

	ψ_1	ψ_2	ψ_3	ψ_4	ψ_5
Eigenvalue	3.2313	1.2430	0.4525	0.0731	0.0001
Eigenvector	0.542	–0.158	–0.146	–0.400	0.708
	0.542	–0.146	–0.153	–0.402	–0.706
	0.137	0.794	–0.583	0.101	0.010
	0.522	–0.238	–0.059	0.817	–0.003
	0.348	0.516	0.783	–0.016	0.000
AP	0.646	0.249	0.090	0.015	0.000
CAP	0.646	0.895	0.985	1.000	1.000

Table 3.5: Major Principal Components

Sl. No.	Major Principal Components		
	ψ_1	ψ_2	ψ_3
Ideal sequence	2.0910	0.7680	-0.1580
1	0.9882	0.1403	-0.4923
2	0.7649	0.4004	-0.3654
3	1.0468	0.6063	-0.2073
4	0.6979	0.5220	-0.4081
5	0.9624	0.4010	-0.2045
6	0.9835	0.6578	-0.2628
7	1.8653	0.1941	-0.3048
8	1.0696	0.7859	-0.3353
9	1.1824	0.7858	0.2397

Table 3.6: Quality loss estimates (for principal components)

Sl. No.	Quality loss estimated corresponding to individual principal components		
	ψ_1	ψ_2	ψ_3
1	1.1028	0.6277	0.3343
2	1.3261	0.3676	0.2074
3	1.0442	0.1617	0.0493
4	1.3931	0.2460	0.2501
5	1.1286	0.3670	0.0465
6	1.1075	0.1102	0.1048
7	0.2257	0.5739	0.1468
8	1.0214	0.0179	0.1773
9	0.9086	0.0178	0.3977

Table 3.7: Utility values related to individual principal components

Sl. No.	Utility values of individual principal components		
	ψ_1	ψ_2	ψ_3
1	1.1555	0.0000	0.7282
2	0.2437	1.3516	2.7301
3	1.4255	3.4261	8.7548
4	0.0000	2.3662	1.9450
5	1.0412	1.3557	9.0000
6	1.1345	4.3947	5.5925
7	9.0000	0.2264	4.1792
8	1.5347	8.9858	3.3876
9	2.1133	9.0000	0.0000

Table 3.8: Overall utility index

Sl. No.	Overall utility index	S/N ratio
1	0.6278	-4.0436
2	1.4417	3.1775
3	4.5350	13.1315
4	1.4369	3.1485
5	3.7986	11.5925
6	3.7069	11.3802
7	4.4681	13.0025
8	4.6356	13.3221
9	3.7041	11.3737

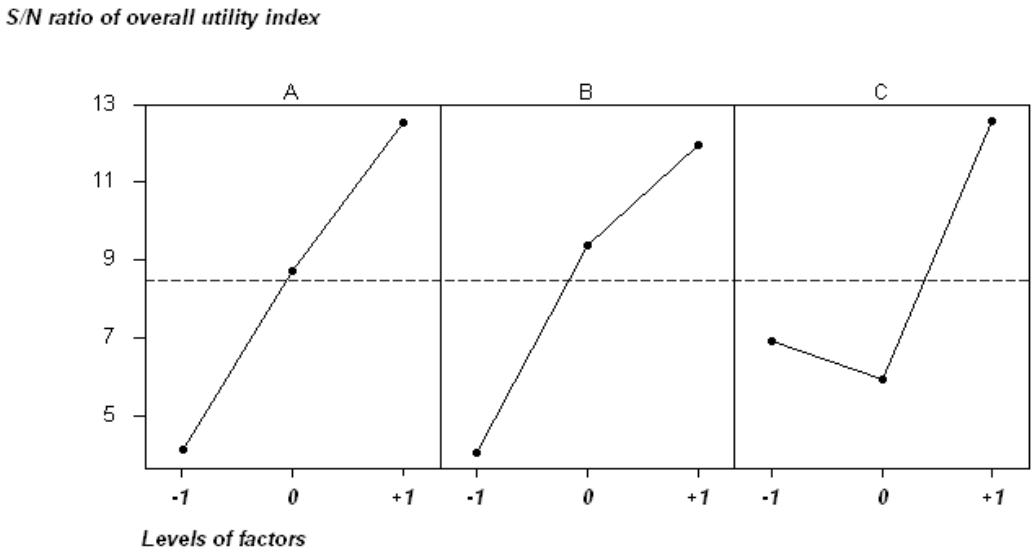

Figure 3.2: S/N ratio plot for overall utility index

Table 3.9: Results of confirmatory experiment

	Optimal setting	
	Prediction	Experiment
Level of factors	$A_1B_1C_1$	$A_1B_1C_1$
S/N ratio of Overall utility index	20.1956	21.1231
Overall utility index	10.2277	11.3803

3.5.3 CONCLUSION

The foregoing study deals with optimization of multiple surface roughness parameters along with material removal rate (MRR) in search of an optimal parametric combination (favorable process environment) capable of producing desired surface quality of the turned product in a relatively lesser time (enhancement in productivity). The study proposes an integrated optimization approach using Principal Component Analysis (PCA), utility concept in combination with Taguchi's robust design of optimization methodology. The following conclusions may be drawn from the results of the experiments and analysis of the experimental data in connection with correlated multi-response optimization in turning.

1) Application of PCA has been recommended to eliminate response correlation by converting correlated responses into uncorrelated quality indices called principal components which have been as treated as response variables for optimization.
2) Based on accountability proportion (AP) and cumulative accountability proportion (CAP), PCA analysis can reduce the number of response variables to be taken under consideration for optimization. This is really helpful in situations were large number of responses have to be optimized simultaneously.
3) Utility based Taguchi method has been found fruitful for evaluating the optimum parameter setting and solving such a multi-objective optimization problem.
4) The said approach can be recommended for continuous quality improvement and off-line quality control of a process/product.

3.6 CASE STUDY 2

OPTIMIZATION OF SURFACE ROUGHNESS PARAMETERS MRR AND CUTTING TOOL FLANK WEAR USING PINCIPAL COMPONENT ANALYSIS (PCA) AND GREY BASED TAGUCHI METHOD

3.6.1 PROCEDURE ADAPTED FOR OPTIMIZATION

Same as discussed before in section 3.5.1 the proposed optimization methodology is as follows. Only difference is this method utilizes grey relation theory instead of utility concept; other things remaining the same. Assuming, the number of experimental runs in Taguchi's OA design is m, and the number of quality characteristics is n. The experimental results can be expressed by the following series: $X_1, X_2, X_3, ..., X_i, ..., X_m$

Here,

$X_1 = \{X_1(1), X_1(2).....X_1(k).....X_1(n)\}$

.

.

.

.

$X_i = \{X_i(1), X_i(2).....X_i(k).....X_i(n)\}$

.

.

.

.

$X_m = \{X_m(1), X_m(2).....X_m(k).....X_m(n)\}$

Here, X_i represents the $i\,th$ experimental results and is called the comparative sequence in grey relational analysis.

Let, X_0 be the reference sequence:

Let, $X_0 = \{X_0(1), X_0(2).....X_0(k).....X_0(n)\}$

The value of the elements in the reference sequence means the optimal value of the corresponding quality characteristic. X_0 and X_i both includes n elements, and $X_0(k)$ and $X_i(k)$ represent the numeric value of $k\,th$ element in the reference sequence and the comparative sequence, respectively, $k = 1, 2, ..., n$. The following illustrates the proposed parameter optimization procedures in detail.

Step 1: Normalization of the responses (quality characteristics)

When the range of the series is too large or the optimal value of a quality characteristic is too enormous, it will cause the influence of some factors to be ignored. The original experimental data must be normalized to eliminate such effect. There are three different types of data normalization according to whether we require the LB (lower-the-better), the HB (higher-the-better) and NB (nominal-the-best). The normalization is taken by the following equations.

(a) LB (lower-the-better)

$$X_i^*(k) = \frac{\min X_i(k)}{X_i(k)} \tag{39}$$

(b) HB (higher-the-better)

$$X_i^*(k) = \frac{X_i(k)}{\max X_i(k)} \tag{40}$$

(c) NB (nominal-the-best)

$$X_i^*(k) = \frac{\min\{X_i(k), X_{0b}(k)\}}{\max\{X_i(k), X_{0b}(k)\}} \tag{41}$$

Here, $i = 1, 2, ..., m;$
$k = 1, 2, ..., n$

$X_i^*(k)$ is the normalized data of the $k\,th$ element in the $i\,th$ sequence.

$X_{0b}(k)$ is the desired value of the $k\,th$ quality characteristic. After data normalization, the value of $X_i^*(k)$ will be between 0 and 1. The series $X_i^*, i = 1,2,3,.....,m.$ can be viewed as the comparative sequence used in the grey relational analysis.

Step 2: Checking for correlation between two quality characteristics

$$Q_i = \{X_0^*(i), X_1^*(i), X_2^*(i), ..., X_m^*(i)\}$$

Let,

$$where,\ i = 1,2,.....,n.$$

It is the normalized series of the $i\,th$ quality characteristic. The correlation coefficient between two quality characteristics is calculated by the following equation:

$$\rho_{jk} = \frac{Cov(Q_j, Q_k)}{\sigma_{Q_j} \times \sigma_{Q_k}}, \tag{42}$$

$$j = 1,2,3.....,n.$$

here, $k = 1,2,3,.....,n.,$

$$j \neq k$$

Here, ρ_{jk} is the correlation coefficient between quality characteristic j and quality characteristic k; $Cov(Q_j, Q_k)$ is the covariance of quality characteristic j and quality characteristic k; $\sigma_{Q_j}\ and\ \sigma_{Q_k}$ are the standard deviation of quality characteristic j and quality characteristic k, respectively.

The correlation is checked by testing the following hypothesis:

$$\begin{cases} H_0 : \rho_{jk} = 0 & (There\ is\ no\ correlation) \\ H_1 : \rho_{jk} \neq 0 & (There\ is\ correlation) \end{cases}$$

Step 3: Calculation of the principal component score

- Calculate the Eigenvalue λ_k and the corresponding eigenvector $\beta_k\ (k = 1, 2, ..., n)$ from the correlation matrix formed by all quality characteristics.
- Calculate the principal component scores of the normalized reference sequence and comparative sequences using the equation shown below:

$$Y_i(k) = \sum_{j=1}^{n} X_i^*(j)\beta_{kj}, \quad i = 0, 1, 2, ..., m; k = 1, 2, ..., n. \tag{43}$$

Here, $Y_i(k)$ is the principal component score of the $k\,th$ element in the $i\,th$ series. $X_i^*(j)$ is the normalized value of the $j\,th$ element in the $i\,th$ sequence, and β_{kj} is the $j\,th$ element of eigenvector β_k.

Step 4: Calculation of the individual grey relational grades

(1) Calculation of the individual grey relational coefficients

Use the following equation to calculate the grey relational coefficient between $X_0(k)$ and $X_i(k)$.

$$r_{0,i}(k) = \frac{\Delta_{\min} + \xi\Delta_{\max}}{\Delta_{0,i}(k) + \xi\Delta_{\max}}, \quad i = 1, 2, ..., m; \quad k = 1, 2, ..., n. \tag{44}$$

Here, $r_{0,i}(k)$ is the relative difference of $k\,th$ element between sequence X_i and the comparative sequence X_0 (also called grey relational grade), and $\Delta_{0,i}(k)$ is the absolute value of difference between $X_0(k)$ and $X_i(k)$.

$$\Delta_{0,i}(k) = \begin{cases} \left| X_0^*(k) - X_i^*(k) \right|, & no\ significant\ correlation\ between\ quality\ characteristics \\ \left| Y_0(k) - Y_i(k) \right|, & Significant\ correlation\ between\ quality\ characteristics \end{cases} \tag{45}$$

$$\Delta_{\max} = \begin{cases} \max\limits_i \max\limits_k \left| X_0^*(k) - X_i^*(k) \right|, & no\ significant\ correlation\ between\ quality\ characteristics \\ \max\limits_i \max\limits_k \left| Y_0(k) - Y_i(k) \right|, & Significant\ correlation\ between\ quality\ characteristics \end{cases} \tag{46}$$

$$\Delta_{\min} = \begin{cases} \min_i \min_k \left| X_0^*(k) - X_i^*(k) \right|, & \textit{no significant correlation between quality characteristics} \\ \min_i \min_k \left| Y_0(k) - Y_i(k) \right|, & \textit{Significant correlation between quality characteristics} \end{cases} \quad (47)$$

Note that ξ is called the distinguishing coefficient, and its value is in between 0 to 1. In general it is set to 0.5, [Deng, 1989].

(2) Calculation of the overall grey relational grade

After the calculation of the grey relational coefficient and the weight of each quality characteristic, the grey relational grade is determined by:

$$\Gamma_{0,i} = \sum_{k=1}^{n} w_k r_{0,i}(k), \qquad i = 1, 2, ..., m. \quad (48)$$

In this section, the multiple quality characteristics are combined into one grey relational grade, thus the traditional Taguchi method can be used to evaluate the optimal parameter combination. Finally the anticipated optimal process parameters are verified by carrying out the confirmatory experiments.

3.6.2 DATA ANALYSES

Experimental data (Table 3.10) have been normalized using Equations (39) and (40). For surface roughness and depth of flank wear (Lower-the-Better) LB; and for material removal rate (MRR) (Higher-the-Better) HB criteria have been selected. The normalized data are shown in Table 3.11.

After normalization, a check has been made to verify whether the responses are correlated or not. Table 3.12 indicates the correlation coefficient among the responses. The coefficient of correlation, between two responses, has been calculated using Equation (42). It has been observed that, all responses are correlated to each other. In order to eliminate response correlations, Principal Component Analysis (PCA) has been applied to derive three independent quality indexes (called principal components), using Equation (43). The analysis of correlation matrix is shown in Table 3.13. The independent quality indexes are denoted as principal components ψ_1 (1^{st} PC) to ψ_3 (3^{rd}

PC). Table 3.14 represents the values of four independent principal components in all experimental runs.

$\Delta_{0i}(k)$ (Table 3.15) for all principal components have been evaluated using Equations (45), (46) and (47). Grey relational coefficients of all three principal components have been calculated using Equation (44). These have been furnished in Table 3.16.

The overall grey relational grade has been calculated using Equation (48), shown in Table 3.17. Thus, the multi-criteria optimization problem has been transformed into a single objective optimization problem using the combination of Taguchi approach and grey relational analyses. Higher is the value of grey relational grade, the corresponding factor combination is said to be close to the optimal.

The S/N ratio plot for the overall grey relational grade is represented graphically in Figure 3.3. The S/N ratio for overall grey relational grade has been calculated using HB (higher-the-better) criterion (Equation 49).

$$SN\,(Higher-the-better) = -10\log\left[\frac{1}{t}\sum_{i=1}^{t}\frac{1}{y_i^2}\right] \tag{49}$$

Here t is the number of measurements, and y_i the measured $i\,th$ characteristic value i.e. $i\,th$ quality indicator. With the help of the Figure 3.3, optimal parametric combination has been determined. The optimal factor setting becomes $A_{-1}B_0C_0$.

After evaluating the optimal parameter settings, the next step is to predict and verify the enhancement of quality characteristics using the optimal parametric combination. Table 3.18 reflects the satisfactory result of confirmatory experiment.

Table 3.10: Experimental data

Sl. No.	Surface roughness R_a in (μm)	MRR $\left(\frac{mm^3}{\min}\right)$	Depth of flank wear (mm)
1	3.153	124.1	0.151
2	4.720	868.7	0.101
3	3.903	2420.0	0.178

Table 3.10 Continued

Sl. No.	Surface roughness R_a in (μm)	MRR $\left(\frac{mm^3}{\min}\right)$	Depth of flank wear (mm)
4	5.757	896.9	0.07
5	3.700	1793.8	0.104
6	3.873	2242.3	0.059
7	1.397	2425.6	0.224
8	3.743	2425.6	0.079
9	3.883	4746.5	0.019

Table 3.11: Normalized data

Sl. No.	Surface roughness (R_a)	MRR	Depth of flank wear
Ideal Sequence	1.0000	1.0000	1.0000
1	0.4431	0.0261	0.1258
2	0.2960	0.1830	0.1881
3	0.3579	0.5098	0.1067
4	0.2427	0.1890	0.2714
5	0.3776	0.3779	0.1827
6	0.3607	0.4724	0.3220
7	1.0000	0.5110	0.0848
8	0.3732	0.5110	0.2405
9	0.3598	1.0000	1.0000

Table 3.12: Check for correlation between the responses

Sl. No.	Correlation between responses	Pearson correlation coefficient	Comment
1	R_a and MRR	0.457	Both are correlated
2	R_a and depth of flank wear	0.275	Both are correlated
3	MRR and depth of flank wear	0.837	Both are correlated

Table 3.13: Eigenvalues, eigenvectors, accountability proportion (AP) and cumulative accountability proportion (CAP) computed for the responses

	ψ_1	ψ_2	ψ_3
Eigenvalue	2.0858	0.7749	0.1393
Eigenvector	$\begin{vmatrix} -0.433 \\ -0.658 \\ -0.617 \end{vmatrix}$	$\begin{vmatrix} 0.883 \\ -0.173 \\ -0.436 \end{vmatrix}$	$\begin{vmatrix} -0.180 \\ 0.733 \\ -0.656 \end{vmatrix}$
AP	0.695	0.258	0.046
CAP	0.695	0.954	1.000

Table 3.14: Principal components in all L_9 OA experimental observations

Sl. No.	Major Principal Components		
	ψ_1	ψ_2	ψ_3
Ideal sequence	-1.7080	0.2240	-0.1030
1	-0.2867	0.3097	-0.1432
2	-0.3646	0.1329	-0.0425
3	-0.5563	0.1634	0.2393
4	-0.3969	0.0511	-0.0832
5	-0.5249	0.1695	0.0892
6	-0.6657	0.0783	0.0701
7	-0.8216	0.7076	0.1389
8	-0.6462	0.1176	0.1496
9	-1.4308	-0.3093	0.0122

Table 3.15: Quality loss estimates $\Delta_{0i}(k)$ (for principal components)

Sl. No.	Quality loss estimated corresponding to individual principal components		
	ψ_1	ψ_2	ψ_3
1	1.4213	0.0857	0.0402
2	1.3434	0.0911	0.0605

3	1.1517	0.0606	0.3423
4	1.3111	0.1729	0.0198
5	1.1831	0.0545	0.1922
6	1.0423	0.1457	0.1731
7	0.8864	0.4836	0.2419
8	1.0618	0.1064	0.2526
9	0.2772	0.5333	0.1152

Table 3.16: Individual grey relational coefficients for the principal components

Sl. No.	Grey relational coefficients for individual principal components		
	ψ_1	ψ_2	ψ_3
1	0.4633	0.9114	0.8777
2	0.4809	0.8977	0.7823
3	0.5304	0.9814	0.3118
4	0.4886	0.7307	0.9999
5	0.5216	1.0000	0.4587
6	0.5635	0.7789	0.4880
7	0.6185	0.4280	0.3968
8	0.5573	0.8609	0.3856
9	1.0000	0.4015	0.6049

Table 3.17: Calculation of overall grey relational grade

Sl. No.	$\Gamma_{0,i}$	S/N Ratio
1	0.7508	-2.48951
2	0.7203	-2.84973
3	0.6079	-4.32336
4	0.7397	-2.61889
5	0.6601	-3.60781
6	0.6101	-4.29198
7	0.4811	-6.35529
8	0.6013	-4.41818
9	0.6688	-3.49407

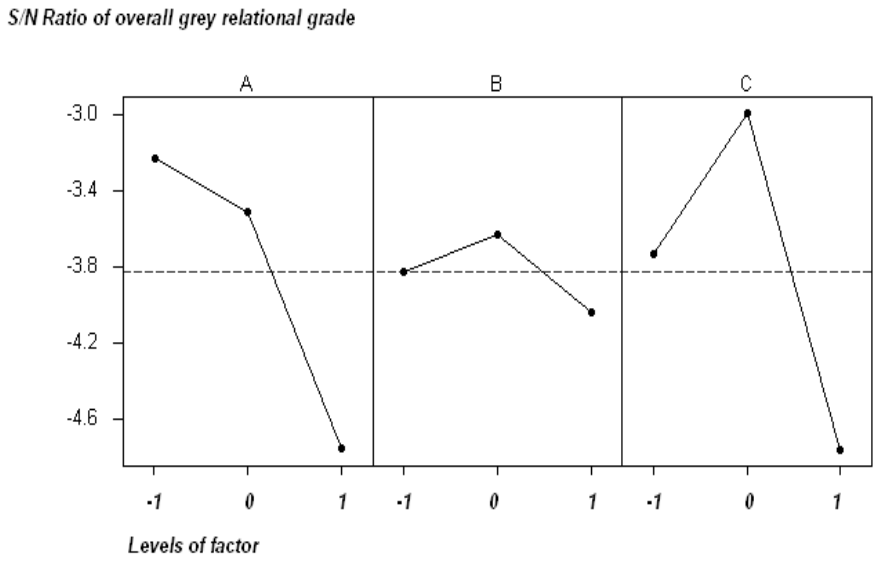

Figure 3.3: S/N Ratio plot of overall grey relational grade

Table 3.18: Results of confirmatory experiment

	Optimal setting	
	Prediction	Experiment
Level of factors	$A_{-1}B_0C_0$	$A_{-1}B_0C_0$
S/N ratio	-2.17838	-2.1500
Overall grey relational grade	0.7782	0.7807

3.6.3 CONCLUSIONS

In the present work, multi-response optimization problem has been solved by searching an optimal parametric combination, capable of producing high surface quality turned product in a relatively lesser time and at the same time ensuring reduced flank wear of the cutting tool. Reduction in cutting tool flank wear also increases tool life. PCA has been used to eliminate correlation among the responses and to convert the correlated responses into independent quality indexes; so as to meet the basic requirement of Taguchi method. Grey relation theory has been found efficient to convert multiple responses into an equivalent single objective function. Thus, a multi-objective optimization problem has been converted into a single objective function optimization problem which can be solved by Taguchi method. The aforesaid extended Taguchi method can be applied for continuous quality improvement of the product/process and off-line quality control.

LIST OF REFERENCES

LIST OF REFERENCES

1. Antony J., (2000), “Multi-response optimization in industrial experiments using Taguchi’s quality loss function and Principal Component Analysis”, Quality and Reliability Engineering International, Volume 16, pp.3-8.
2. Ahmed S. G., (2006), “Development of a Prediction Model for Surface Roughness in Finish Turning of Aluminium”, Sudan Engineering Society Journal, Volume 52, Number 45, pp. 1-5.
3. Abburi N. R. and Dixit U. S., (2006), “A knowledge-based system for the prediction of surface roughness in turning process” Robotics and Computer-Integrated Manufacturing, Volume 22, pp. 363–372.
4. Al-Ahmari A. M. A., (2007),”Predictive machinability models for a selected hard material in turning operations”, Journal of Materials Processing Technology, Volume 190, pp. 305–311.
5. Choudhury S. K. and Bartarya G., (2003), “Role of temperature and surface finish in predicting tool wear using neural network and design of experiments”, International Journal of Machine Tools and Manufacture, Volume 43, pp. 747–753.
6. Chien W.-T. and Tsai C.-S., (2003), “The investigation on the prediction of tool wear and the determination of optimum cutting conditions in machining 17-4PH stainless steel”, Journal of Materials Processing Technology, Volume 140, pp. 340–345.

7. Biswas C. K., Chawla B. S., Das N. S., Srinivas E. R. K. N. K., (2008), “Tool Wear Prediction using Neuro-Fuzzy System”, Institution of Engineers (India) Journal (PR), Volume 89, pp. 42-46.
8. Doniavi A., Eskanderzade M. and Tahmsebian M., (2007), “Empirical Modeling of Surface Roughness in Turning Process of 1060 steel using Factorial Design Methodology”, Journal of Applied Sciences, Volume 7, Number17, pp. 2509-2513.
9. Datta S., Bandyopadhyay, A. and Pal, P. K., (2008), “Application of Taguchi Philosophy for Parametric Optimization of Bead Geometry and HAZ Width in Submerged Arc Welding Using Mixture of Fresh Flux and Fused Slag”, for International Journal of Advanced Manufacturing Technology, Volume 36, pp. 689-698.
10. Datta S., Nandi G., Bandyopadhyay A. and Pal P. K., (2009), “Application of PCA based hybrid Taguchi method for multi-criteria optimization of submerged arc weld: A case study”, For International Journal of Advanced Manufacturing Technology. (Article In press) DOI 10.1007/s00170-009-1976-0.
11. Feng C. X. (Jack) and Wang X., (2002), “Development of Empirical Models for Surface Roughness Prediction in Finish Turning”, International Journal of Advanced Manufacturing Technology, Volume 20, pp. 348–356.
12. Fnides B., Aouici H., Yallese M. A., (2008), “Cutting forces and surface roughness in hard turning of hot work steel X38CrMoV5-1 using mixed ceramic”, Mechanika, Volume 2, Number 70, pp. 73-78.

13. Fu P. and Hope A. D., (2008), “A Hybrid Pattern Recognition Architecture for Cutting Tool Condition Monitoring” Technology and Applications, Volume 24, Number 4, pp. 548-558.
14. Kirby E. D., Zhang Z. and Chen J. C., (2004), “Development of An Accelerometer based surface roughness Prediction System in Turning Operation Using Multiple Regression Techniques”, Journal of Industrial Technology, Volume 20, Number 4, pp. 1-8.
15. Kohli A. and Dixit U. S., (2005),”A neural-network-based methodology for the prediction of surface roughness in a turning process”, International Journal of Advanced Manufacturing Technology, Volume 25, pp.118–129.
16. Kumanan S., Saheb S. K. N. and Jesuthanam C. P., (2006), “Prediction of Machining Forces using Neural Networks Trained by a Genetic Algorithm”, Institution of Engineers (India) Journal, Volume 87, pp. 11-15.
17. Kassab S. Y. and Khoshnaw Y. K., (2007), “The Effect of Cutting Tool Vibration on Surface Roughness of Work piece in Dry Turning Operation”, Engineering and Technology, Volume 25, Number 7, pp. 879-889.
18. Lin W. S., Lee B. Y., Wu C. L., (2001), “Modeling the surface roughness and cutting force for turning”, Journal of Materials Processing Technology, Volume 108, pp. 286-293.
19. Lee S. S. and Chen J. C., (2003), “Online surface roughness recognition system using artificial neural networks system in turning operations” International Journal of Advanced Manufacturing Technology, Volume 22, pp. 498–509.

20. Lan T.-S., Lo C. Y., Wang M.-Y. and Yen A-Y, (2008), “Multi Quality Prediction Model of CNC Turning Using Back Propagation Network”, Information Technology Journal, Volume 7, Number 6, pp. 911-917.
21. Mahmoud E. A. E. and Abdelkarim H. A., (2006), “Optimum Cutting Parameters in Turning Operations using HSS Cutting Tool with 45^0 Approach Angle”, Sudan Engineering Scoeiety Journal, Volume 53, Number 48, pp. 25-30.
22. Natarajan U., Arun P., Periasamy V. M., (2007), “On-line Tool Wear Monitoring in Turning by Hidden Markov Model (HMM)” Institution of Engineers (India) Journal (PR), Volume 87, pp. 31-35.
23. Özel T. and Karpat Y., (2005), “Predictive modeling of surface roughness and tool wear in hard turning using regression and neural networks”, International Journal of Machine Tools and Manufacture, Volume 45, pp. 467–479.
24. Özel T., Karpat Y., Figueira L. and Davim J. P., (2007), “Modeling of surface finish and tool flank wear in turning of AISI D2 steel with ceramic wiper inserts”, Journal of Materials Processing Technology, Volume189, pp.192–198.
25. Pal S. K. and Chakraborty D., (2005), “Surface roughness prediction in turning using artificial neural network”, Neural Computing and Application, Volume14, pp. 319–324.
26. Reddy B. S., Padmanabhan G. and Reddy K. V. K., (2008), “Surface Roughness Prediction Techniques for CNC turning”, Asian Journal of Scientific Research, Volume 1, Number 3, pp. 256-264.

27. Su, C. T. and Tong, L. I., 1997, “Multi-response robust design by principal component analysis”, Total Quality Management, Volume 8, Issue 6, pp. 409-416.
28. Suresh P. V. S., Rao P. V. and Deshmukh S. G., (2002), “A genetic algorithmic approach for optimization of surface roughness prediction model”, International Journal of Machine Tools and Manufacture, Volume 42, pp. 675–680.
29. Singh H. and Kumar P., (2006), “Optimizing Feed Force for Turned Parts through the Taguchi Technique”, Sadhana, Volume 31, Number 6, pp. 671–681.
30. Srikanth T. and Kamala V., (2008), “A Real Coded Genetic Algorithm for Optimization of Cutting Parameters in Turning IJCSNS”, International Journal of Computer Science and Network Security, Volume 8 Number 6, pp. 189-193.
31. Sahoo P., Barman T. K. and Routara B. C., (2008), “Taguchi based practical dimension modeling and optimization in CNC turning”, Advance in Production Engineering and Management, Volume 3, Number 4, pp. 205-217.
32. Shetty R., Pai R., Kamath V. and Rao S. S., (2008), “Study on Surface Roughness Minimization in Turning of DRACs using Surface Roughness Methodology and Taguchi under Pressured Steam Jet Approach”, ARPN Journal of Engineering and Applied Sciences, Volume 3, Number 1, pp. 59-67.
33. Thamizhmanii S., Saparudin S. and Hasan S., (2007), “Analysis of Surface Roughness by Using Taguchi Method”, Achievements in Materials and Manufacturing Engineering, Volume 20, Issue 1-2, pp. 503-505.
34. Thamma R., (2008), “Comparison between Multiple Regression Models to Study Effect of Turning Parameters on the Surface Roughness”, Proceedings of the 2008

IAJC-IJME International Conference, ISBN 978-1-60643-379-9, Paper 133, ENG 103 pp. 1-12.

35. Walia R. S., Shan H. S. and Kumar, P., (2006), "Multi-Response Optimization of CFAAFM Process Through Taguchi Method and Utility Concept", Materials and Manufacturing Processes, Volume 21, pp. 907-914.
36. Wang M. Y. and Lan T. S., (2008), "Parametric Optimization on Multi-Objective Precision Turning Using Grey Relational Analysis". Information Technology Journal, Volume 7, pp.1072-1076.
37. Wannas A. A., (2008), "RBFNN Model for Prediction Recognition of Tool Wear in Hard Turning", Journal of Engineering and Applies Science, Volume 3, Number 10, pp. 780-785.
38. Zhou Q., Hong G. S. and Rahman M., (1995), "A New Tool Life Criterion For Tool Condition Monitoring Using a Neural Network", Engineering Application Artificial Intelligence, Volume 8, Number 5, pp. 579-588.
39. Zhong Z. W., Khoo L. P. and Han S. T., (2006), "Prediction of surface roughness of turned surfaces using neural networks", International Journal of Advance Manufacturing Technology, Volume 28, pp. 688–693.
40. Bhattacharyya, A., Reprinted 2006, "Metal Cutting: Theory and Practice", New Central Book Agency, Page No. 495 – 501. ISBN: 81-7381-228-4.
41. DIN 4760: Form deviations; concepts; classification system. Deutsches Institute Fuer Normung, e.V., 1982.
42. Groover, Mikell P. (2007). "Theory of Metal Machining", Fundamentals of Modern Manufacturing, 3rd ed, John Wiley & Sons, Inc. ISBN 0471744859.

43. Kaczmarek J., 1983 “Principles of machining by cutting”, abrasion and erosion. London: Peter Peregrinus.
44. Kalpakjian S. and Schmid Steven R. (2000), “Manufacturing Engineering and Technology”, 4th ed, Pearson Education Asia. ISBN 81-7808-157-1.
45. Manly, B. F. J., (1994), “Multivariate Statistical Methods: A Primer”, Chapman and Hall, London.
46. Peace, G., S., (1993), “Taguchi Methods- A Hands-On Approach”, Addison-Wesley Publishing Company. Massachusetts.
47. Rao, P. N. (2001). “Manufacturing Technology – Metal Cutting and Machine Tools”, First reprint 2001, Tata McGraw-Hill. ISBN 0-07-463843-2.
48. Taguchi, G., (1986), “Introduction to Quality Engineering,” *Proceedings of* Asian Productivity Organization, UNIPUB, White Plains, NY.
49. Taguchi, G., (1987), “System of Experimental Design: Engineering Methods to Optimize Quality and Minimize Cost,” *Proceedings of* UNIPUB/Kraus International, White Plains, NY.

COMMUNICATIONS

COMMUNICATIONS

1. U. Khandey, S. Datta, S. S. Mahapatra and A. Bandyopadhyay, "***Optimization of Surface Roughness, Material Removal Rate and Cutting Tool Flank Wear in Turning Using Extended Taguchi Method***", Proceedings of International Conference on Advances in Mechanical Engineering (ICAME 2009) to be held on August 3-5, 2009; organized by Department of Mechanical Engineering at Sardar Vallabhbhai National Institute of Technology (SVNIT), Surat-395007, Gujarat. (Accepted)

2. U. Khandey, S. Datta, S. S. Mahapatra and A. Bandyopadhyay, "***Taguchi Approach coupled with PCA and Utility Concept for Optimization of Correlated Multi-Quality Characteristics in Straight Turning of Mild Steel***", For International Journal of Machining and Machinability of Materials,, Inderscience Publications. (Under Review) (Manuscript ID: IJMTM 8950)

APPENDIX

APPENDIX

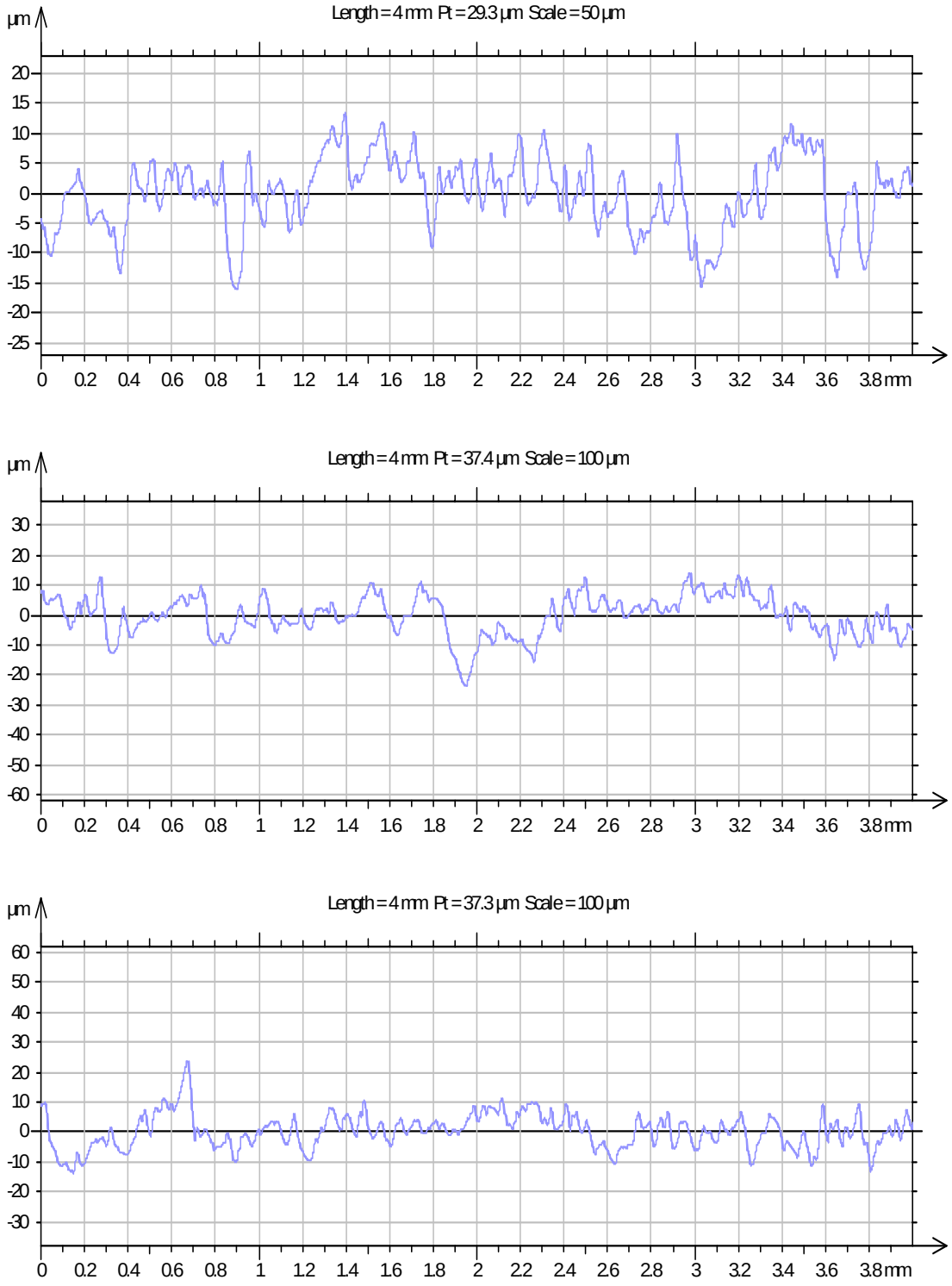

(**Sample 1**) Surface roughness and waviness profile curve at factor setting:

Spindle speed 220 rpm, feed rate 0.044 mm/rev and depth of cut 0.4 mm

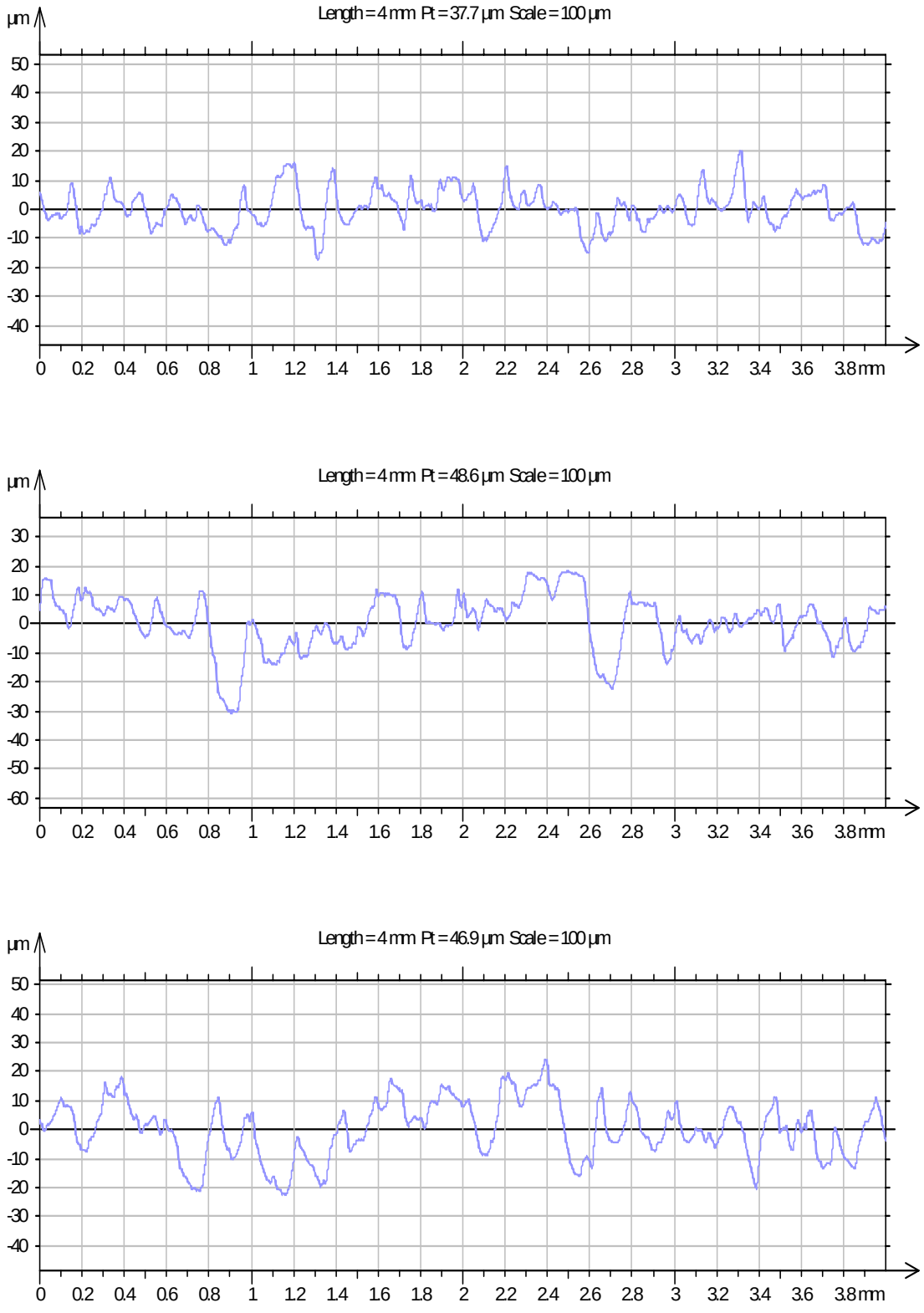

(**Sample 2**) Surface roughness and waviness profile curve at factor setting:

Spindle speed 220 rpm, feed rate 0.088 mm/rev and depth of cut 0.8 mm

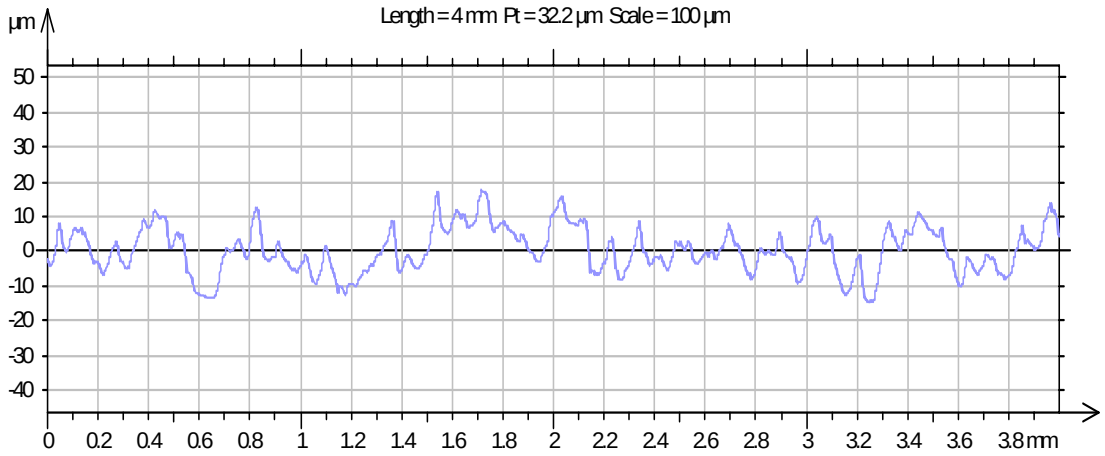

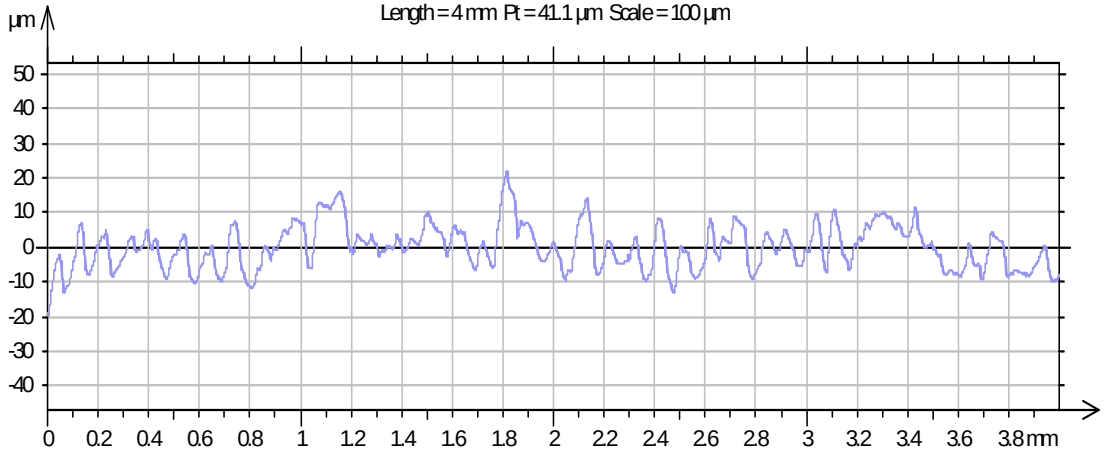

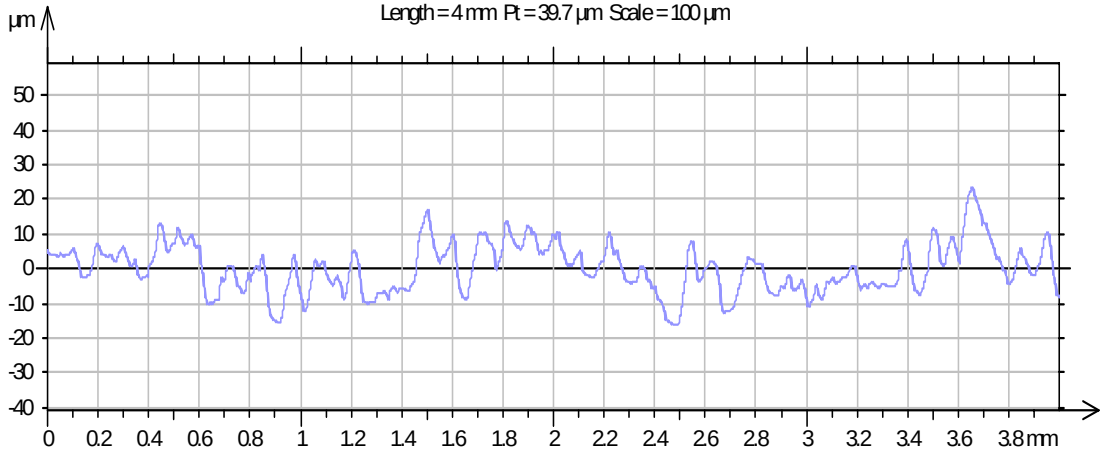

(**Sample 3**) Surface roughness and waviness profile curve at factor setting:

Spindle speed 220 rpm, feed rate 0.132 mm/rev and depth of cut 1.2 mm

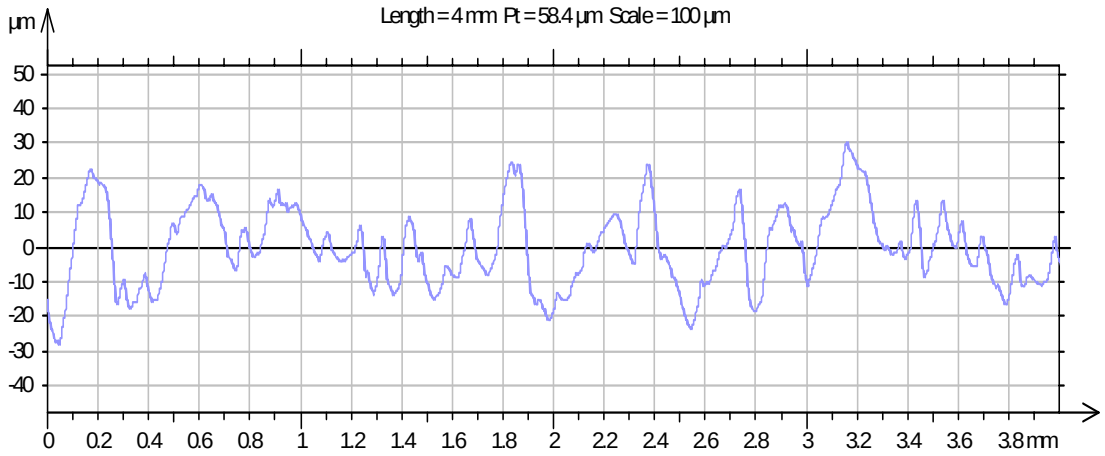

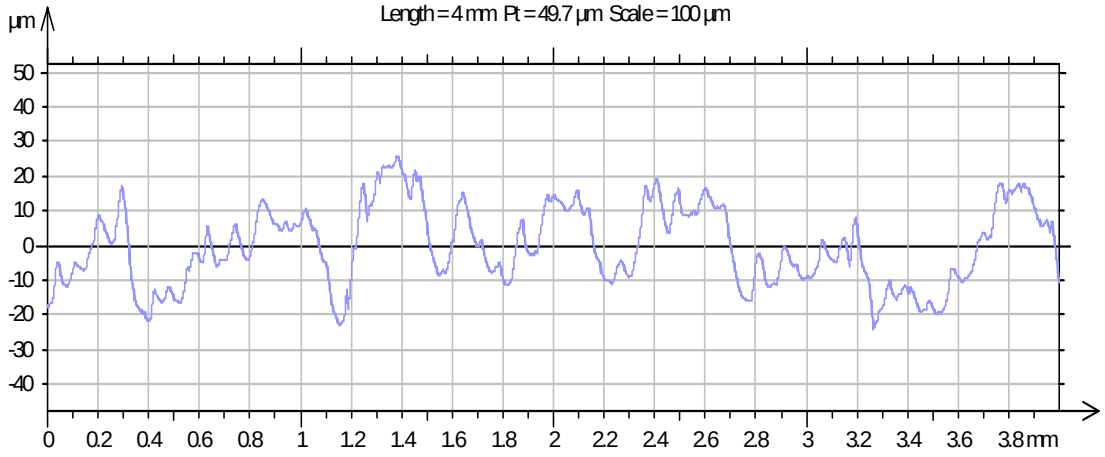

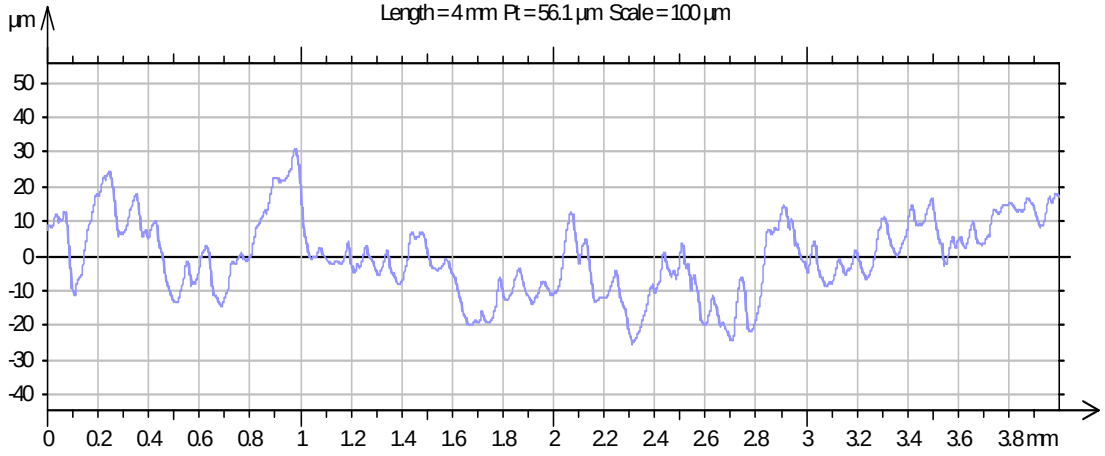

(**Sample 4**) Surface roughness and waviness profile curve at factor setting:

Spindle speed 530 rpm, feed rate 0.044 mm/rev and depth of cut 0.8 mm

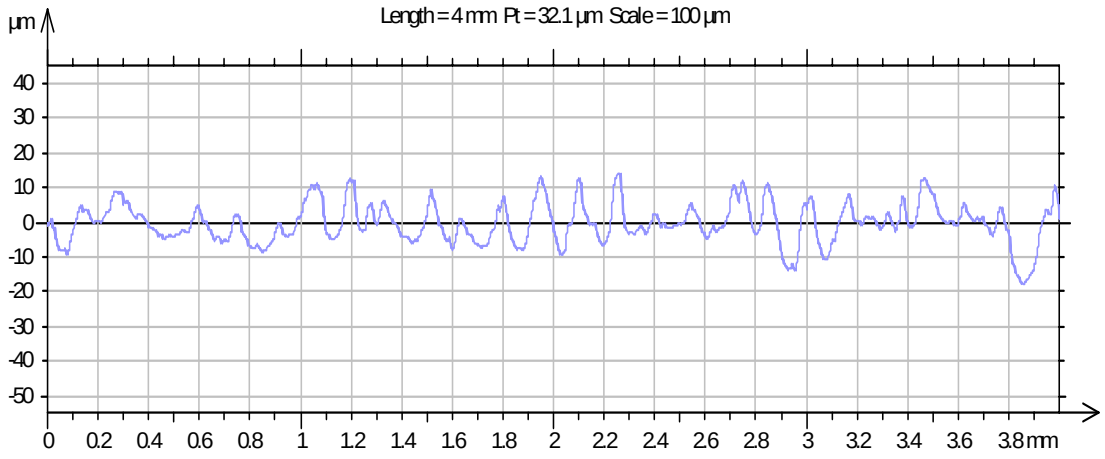

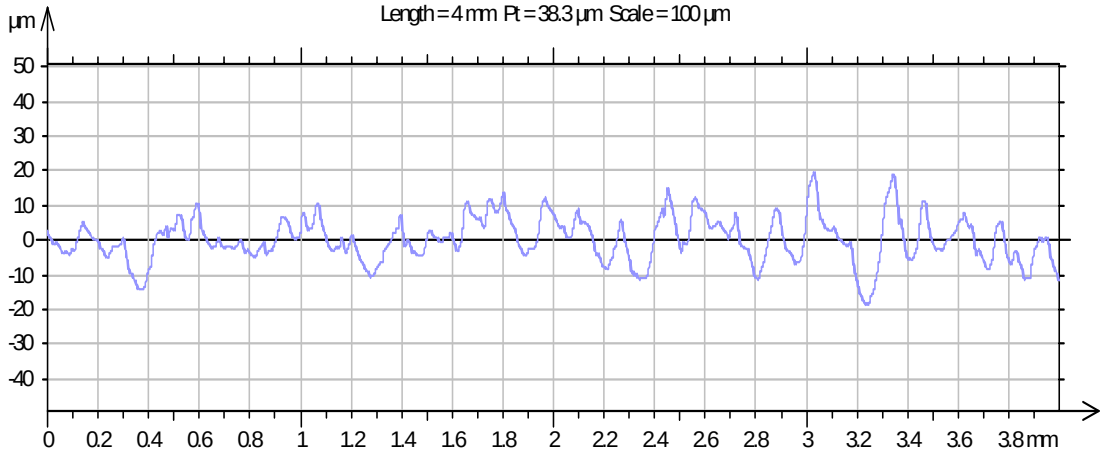

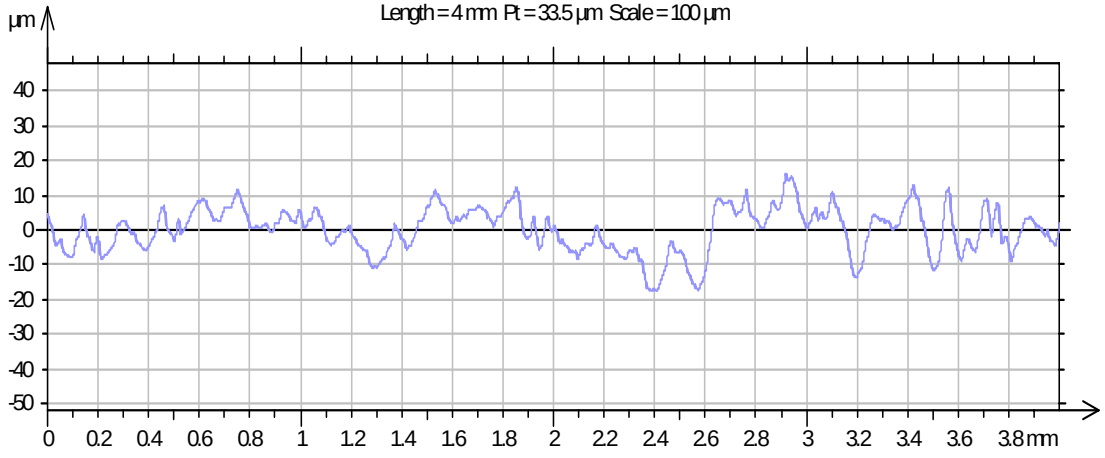

(**Sample 5**) Surface roughness and waviness profile curve at factor setting:

Spindle speed 530 rpm, feed rate 0.088 mm/rev and depth of cut 1.2 mm

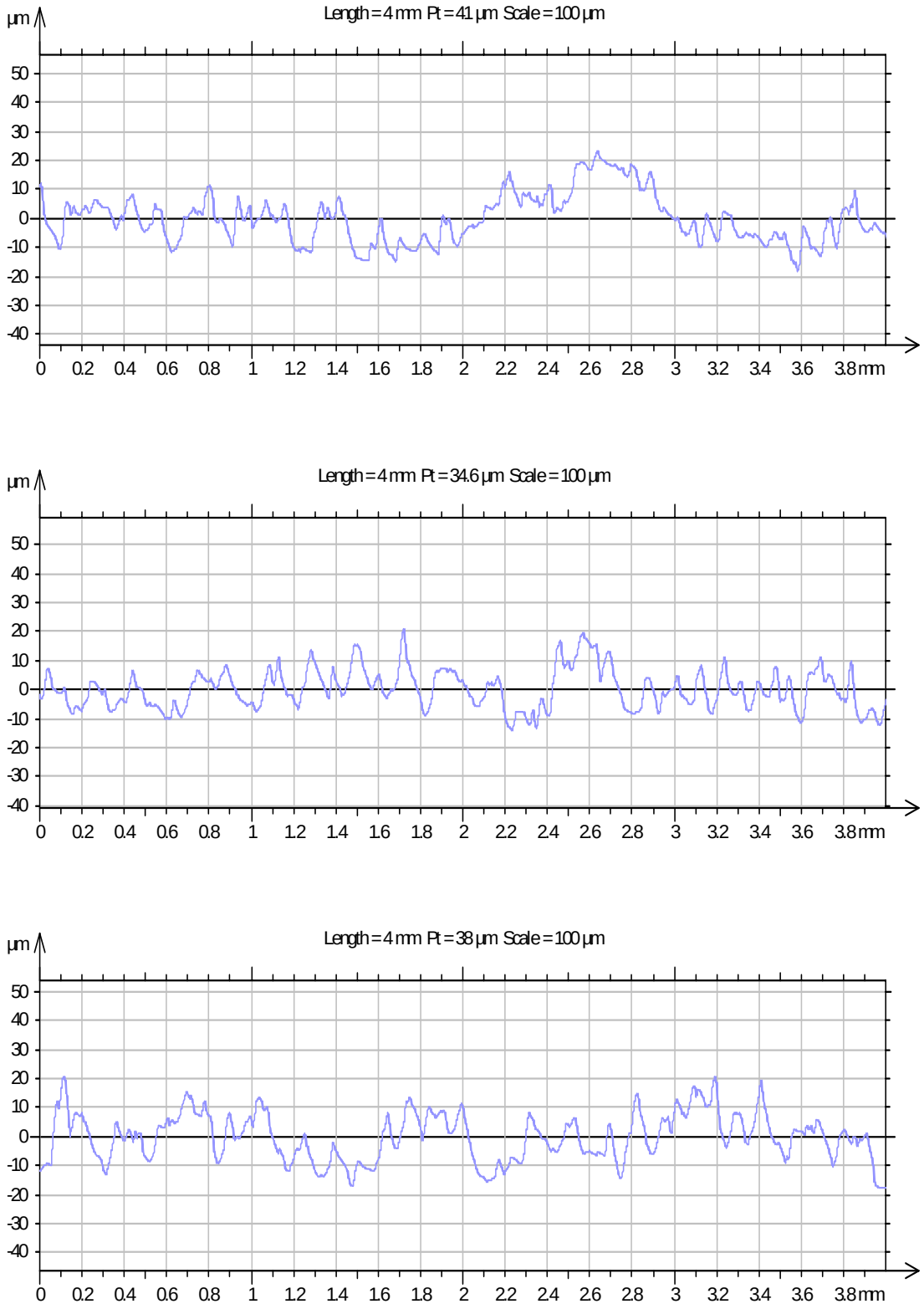

(**Sample 6**) Surface roughness and waviness profile curve at factor setting:

Spindle speed 530 rpm, feed rate 0.132 mm/rev and depth of cut 0.4 mm

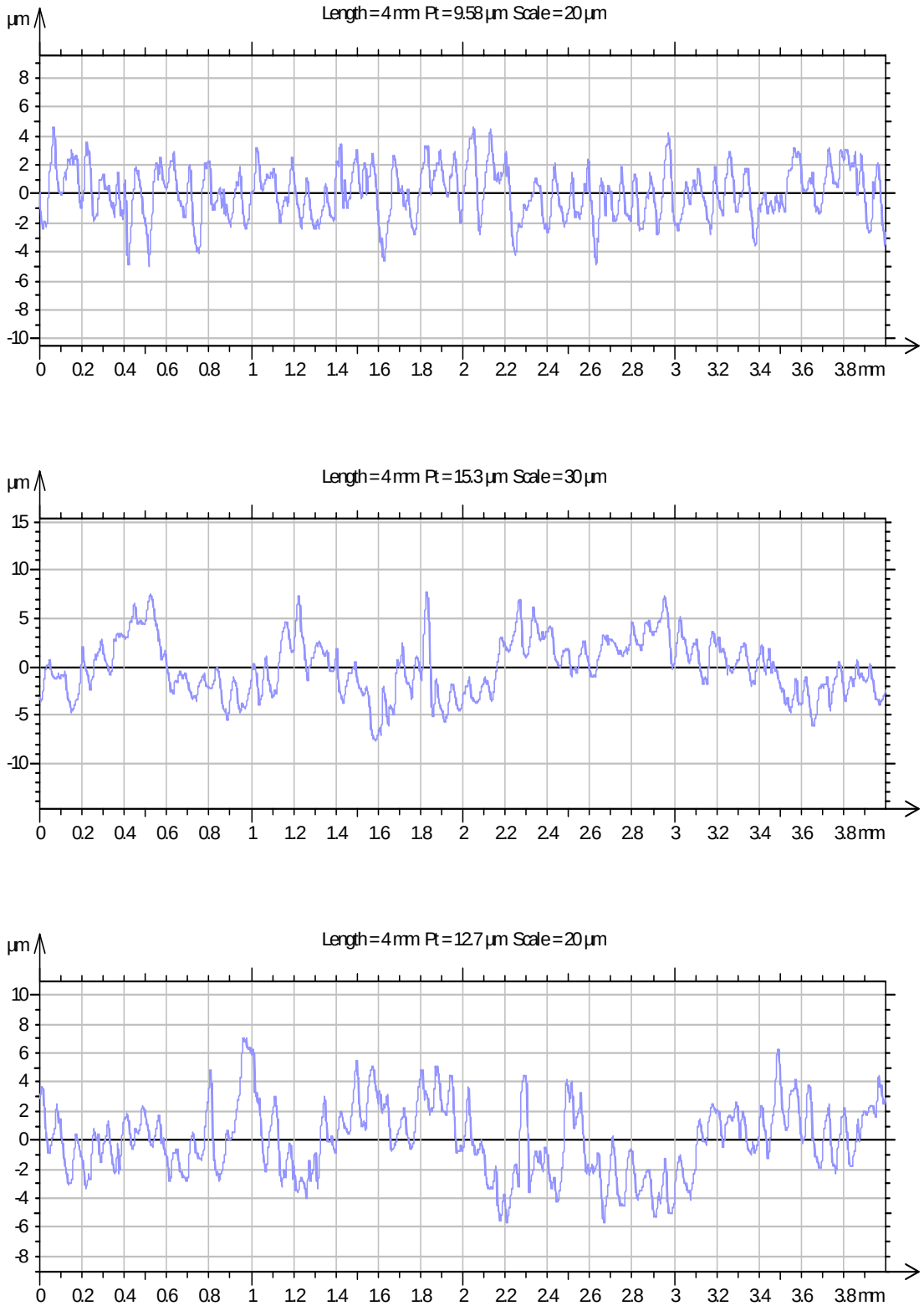

(**Sample 7**) Surface roughness and waviness profile curve at factor setting:

Spindle speed 860 rpm, feed rate 0.044 mm/rev and depth of cut 1.2 mm

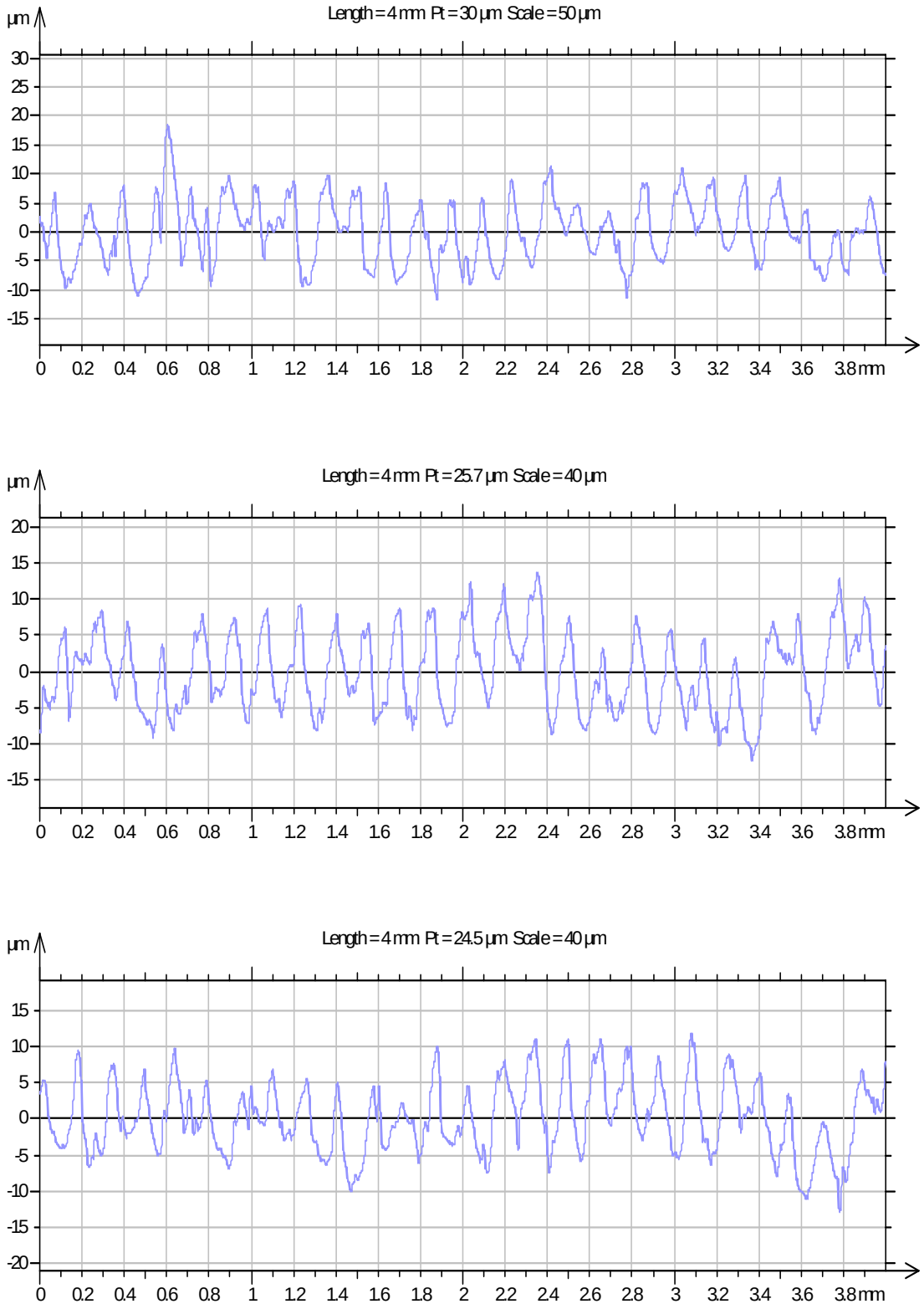

(**Sample 8**) Surface roughness and waviness profile curve at factor setting:

Spindle speed 860 rpm, feed rate 0.088 mm/rev and depth of cut 0.4 mm

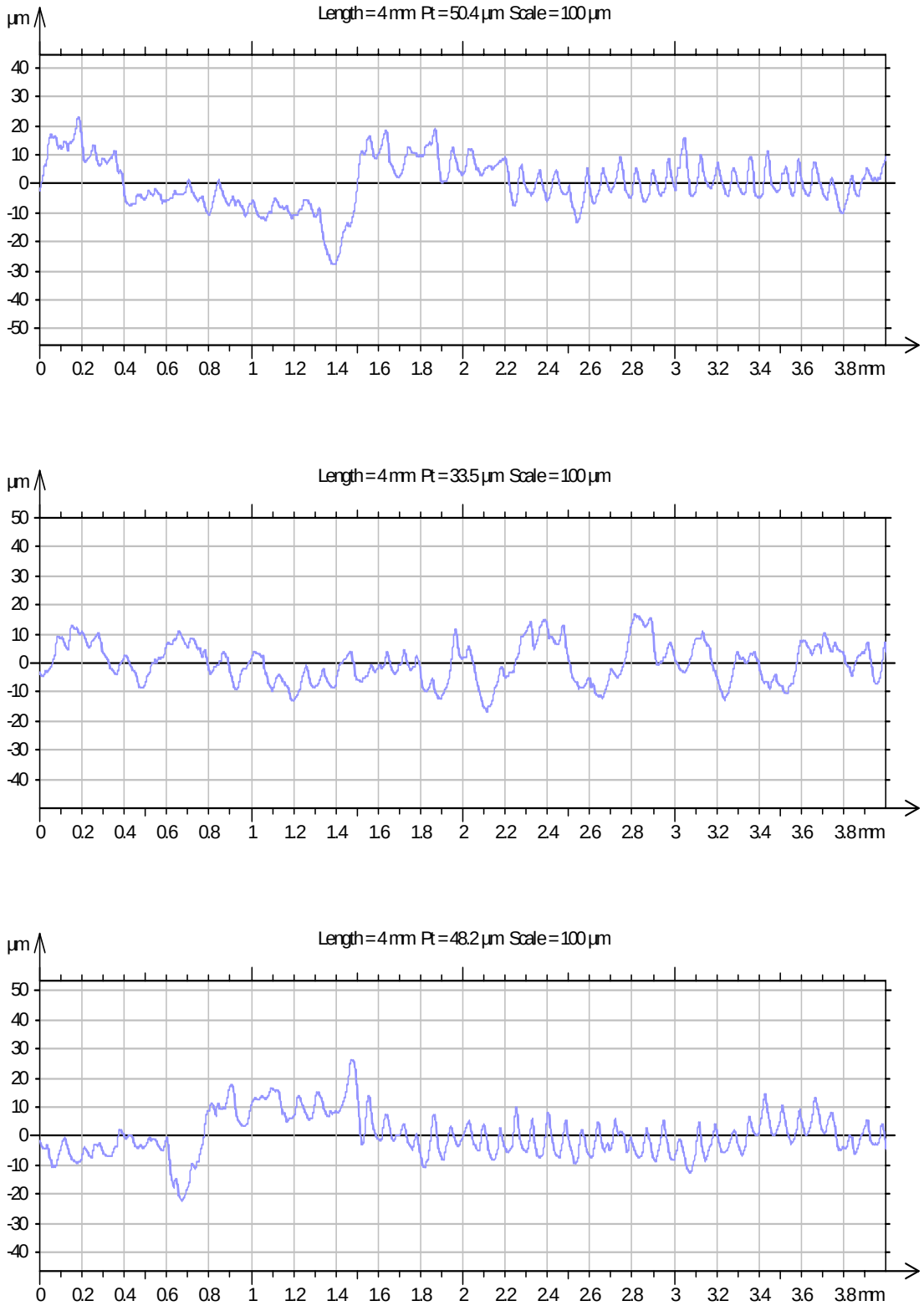

(**Sample 9**) Surface roughness and waviness profile curve at factor setting:

Spindle speed 860 rpm, feed rate 0.132 mm/rev and depth of cut 0.8 mm